Targeting the Oligomannose Biomarker Present on Distinct Subsets of Non-Hodgkin Lymphomas

by

Butaek Lim

DISSERTATION

Submitted in partial fulfillment of the requirements
for the degree of Doctor of Philosophy in Biomedical Engineering at
The University of Texas at Arlington
August 2020

Arlington, Texas

Supervising Committee:

Justyn W. Jaworski, Ph.D., Supervising Professor
Mark Pellegrino, Ph.D.
Young-Tae Kim, Ph.D.

ACKNOWLEDGEMENTS

I would like to thank University of Texas at Arlington and department of Bioengineering for the scientific support, financial aids, and quality education throughout my graduate study. I would express my sincere appreciation to my P.I., Dr. Justyn Jaworski for his advice and guidance. He is my true friend and gives me the freedom during these years of doctorate that enabled me to become a good person as well as a researcher. I also thank professors and employees (Julia Rockow, Cynthia Bradfield, and Alicia Gill) in the bioengineering department that made possible this accomplishment of my academic progress. I would give my genuine gratitude to my committee members, Dr. Young-Tae Kim, and Dr. Mark Pellegrino, for participating in my dissertation defense and leading me in the right direction to achieve academic goal. Thanks to my former and current colleges Dr. Rahul Kumar, Lenaiya Kydd, Anindita Arpa, and Priyanka Shiveshwarkar in Dr. Jaworski's Lab for direct or indirect contribution to my research. I am grateful Dr. Nguyen, Dr. Weidanz and Dr. Pellegrino and their Labs for receiving me without hesitation in their Labs so that I could assess much of the researches presented here; especially thanks to Manoj, Aneetta, Madhab, and Siraje. Special thanks to Mohammed who gladly helped me settle down on campus in the very beginning with a packet of nuts! Thanks also to pastors and families in KCUMC of Dallas, especially Zoe ministry, Mingu/Hana and No.1 lovely nephew Minha and Naim. Especially thanks to Daniel and Ellen, my spiritual parents, for presenting and teaching us what the actual life of Christianity is. Thanks to my parents Jong-Keun Lim, Pan-Sim Jung and my sister Ahreum Lim and all my relatives for unconditional love and for always supporting and completely trusting me on my side. I would give my appreciation to my parents in law Seung-Woon Myung, Eun-Hee Jung and my brother in law Ji-Won Myung for accepting me, who have so many flaws, but still encouraging and praying for me. I am in her debt to my wife Chi Ye Myung for being always by my side in the most difficult time. During four years you are on all occasions around and it was my safe harbor, your love and inspiration braced my strength and reawakened my purpose in life, helping me never pursuing worldly values. Thank you for your support and understanding and for waiting for me, always a little late me. Above all, I thank God, for being my true Lord who gives me the strength and motivation not to forget his purpose and lose my goal. To Almighty God I dedicate this work, "I consider everything a loss compared to the surpassing greatness of knowing Christ Jesus my Lord"

Abstract

Targeting the Oligomannose Biomarker Present on Distinct Subsets of Non-Hodgkin Lymphomas

Butaek Lim, Ph.D.

The University of Texas at Arlington, 2020

Supervising Professor: Dr. Justyn Jaworski

Subtypes of B cell non-Hodgkin's lymphomas, including follicular lymphomas, have shown a unique high oligomannose presentation on their immunoglobulins that will interact with natural receptors of the innate immunity, reportedly causing stimulation and proliferation. From next generation deep sequencing of the variable heavy and light chain sequences of follicular lymphoma involved tissue sections, we identified the consensus variable sequences possessing glycosylation sites at the complementarity determining region. Using this information, we developed a cell line, referred to here as BZ, which displays the consensus variable segments as part of a surface antibody (IgM) and confirmed its presentation of high oligomannose on the heavy chain both in vitro and in vivo. An mCherry expressing variant provided a reporter cell line displaying the high oligomannose surface biomarker while affording clear fluorescent signals for FACS screening as well as for fluorescent in vivo imaging of ectopic xenograft tumors. In developing this reporter cell line displaying the biomarker glycan of follicular lymphoma, we provide a tool that may be used for future screening and validation of receptive moieties for selectively binding high oligomannose for development of targeted diagnostics or therapeutics to such B cell malignancies that display this unique glycan. In our examination and development of oligomannose receptive moieties, we have investigated a potential antibody (2G12), engineered an existing lectin (*Pseudomonas Fluorescens Agglutinin*), as well as conducted phage display screening for candidate oligomannose receptors.

Contents

Chapter 1: Background on Follicular Lymphoma and Potential Oligomannose Receptors

1.1) Follicular Lymphoma

The IgH:BCL-2 translocation had been considered the hallmark of follicular lymphoma (FL), as it was found to exist in the majority of follicular lymphomas. However, extensive genomic analysis of this interesting translocation revealed that IgH:BCL-2 rearrangements occur naturally with age progression and are seen in 46% of healthy individuals(1, 2). It has been confirmed that this rearrangement alone is not primarily responsible for oncogenesis thereby bringing into question what additional factors cause such B-cell oncogenesis(4). While not the lone transformative factor, this chromosomal rearrangement undoubtedly plays a key role, since it result in the over-production of BCL2 protein to inhibit apoptosis(6). In contrast to this classic model of germinal center entry of naïve B cells harboring these translocation, several multistep routes have been proposed for oncogenesis in which the anti-apoptotic behavior of the IgH:BCL-2 translocation is coupled with additional factors that stimulate continuous proliferation. The subsequent collection of chromosomal aberrations over time resulting in an eventual transformation of FL to aggressive DLBCL (Diffuse Large B Cell Lymphoma) at a cumulative probability of 3% for each year after diagnosis(7). An additional proliferative factor leading to oncogenesis has shown that membrane immunoglobulin (antibody) displayed as part of

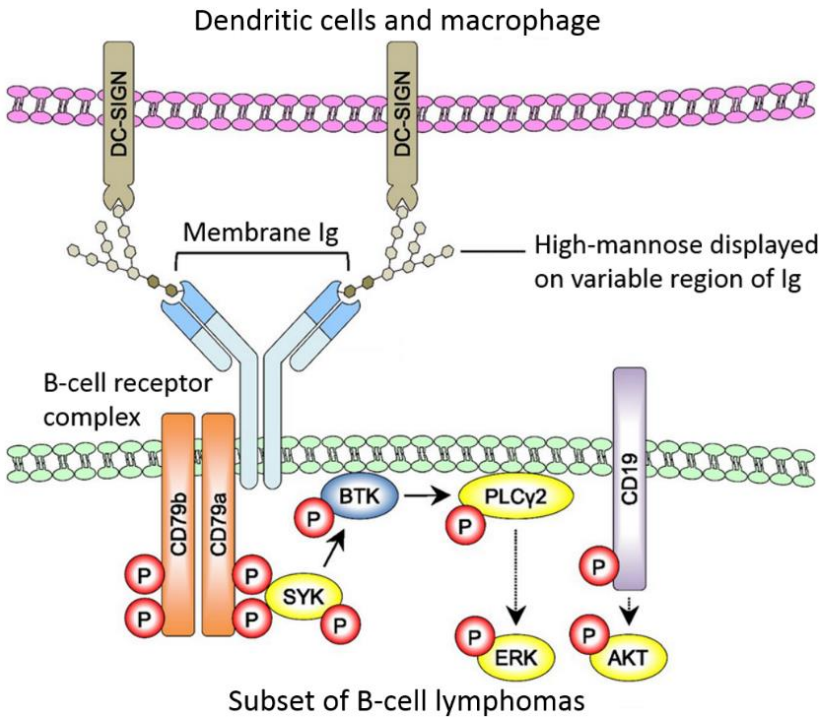

Figure 1: Simplified model by which certain B-cell lymphomas possessing oligo-mannosylated B cell receptors can receive antigen-independent stimulation by interaction with endogenous lectins on nearby dendritic cells and macrophage.

the B cell receptor (BCR) may be providing this additional stimulating signal by constant activation with a "self-antigen"(8).

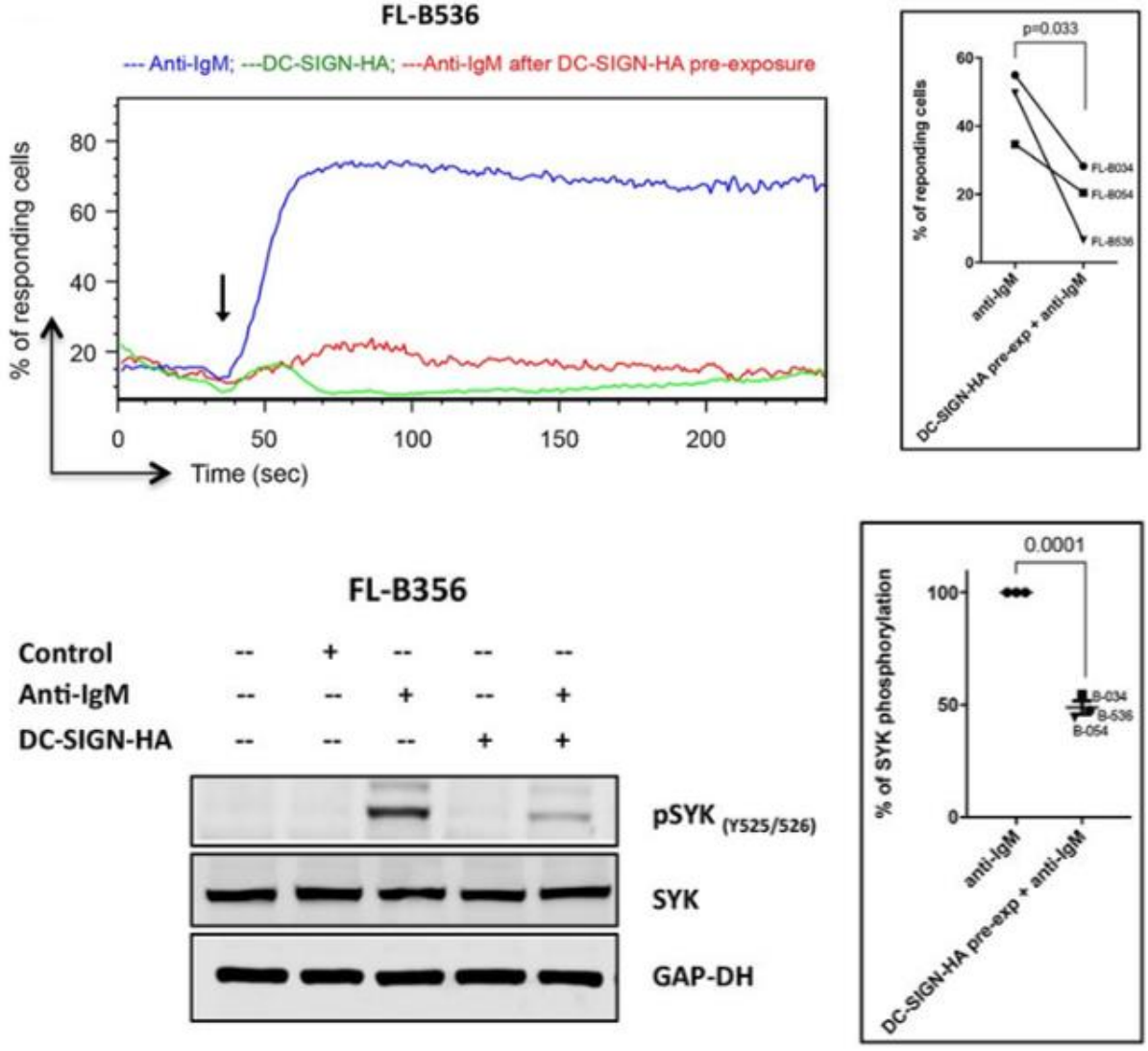

Figure 2: Shows stimulation of follicular lymphoma cells by anti-IgM and blocking of BCR by DC-SIGN for a monovalent form of soluble DC-SIGN. From Ref (2)

Several studies had previously revealed, the antibody displayed by patient derived lymphomas to recognize a natural human protein to provide this persistent signal for proliferation(9), but previously no common protein target was found across different patients until a recent analysis. A new discovery from a large cohort of lymphoma patients revealed that the Ig variable regions of a large cohort of lymphoma patients has shown that an interesting common signal does exist and is found on the variable heavy chain of B-cell receptors of approximately 79% of FL patients and

41% of DLBCL patients, namely the presence of an N-linked glycosylation site in the CDR (complementary determining region) segment of the Ig (immunoglobulin) resulting in the display of high oligomannose(10, 11). Such high oligo-mannose sites on the CDR are generally absent in naive human B cell repertoires(12), yet were found prevalent in the majority of follicular lymphomas (FL) and also in a large proportion of DLBCLs(13). In our own research, we have also found such glycosylation sites in the complimentary determining region (CDRs) of follicular lymphomas resulting in the display of high-mannose. While other forms of Ig glycosylation such as sialylation has been observed in 15% of serum antibodies, the appearance of high oligomannose appears to be unique to this subset of lymphomas(12). Presentation of high oligomannose on the variable heavy chain of B-cells has since been validated to result in BCR crosslinking by interaction with common endogenous receptors presented by cells in the lymph node. These endogenous oligomannose receptors include DC-SIGN and DC-SIGNR present on macrophage and dendritic cells. Such BCR crosslinking has been confirmed to result in persistent activation of B cell proliferation evident in these B cell lymphomas.

The DC-SIGN is upregulated in macrophage and dendritic cells associate with follicular lymphoma involved nodes; however, these in vitro studies with soluble DC-SIGN did not stimulate SYK phosphorylation pathway of FL cells but rather attenuated it by blocking access to anti-IgM induced Ca^{2+} flux. These results showed that soluble DC-SIGN alone provided a low level signal without loss of surface IgM to endocytosis. Shortcomings of this in vitro model is that the soluble DC-SIGN is not multivalent while the multivalent surface display of DC-SIGN or DC-SIGNR would facilitate BCR crosslinking(3).

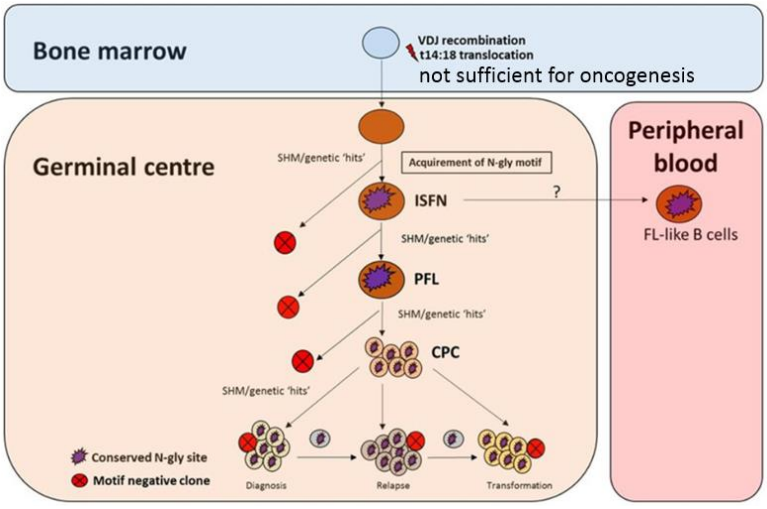

Figure 3: Overview of follicular lymphoma acquiring translocation followed by N-gly motif sites which are found to be conserved both in the heterogeneous subclonal population and the overall tumor mass. The sites are also retained in progression-associated subclones while rare motif-negative subclones disappear

Acquired N-linked glycosylation motif sites are a clonal feature in the complementary determining regions of FL and this motif is conserved

both in the heterogeneous subclonal populations and in the overall tumor mass. It is also found that these glycosylation sites are retained in progression-associated subclones while rare motif-negative subclones disappear(3). The B-cell receptor (BCR) signaling pathway for B-cell survival can be stimulated in an antigen-independent manner when oligomannosylated. Displayed oligomannose on the variable Ig domains of can be bound by endogenous lectins on dendritic cells or macrophage like DC-SIGN in the lymphoid tissue as part of innate immunity.

1.2) DLBCL and Other Oligomannose Presenting Cancers

DLBCL is a heterogeneous group of lymphomas that makes of 30% of non-Hodgkin's lymphoma cases and is characterized as a particularly aggressive disease with large neoplastic B cells in a diffuse growing pattern. While autoimmune diseases, pesticides, hair dyes, and UV radiation can confer increased risk of DLBCL, it also is known to arise by direct transformation from follicular lymphoma B cells when mutations or chromosomal translocation continue to accumulate with the disease at gene loci such as MYC, TP53, or CARD11. The classifications of DLBCL have evolved overtime due to improvements in identifying the pathology of this clinically heterogeneous class of B cell neoplasms but for a clear understanding of the variety of the underlying molecular abnormalities necessitates further improvements in immunophenotyping and other diagnostic tools. Three DLBCL subtype classifications exist based on gene expression patterns and are device as GCB (germinal center B cell), ABC (activated B cell), and PMBL (primary mediastinal large B cell lymphoma) with the highest survival seen for GCB DLBCL among these three. Diagnostic use of IHC staining was previously validated as a means for distinguishing between GCB and ABC utilizing markers of CD20, CD10, BCL6, and MUM1 (17). In recent years however since the implementation of rituximab immunotherapy which targets CD20, there is a propensity for patients losing the CD20 marker (18) and as such no longer does this panel provide prognostic information. A new biomarker panel would thus provide significant prognostic value in classifying between these DLBCL subtypes. Interesting 41% of DLBCL possess a glycosylation site on their BCR (B cell receptor) as confirmed by sequence analysis and are manifested exclusively in GCB type DLBCL making this a strong biomarker candidate for distinguishing these subtypes; hence, we explore the development of a diagnostic immunophenotyping probe based on the recognition of oligomannosylation of the BCR (19).

Table 1: Overview of literature reports of rates of identified glycosylation of the variable heavy and light chain of B cell receptors in distinct B cell non-Hodgkin lymphoma subtypes.

Lymphoma subtype	% possessing glycosylation site on Ig variable H/L chain	Literature Citation
Follicular Lymphoma (FL)	79-100%	Ref (10)
Diffuse Large B-Cell Lymphoma (DLBCL)	41% (GCB)	Ref (14)
Burkitt's Lymphoma	57% (endemic/sporadic)	Ref (14)
Chronic Lymphocytic Leukemia (CLL)	13% (Unmutated-CLL)	Refs (10, 15, 16)

Epidermal growth factor receptor in human epidermoid carcinoma A431 cell line(20) and gastric cancer cell line MKN28 (21). Unspecified upregulation of oligomannose type glycans in human lung adenocarcinoma(22) and colorectal cancer(23). Anti-oligomannose immune repertoires were found to develop naturally in patients with high grade prostate cancer(24). The appearance of oligomannose in patient tumors with prostate cancer follows directly with the Gleason grade of the cancer which is a predictor of recurrence. Related works have shown that tumor cell-based vaccines of melanoma cells could elicit immune responses in animal studies resulting in anti-Man9-cluster antibodies(25), which have been claimed to show strong binding to a number of murine and human tumor cell lines such as ovarian, breast, and prostate cancer; however, no follow up studies have been reported leading the specificity of the produced antibodies to be in question.

1.3) Oligomannose Glycans

Oligomannose in the context of healthy mammalian systems are masked by other sugar moieties capped onto the end and typically only exist as precursors, or core/internal sequences of mature glycans. The biosynthesis of N-linked glycans begins through the transfer of a "high-mannose" oligosaccharide composed of Glc3Man9GlcNAc2 to a nascent polypeptide chain in the endoplasmid reticulum at canonical glycosylations sites having the amino acid sequence (N-X-S/T). Reactions with glucosidases begin trimming the ends to remove glucose unit while a series of mannosidases would follow to remove all but three mannose residues as the protein enters the

early Golgi. While capping with galactose and sialic acid as terminal sugar residues should occur naturally, recognition of oligomannose at key checkpoint stages can be indicative of improper folding whereby such oligomannosylated proteins would be targeted for degradation(26). To understand how then certain surface proteins such a IgM could display oligomannose without being targeted for degradation, it is critical to understand that the trafficking machinery will be ineffective if it is for any steric reason physically blocked for binding the oligomannose. Such steric blocking of trimming enzymes as well as trafficking proteins is believed to arise for the case of oligomannosylation in the complementary determining region (CDR) of immunoglobulin as these CDR antigen binding sites are notoriously concave and thus could effectively restrict any interaction with processing/trafficking machinery. The consistent distinct glycosylation pattern of oligomannose presented on the variable regions of immunoglobulins in follicular lymphoma while the constant domains possess properly processed glycosylation sites provides a clear internal control that normal transit and processing through the Golgi is occurring but with an inability to process mannose trimming in the variable region due to some form of steric blocking. Importantly, endogenous lectins present on the surface of macrophage and dendritic cells in the germinal center will interact with the displayed immunoglobulin providing activation of those B cells displaying oligomannose. This conservation of the CDR glycosylation site during somatic hypermutation suggest it as a critical factor that restricts a key dependence of follicular lymphomas on the surrounding tumor microenvironment and follows rationally why there continues to be great difficulty in generating a follicular lymphoma cell line or in vivo model(13).

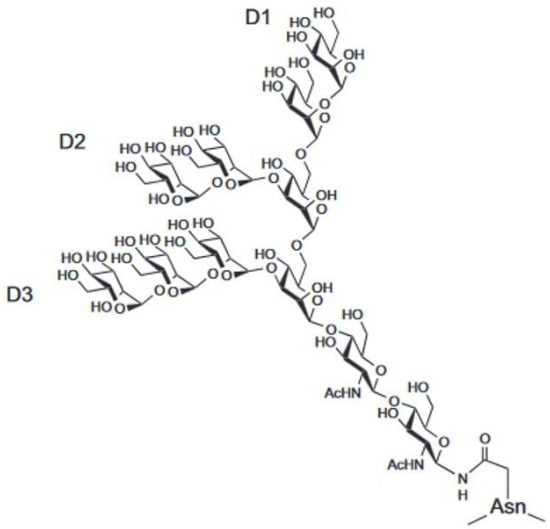

Figure 4: Structure of Man-9 oligomannose possessing alpha 1,2 linkages between linear mannose units and alpha 1,3 and alpha 1,6 linkages at branch points. A beta 1,4 linkage at the linear stem comprised of two GlcNAc units is N-linked to asparagine.

1.4) Lectins and Antibodies

Lectins are natural carbohydrate-binding proteins that have a critical role in trafficking of glycoproteins and play other key roles including adhesion and recognition of cells and pathogens.

Here we will discuss about two broad categories of lectins specific for oligomannose: those from humans that are endogenous to lymphoid tissue; and those from plants and microorganisms. A number of human lectins are found throughout lymphoid tissue that are capable of binding to oligomannose and most typically fall into the category of calcium-dependent (C-type) lectins. C-type lectins include DC-SIGN (dendritic cell-specific intercellular adhesion molecule-3 grabbing non-integrin) present on the surface of macrophage and dendritic cells which plays a critical role in the innate immunity by virtue of binding to mannose presented by a range of pathogens including rotovirus, HIV, and a number of fungi. By virtue of oligomannose also being present on the B cell receptor (BCR) of follicular lymphoma, such endogenous lectins present in lymphoid tissue can inherently bind to the BCR causing activation of signaling pathways. Indeed, it has been demonstrated that ERK and AKT phosphorylation signaling in primary follicular lymphomas can be activated by DC-SIGN (27). This ability of the DC-SIGN lectin to bind follicular lymphoma cells could serve two key roles in the pathology by providing both an adhesion signal by retention on lymphatic endothelium as well as a means for antigen-independent BCR signaling to stimulate survival and proliferation of the oligomannose motif on this form of B cell malignancy. DC-SIGN is but one of a handful of other C-type lectins that could potentially serve as an activating receptor of the oligomannosylated BCR. For these C-type lectins with affinity for mannose (DC-SIGN, DC-SIGNR, MBL, Endo180, and Langerin), the oligomannose form coordination bonds with the conserved Ca^{2+} as well as additional hydrogen bonding with groups in the receptor site depending on the position where the overall carbohydrate structure dictates the specificity and affinity. In contrast to human C-type lectins, there are a number of plant and microbe derived lectins capable of recognizing oligomannose that proceed in a calcium independent manner. The *Oscillatoria agardhii* agglutinin homologue (OAAH) family of lectins, with *Pseudomonas fluorescens* agglutinin (PFA) being a specific example, are capable of recognizing the Man alpha(1-3) Man alpha(1-6) Man core of oligomannose directly and with high affinity. The ability of the OAAH family of lectins to recognize oligomannose has been of particular interest for its inactivating properties on HIV replication and transmission (28). Specifically, the OAAH family of lectins exhibit a unique recognition of the core mannopentaose providing it with broader selectivity for Man-6 to Man-9 oligomannose variants as compared to other lectins that merely recognize the terminal mannoses (29, 30). The PFA lectin exhibits two binding sites for oligomannose on opposing ends of the beta-barrel like architecture. The potential for using this form of receptor for

targeting to the oligomannose presented by follicular lymphoma cells but would need careful consideration of the ramifications of having a bi-valent binder of oligomannose as this may result in BCR cross-linking that would inherently stimulate activation of these malignant B cells.

The pursuit of antibodies with specificity for oligosaccharides has seen significant research attention given the high impact that such targets could serve; however, the development of anti-glycan antibodies has historically seen little success due to relatively poor affinities and corresponding weak specificities which was noted by the National Academy of Sciences as a key barrier for advancing basic research and clinical applications(31, 32). The development of an effective oligomannose antibody in particular has seen substantial interest as a potential broadly neutralizing antibody for HIV since the HIV envelope protein gp120 contains clusters of oligomannose residues which it uses to bind to and subsequently infect macrophage and dendritic cells. One monoclonal antibody was serendipitously discovered from an HIV-1 patient that specifically recognized the oligomannose carbohydrate epitope presented by the HIV gp120 envelope protein and marked a key candidate for a broadly neutralizing antibody. With significant attention on this monoclonal antibody, crystallographic studies of the 2G12 interaction with the oligomannose were conducted and revealed a very unique domain swapped confirmation of an interlocked variable heavy (V_H) domain dimer which provide an extended complementary determining region optimized for interaction with clustered oligomannose to provide a high-affinity binding surface.(5) The affinity was found to be conveyed by a large number of acidic

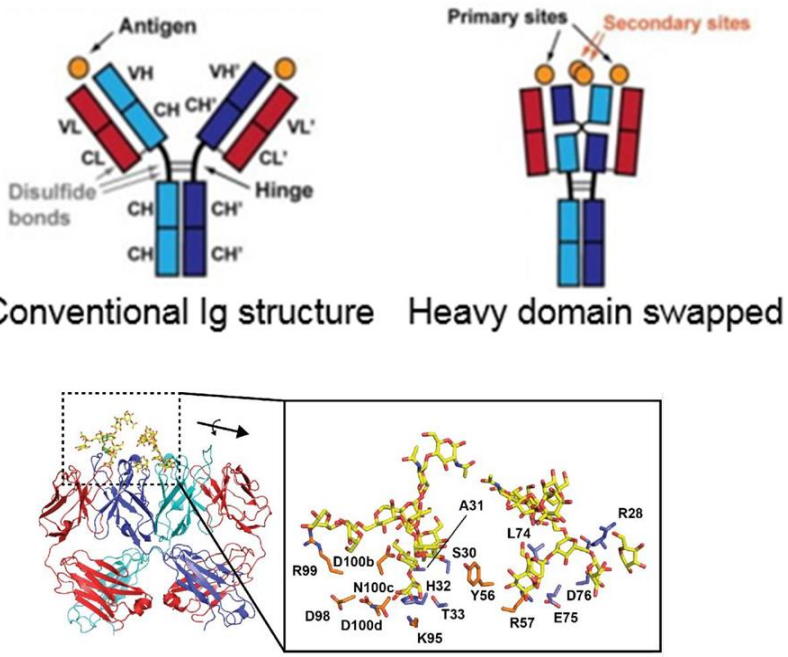

Figure 5: Schematic (top) and 3D model of 2G12 recognition of oligomannose from gp120 (bottom) based on the crystal structure of 2G12 having dimerized Fab (antibody fragments) due to variable heavy domain cross-over through a swapping of segments in the two variable heavy domains creating a new interface as well as an increased surface area of the complementary determining region. From Ref (3).

residues that played a critical role in recognition of the alpha1-2 mannose disaccharide units. Assessment of the 2G12 antibody revealed it to be highly mutated from the germline sequence possessing a critical proline resulting in an elbow between the variable and constant heavy chain domains with a significant amount of hydrophobic residues to facilitate the coupling of the interface for heavy domain exchange(33). The higher local concentration of alpha1-2 mannose recognition regions facilitated by the domain cross-over of 2G12 allow for potential avidity effects for multivalent binding across a larger binding surface. It is worth noting that while 2G12 is an effective broadly neutralizing antibody against infection of certain HIV subtypes in animal models, it is still the only domain cross-over antibody to have been discovered. Attempts to create a 2G12 like antibody with altered specificity have been attempted by several groups(34). In this work, we utilize the 2G12 antibody for its oligomannose recognition capabilities and explored its utility for targeting the oligomannose displayed by follicular lymphoma and distinct subtypes of diffuse large B cell lymphoma. The rationale for utilizing the 2G12 antibody lies in its unique specificity for the alpha1-2 mannose epitope of the D1 arm of $Man_9GlcNAc_2$ glycan on the gp120 which is identical to that of the $Man_9GlcNAc_2$ glycan found on the B cell receptors of these lymphoma subsets. The selectivity of 2G12 for Manα1→2Man terminating glycans is thus expected to provide a means for targeted discrimination of distinct lymphoma subsets which possess oligomannosylated B cell receptors (35, 36).

Chapter 2: Confirmation of Glycosylation in FL and Generating a Cell Model

2.1) Introduction

In beginning of this dissertation work, a notable study had just been released on the meta-analysis of follicular lymphoma patient lymph node specimens looking at the nucleotide sequences of the Ig variable heavy domain. The findings revealed that in a dominant proportion of follicular lymphoma patients the IgH VDJ recombination sites possessed canonical glycosylation tags that when expressed would present the amino acid sequence N-X-T/S. This discovery is significant as the naive human immune repertoire is nonexistent in such sequences notably within the CDRs (complementary determining regions). Given our interests in receptor screening, this unique glycosylation presented itself as an interesting unique incomparable biomarker for receptor discovery and development; however, before moving forward we needed to confirm the biomarker oligomannose was truly presented on the expressed variable heavy chain sequence derived from the follicular lymphoma B cell tissue specimen.

Indeed there has been much work in suggesting that B cell follicular lymphoma as well as subsets of other B cell lymphomas display a unique high oligomannose glycan on their membrane bound immunoglobulin (Ig)(1-6). Works examining the Ig variable regions of follicular lymphoma (FL) patients has shown an intriguing common trait of presentation of a glycosylation site sequence within the variable segment, typically at the CDR (complementarity determining region)(4,7,8). This site has been formerly reported in the variable heavy chain of B-cell receptors of at least 90% of FL patients and at least 41% of Diffuse Large B-Cell Lymphoma (DLBCL) patients(1,2,4,8,9), where the unique display of a high oligomannose glycan is arisen from such N-linked glycosylation sites of the CDR. This display of high oligomannose on the CDR are absent in naive human B cell repertoires and are selected in opposition to, since high oligomannose binds to receptors present on natural innate immune cells(3,10). Whereas, other forms of glycosylation such as sialylation are readily observable at other sites along the Ig but not at the CDR(10). DC-SIGN and DC-SIGNR are comprised of endogenous oligomannose receptors presented by macrophage and dendritic cells, and the interaction of DC-SIGN with the oligomannosylated Ig of FL B-cells has been validated to cause B-cell receptor crosslinking for persistent activation of B cell proliferation(11,12). The acquiring of this N-linked glycosylation motif is obvious to be a necessary feature among certain B cell lymphomas. The conserved glycosylation at the

complementarity determining regions of FL B cells can be observed within heterogeneous subclonal populations of FL, whereas the glycosylation motif-negative subclones will disappear from the overall tumor mass, while glycosylation sites are retained in the progression-associated subclones(9,11,13). A reported rationale of this is the endogenous lectins present on the surface of macrophage and dendritic cells in the germinal center which react to the displayed oligomannose on the immunoglobulin providing activation of those B cells displaying this unique glycan[4]. This conservation of the CDR glycosylation site during somatic hypermutation indicate that it is a critical factor that confines dependence of follicular lymphomas on the neighboring tumor microenvironment[9]. It thus describes rationally why there continues to be great difficulty in generating a follicular lymphoma cell line or in vivo model given this dependence(3).

While we now know that displayed oligomannose on the variable Ig domains can be bound by endogenous lectins of innate immune cells within lymphoid tissue, future studies may observe to identify mechanisms to block this B-cell receptor signaling required for FL B-cell survival. In looking to understand how this unique oligomannose can be presented as a hallmark on the CDR of Ig, it is essential to consider that in the context of healthy mammalian systems these terminal mannose units of oligomannose are typically masked by other sugar moieties capped onto the end and thus oligomannose is commonly only present as precursors, or core/internal sequences of more mature glycans. This biosynthesis of N-linked glycans initiates through the transfer of an oligosaccharide constituted $Glc_3Man_9GlcNAc_2$ to a nascent polypeptide chain in the endoplasmic reticulum at canonical glycosylation sites having the amino acid sequence (N-X-S/T). Trimming of the glucose terminal units is initiated by glucosidase reactions while a series of mannosidases would succeed to remove all but three mannose residues as the protein passes into the early Golgi to follow with capping of terminal sugar residues such as fucose and sialic acid(14,15). Natural recognition of high oligomannose at key checkpoint stages is an indication of improper folding whereby such oligomannosylated proteins would be targeted for degradation(16). However, for an Ig of FL to display oligomannose without being directed for degradation, it is believed that the generally concave shape of the CDR(17) may sterically hinder the glycan trimming enzymes as well as trafficking machinery from binding the oligomannose within the CDR pocket and in response interrupt the ability to degrade the high oligomannose displaying Ig. This distinct high oligomannosylation is persistently presented on the variable regions of the Ig in follicular lymphoma, whilst the constant domains acquire properly processed glycosylation sites (12,15).

This feature sustains a clear internal control that normal transit and processing through the Golgi is happening but with an inability to process mannose trimming in the variable region due to some form of steric hinderance as mentioned above. In order to allow a system for the display of the high oligomannose biomarker presented by the immunoglobulin of FL B cells, we have constructed here a reporter cell-line which presents the variable domains from a FL B cell as a membrane bound surface antibody and substantiated its display of the high oligomannose glycan.

It has been reported that the availability of mouse models for investigating follicular lymphoma are limited due to the toughness to establish follicular lymphoma xenografts, as the local tumor microenvironment is vital for their survival and immuno-compromised mice are inadequate necessary supportive interaction or mature secondary lymphoid organs(18). Because of the requirement of this supportive cellular framework, in vitro growth has also shown very restricted survival and as such there are believed to be no true follicular lymphoma B-cell lines(18). Nonetheless, a number of reports have demonstrated FL-like cell lines, often with co-culture of helper cells, can serve as necessary tools for studying different perspectives of follicular lymphoma such as chromosomal features, apoptosis, and cytokine-mediated growth regulation(19-24). In the present work we do not try to provide a follicular lymphoma cell line but rather suggest an engineered reporter cell line that produces a high oligomannosylated surface antibody as to mimic that presented by FL B cells. Here, we explain our approach to using deep sequencing of variable domains from FL tissue sections to identify and generate a genetic engineering for expression of a membrane bound IgM that displays the canonical high oligomannose on the heavy chain CDR. Herein, two engineered cell lines were created using a HEK293 background and were observed to stably express the oligomannoyslated antibody with one carrying a cytosolic mCherry fusion as a reporter. We anticipate contributing these cell lines as tools for the research and development of receptive moieties for high oligomannose will help to bring new diagnostic or therapeutic technologies. The potential use of this reporter cell line for *in vitro* screening or *in vivo* imaging studies may deliver as a starting point toward recognizing relevant high oligomannose receptors that may ultimately be advanced into clinically beneficial probes.

2.2) Materials and Methods

I first processed FFPE slide sections of lymph node specimens from FL involved lymph nodes for DNA extraction by 15 minute incubation twice in xylene followed by incubation in ethanol to

displace paraffin for following extraction using the Qiagen FFPE DNA extraction kit as per the protocol for FFPE tissue. Deep sequencing of the variable heavy and light chain sequences presented in the samples were achieved by first generating amplicons using 20 cycles of PCR with the primer sets referred to as "1st PCR Extension" in the Supplementary Methods (see Supplementary Information) which were based on available primers optimized for creating libraries of the human Ig repertoire(31,32). After I confirmed amplicon sizes by agarose gel electrophoresis and purified them by column purification, I performed a second fusion amplification of 5 cycles using the primer sets referred to in the Supplementary Methods as "2nd PCR extension" to adjoin the amplicons with the Nextera adaptor sequences. I then analyzed the amplicon sizes by gel and cleanup before providing 58uL of eluted DNA at 277ng/uL of dsDNA for NGS sequencing by MiSeq. Samples were processed and sequenced by Macrogen where first the Nextera XT indexing primers Index 1 Read (CAAGCAGAAGACGGCATACGAGAT[i7]GTCTCGTGGGCTCGG) and Index 2 Read (AATGATACGGCGACCACCGAGATCTACAC[i5]TCGTCGGCAGCGTC) were added where i7 and i5 are sets of distinct indexing sequences used as part of Macrogen's Illumina MiSeq NGS workflow. The resulting sets of samples yielded 452787 and 358961 paired end (2x300nt read length) MiSeq reads of the NGS data obtained as FASTQ files.

The amplicon data was processed using Bioconductor v3.11 in R v4.0.0 with the DADA2 package v1.16.0 (33). The mean quality score at each base position was approved, and filtering was conducted based on the quality profile standard using truncation of the forward reads at position 250 and the reverse reads at position 180 in order to only collect the positions in which there was a high mean quality score distribution above 30. The parametric error model of the DADA2 algorithm was employed to learn the error rates of our amplicon dataset and to conclude the true sequence variants at the same time as de-noising to remove withdraw spurious reads. The model merged unique pairings where paired reads that did not overlap were removed. Data processing workflow in R is explained in the Supplementary Methods. After amplicons were analyzed by IMGT/HighV-QUEST which translates them to the amino acid sequences, separately aligned to their respective heavy or light chain sequences designated by subtype (heavy, kappa, lambda), and executed mutational analysis towards the germ line sequence. Multiple sequence alignment of the translated sequences using MAFFT was arranged via NGPhylogney.fr(34). The consensus sequence of the most frequent amino acids was selected from the sequence logo

provided by the aligned clonotypes as analyzed by WebLogo for both the heavy and light chain variable domains(35). These consensus sequences for the light chain and heavy chain were then used to express the antibodies to be displayed in our engineered cell line.

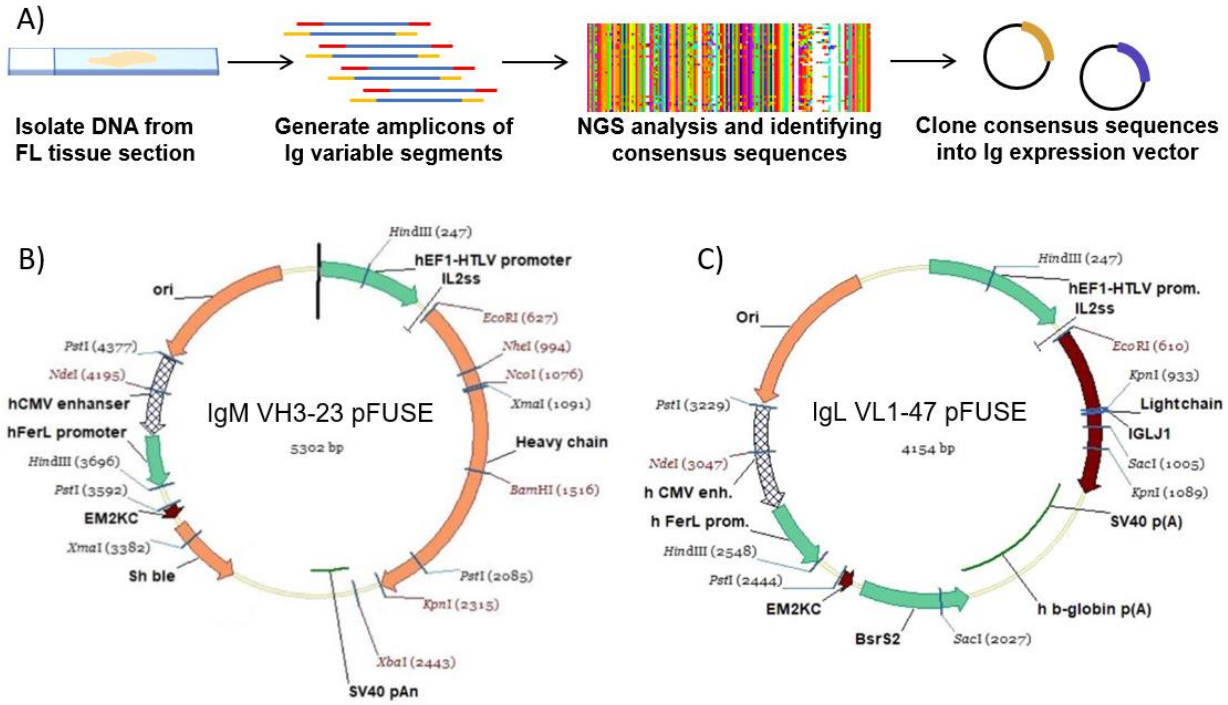

Figure 6: Schematic method to create Ig expression vectors retaining variable domains from follicular lymphoma B cells. A) Process of our approach to discover consensus variable segment sequences from follicular lymphoma B cell FFPE tissue sections. B) Plasmid map (drawn by VectorNTI software) of IgM VH3-23 pFUSE vector and C) IgL VL1-47 pFUSE vector for expression of surface antibody displaying the variable heavy and light chain consensus segments identified from FL B cell tissue sections and possessing genes for zeocin and blasticidin resistance, respectively.

The following primers were used in preparation of amplicons for deep sequencing of Ig variable segments. (Note: R=A,G; W=A,T; S=C,G; D=A,G,T; B=C,G,T; N=A,C,G,T; Y=C,T; M=A,C; K=G,T; H=A,T,C; V=A,C,G)

1st PCR extension

Vlambda primers

IGLam V1for: ATC TAA CTC GAG CAG TCT GYS YTG ACK CAG CCK SC

IGLam V2for: ATC TAA CTC GAG AAT TTT ATG CTG ACT CAG CCC CA

IGLam V3for: ATC TAA CTC GAG TCY TMT GWG CTG ACT CAG SMM CC

IGLam Jrev: TAA ACT ATG CGG CCG CAC CTA RRA CGG TSA SCT KGG TCC C

Vkappa primers

IGKap V1for: ATC TAA CTC GAG GAA ACG ACA CTC ACG CAG TCT CC

IGKap V2for: ATC TAA CTC GAG GAY RTY GTG ATG ACY CAG TCT CC

IGKap V3for: ATC TAA CTC GAG GAA ATT GTG YTG ACK CAG TCT CC

IGKap V4for: ATC TAA CTC GAG GAC ATC CAG ATG ACC CAG TCT CC

IGKap Jrev: TAA ACT ATG CGG CCG CAC GTT TRA THT CCA SYY KKG TCC C

Vheavy primers

Vh1for: ATC TAA CTC GAG SAR RTV CAG CTS BWR SAG TCN GG

Vh2for: ATC TAA CTC GAG GAG GTG CAG CTG TTG CAG TCT GC

Vh3for: ATC TAA CTC GAG CAG GTA CAG CTG CAG CAG TCA GG

IGH Jrev: TAA ACT ATG CGG CCG CAC CTG ARG AGA CRG TGA CC

2nd PCR extension

Adapter primers

NGS Vhfor: (FPOA)-AATCTAACTCGAGSARRTVCAGC

NGS Vlambdafor: (FPOA)-TATCTAACTCGAGYMBTMTGHS

NGS Vkappafor: (FPOA)-GATCTAACTCGAGGAHRYBVHRHTYAC

NGS IGmix Jrev: (RPOA)-TAAACTATGCGGCCGCACSTD

Where FPOA is the Forward Primer Overhang Adapter (TCGTCGGCAGCGTCAGATGTGTATAAGAGACAG) and RPOA is the Reverse Primer Overhang Adapter (GTCTCGTGGGCTCGGAGATGTGTATAAGAGACAG).

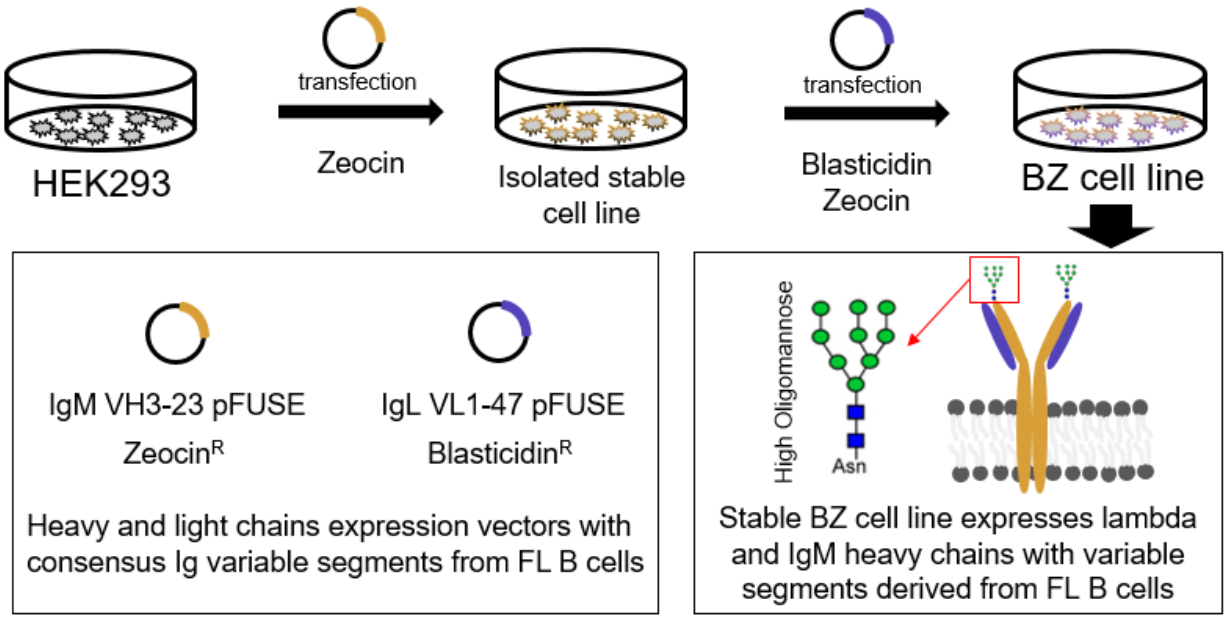

Figure 7: Schematic illustration of approach for generating engineered BZ cell line. A) Expression vectors based of pFUSE were constructed with variable segments derived from consensus deep sequencing results of follicular lymphoma B cells. Sequential separation of stable cell lines under antibiotic selection and examination of expression were carried out to identify the BZ cell line which provided the surface display of antibody possessing variable domains derived from the FL B cell.

After consensus sequences of the variable heavy and variable lambda light domains were identified from the follicular lymphoma involved nodes as shown in Figure 6, each variable sequence was cloned into separate modified pFUSE mammalian expression vector as describe in detail in the Supplementary Methods. Two different pFUSE expression vectors were utilized, one for expression of the heavy chain IgM containing zeocin resistance and one for expression of the lambda light chain containing blasticidin resistance. The IgM VH3-23 pFUSE was engineered to possess a canonical IgM transmembrane domain as to present the B cell receptor on the cell surface when the heavy and light chain pair are co-expressed. Co-transfection of 50% confluent HEK293 cells with the IgM VH3-23 pFUSE and IgL VL1-47 pFUSE plasmids was attempted in sequential transfection and selection step utilizing polyethyleneimine as carrier vesicles in 24 well plates. An overview of the procedure is provided in Figure 7. For the selection of stable transfectants with IgM VH3-23 and IgL VL1-47 integrated into the genome, zeocin and blasticidin were used for selection, respectively. The antibiotic was added to the culture media as selection markers beginning from 48 hours after transfection and transfected cells were allowed to grow for 4 days

until colonies were isolated for subsequent screening. Screening of stable transfectants carrying the heavy and light chain after 3 weeks were carried out by separation on 96 well plates and inspecting replicate plates by IHC staining with biotinylated anti-IgLambda and anti-IgM primary antibody and strep-HRP secondary. The isolated cell lines possessing both blasticidin and zeocin resistance that were confirmed to display IgLambda and IgM were passaged to provide sufficient cells for examination of the lysate by western blot using biotinylated anti-IgM and anti-IgLambda primary followed by strep-HRP secondary. To resolve the bands on the nitrocellulose membrane, AEC staining was used and the expression of heavy and light chains was confirmed. The BZ-mCherry cell line was established by the above identical method but with automated screening by FACS (BD FACS Melody) and visual evaluation by fluorescence microscopy (Nikon ECLIPSE Ti2-A).

Using pFUSE for the heavy chain, the gene segment for the consensus sequence of the variable heavy chain from the FL involved node (referred to here as VH3-23 and seen in Figure 7) was cloned into a pUC19 vector. To utilize the constant region of the IgM heavy chain, the CHIg-mM fragment of pFUSE-CHIg-mM vector was amplified with forward (F-EcoRI-NheI-CHIg) and reverse (R-XbaI-KpnI-CHIg) primers and cloned into pUC19 vector. After amplifying VH3-23 sequence using forward (F-EcoRI-VH3-23) and reverse (R-NheI-VH3-23) primers, it was cloned and placed in the upstream of CHIg-mM to construct VH3-23-CHIg-mM. A transmembrane domain (TMD) was subcloned into the 3’ end of CHIg-mM after amplifying with forward (F-KpnI-TMD) and reverse (R-XbaI-TMD) primers and VH3-23-CHIg-mM-TMD was successfully constructed in pUC19 vector. After the whole insert was cut with EcoRI and XbaI, it was transferred to the pFUSE backbone vector to construct pFUSE-VH3-23-CHIg-mM-TMD vector. Light chain cloning was performed after expanding the consensus variable lambda light chain (referred to here as VL1-47 and seen in Figure 7) by using forward (F-VL1-47) and reverse (R-VL1-47) primer and directly delivered into the pFUSE2ss-CLIg-mL1 vector to form pFUSE2ss-VH1-47-CLIg-mL1. The following primer sets for cloning are listed below:

F-EcoRI-NheI-CHIg: AAAGGAATTCCCTAGCTAGCTCAGAGAGTCAGTCCTTCCC

R-XbaI-KpnI-CHIg: ATGCTCTAGAGCGGTACCAGTGGACTTGTCCACGGTCCTC

F-EcoRI-VH3-23: AAAGGAATTCCGAAGTACAGCTCTTAGAGTCGG

R-NheI-VH3-23: AACTAGCTAGCTGAGGAGACAGTGACCAGG

F-KpnI-TMD: ATTGAGGGTACCGAAGGAGAAGTGAACG

R-XbaI-TMD: TGTTTTCTAGATCACTTAACCTTGAACAAGGTAACAG

F-VL1-47: ATGGAATTCCAGTCCTATGTGCTGACTCAGGACCC

R-VL1-47:
TATCAGGTACCTGTCCCGAATACACGGCCACTCAGGCTGTCATCCCATGCTGC

To specify the presence of oligomannosylation on the heavy chain or light chain, the lysate of BZ cell line was treated with glycosidases Endo H, PNGase F, or Mannosidase and compared by western blot to lysate of the HEK293 background cell. Approximately, 10^6 cells were lysed with 100 µL of RIPA buffer on ice for 30 minutes and centrifugated for 10 minutes at 13,000 rpm to pellet cell debris, and the supernatant was stored for further experiments. Enzyme reaction conditions were prepared by the supplier's (New England Biolabs, MA, USA) instructions and their supplied buffers. Briefly, mannosidase reaction was prepared by combining 8 µL of the above-mentioned cell lysate, 1 µL of 10X GlycoBuffer 4 (1X is 50mM sodium acetate pH 4.5) and 1 µL of Mannosidase, and the mixture was incubated at 37°C for 1 hour. For Endo H and PNGase F enzyme reaction, the cell lysate was denatured by combining 9 µL of cell lysate and 1 µL of 10X denaturing buffer (1X is 0.5% SDS and 40 mM DTT) and incubated at 100°C for 10 minutes. 8 µL of denatured cell lysate, 1 µL of 10X Glycobuffer 3 (1X is 50 mM sodium acetate pH 6.0) and 1 µL of Endo H were combined and incubated for 1 hour at 37°C. For PNGase F reaction, 7 µL of denatured cell lysate, 1 µL of 10X Glycobuffer 2 (1X is 50 mM sodium phosphate pH 7.5), 1 µL of 10% NP-40 and 1µL of PNGase F were mixed and incubated at 37°C for 1 hour. Each reactant was mixed with protein loading dye and heated at 100°C for 10 minutes. Samples were loaded and resolved by SDS-PAGE for 2 hours at 120V followed by overnight transfer to nitrocellulose membrane at 4°C. Membranes were blocked overnight in 1 % bovine serum albumin (BSA) in 10 mM PBS buffer. 1 µL of primary antibody was diluted with washing buffer (1 % BSA and 0.5% Tween-20 in 10 mM PBS) to 1 mL and incubated overnight at 4°C with slow horizontal agitation (50 rpm). The membrane was washed with 10 mL of washing buffer for 10 minutes three times with horizontal agitation. 1 µL of secondary antibody conjugated with HRP was diluted to 2 mL and incubated for 30 minutes at room temperature with agitation followed by three times

washing. 10 mL of 0.05% AEC and 0.015% H_2O_2 in 50 mM acetate buffer pH 5.5 was added to develop the membrane until primary bands appeared.

2.3) Results

2.3.1) Identifying established follicular lymphoma B cell antibody sequence possessing characteristic CDR glycosylation site.

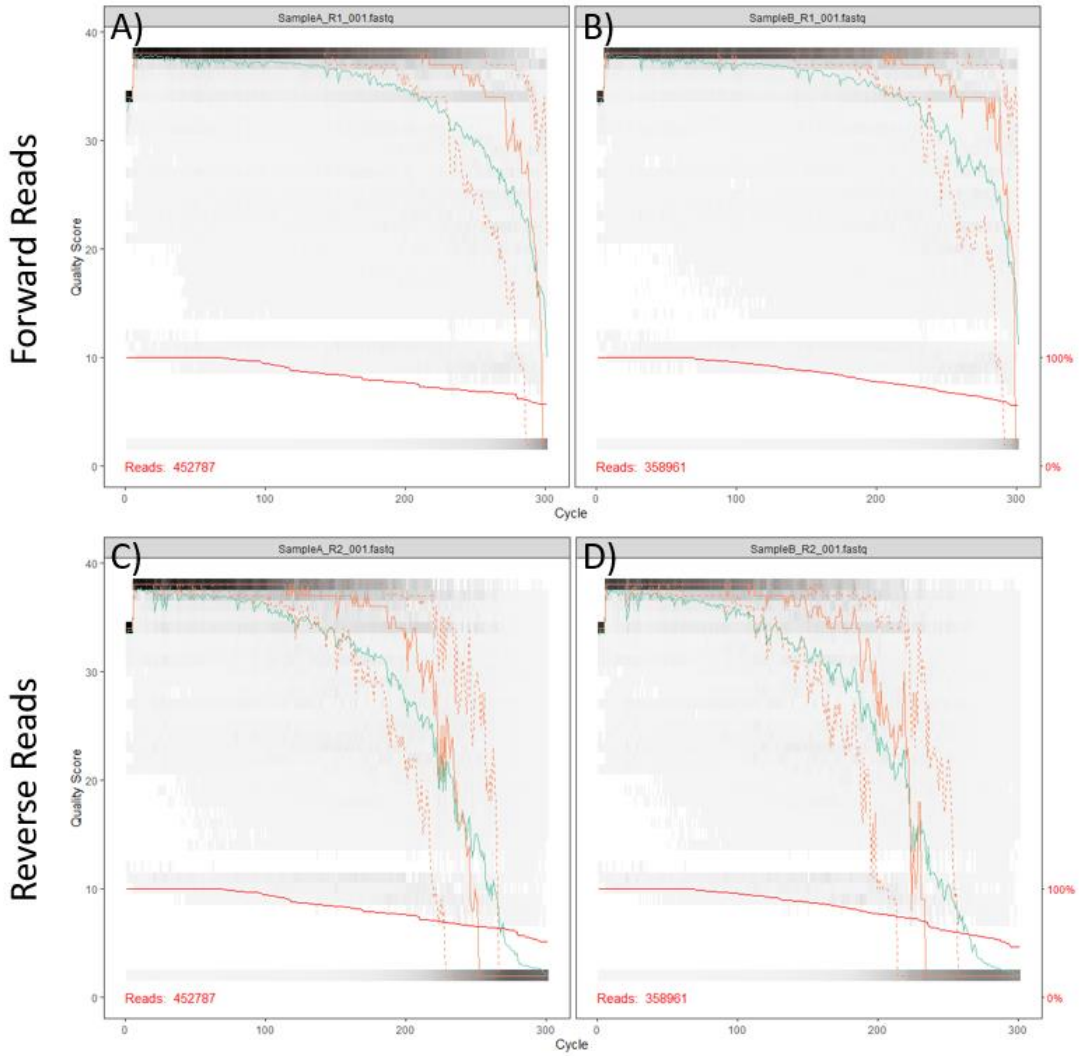

Figure 8: Quality scores for the forward reads of (A) sample 1 and (B) sample 2 as well as for the reverse reads of (C) sample 1 and (D) sample 2. The gray scale provides a heat map of the frequency of the quality score at that particular base position (with dark colors being equal to higher frequencies). The mean quality score is depicted in green with reference to each base position. The orange line grants the median quality score distribution with the lower quartile 25th percentile and upper quartile 75th percentile in dashed orange lines. The red line shows the proportion of reads that extend at least to that base position.

Unusual glycosylation sites on the complimentary determining regions of the immunoglobulin presented by follicular lymphoma B cells have been broadly documented as a feature of this subset of lymphoma. To produce an engineered cell line which expresses an established FL-derived antibody sequence, we conducted next generation deep sequencing (NGS) of the variable heavy and light chains presented from follicular lymphoma involved lymph node tissue sections. We confirmed 9931 unique sequence pairs (5228 unique to sample 1 among 216053 paired-reads and 4797 unique to sample 2 among 155596 paired-reads) of the variable domain amplicons from NGS results.

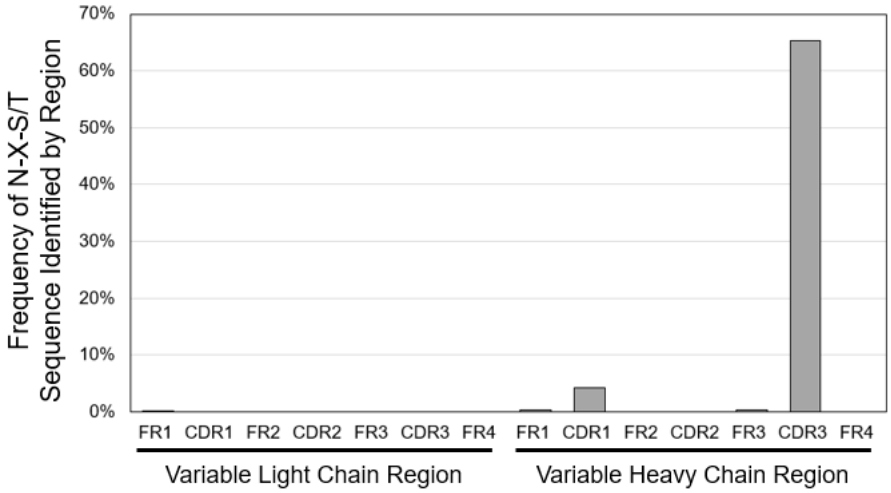

Figure 9: Frequency and region of glycosylation site sequences appeared in variable segments. Deep sequencing results of tissue sections from a follicular lymphoma involved lymph node were analyzed to detect the region and frequency of total reads possessing an N-glycosylation site sequence N-X-S/T (where X is not Proline) indicating that the B cells present in the section had preferential glycosylation of the CDR3 region.

Examination of the amplicons by IMGT/HighV-QUEST revealed 3225 recombination to be dynamic which were scattered as 1798 heavy chain V-D-J recombinations, 1420 lambda light chain V-J recombinations, and only 7 kappa light chain V-J recombinations. While in normal reactive lymphoid populations there is a mixture of kappa vs lambda light chains, we expected our observed lambda light chain is dominant within the population since light chain restriction is a common feature of lymphomas (25). Alignment and translation by IMGT/HighV-QUEST[26-29] presented 260 unique variable heavy chain and 792 unique variable light chain domain among which 174 heavy chains and 1 light chain possessed the consensus N-X-S/T glycosylation sequence. Since the distance created by proline between the acceptor asparagine and that of the hydroxyl of serine or threonine is too far in the glycosylation machinery, N-linked glycosylation

does not typically develop when the X residue is a proline and as such those sequences retaining an N-P-S/T sequence were not assessed glycosylation sequences in our analysis (30). From Figure 9, predominant distribution of these glycosylation sequences were located at CDR3 and to a lesser extent at CDR1 of the heavy chain. This accords with recent studies of abnormal glycosylation sites detected on the antibodies of follicular lymphoma B cells (9).

Multiple sequence alignment was implemented by using MAFFT (multiple alignment using fast Fourier transform) for the heavy chain and lambda light chain variable domains and the sequence pattern of the clones existing in the follicular lymphoma B cells are depicted in Figure 10 as a sequence logo. The consensus heavy chain clonotype was found to be derived from the IGH V3-23 germline whereas that of the lambda light chains were derived from IGL V1-47. Significantly, an N-D-S glycosylation site at the heavy chain CDR3 was highly conserved, where studies have demonstrated such aberrant glycosylation sites at the CDR to be hallmark of follicular lymphoma.

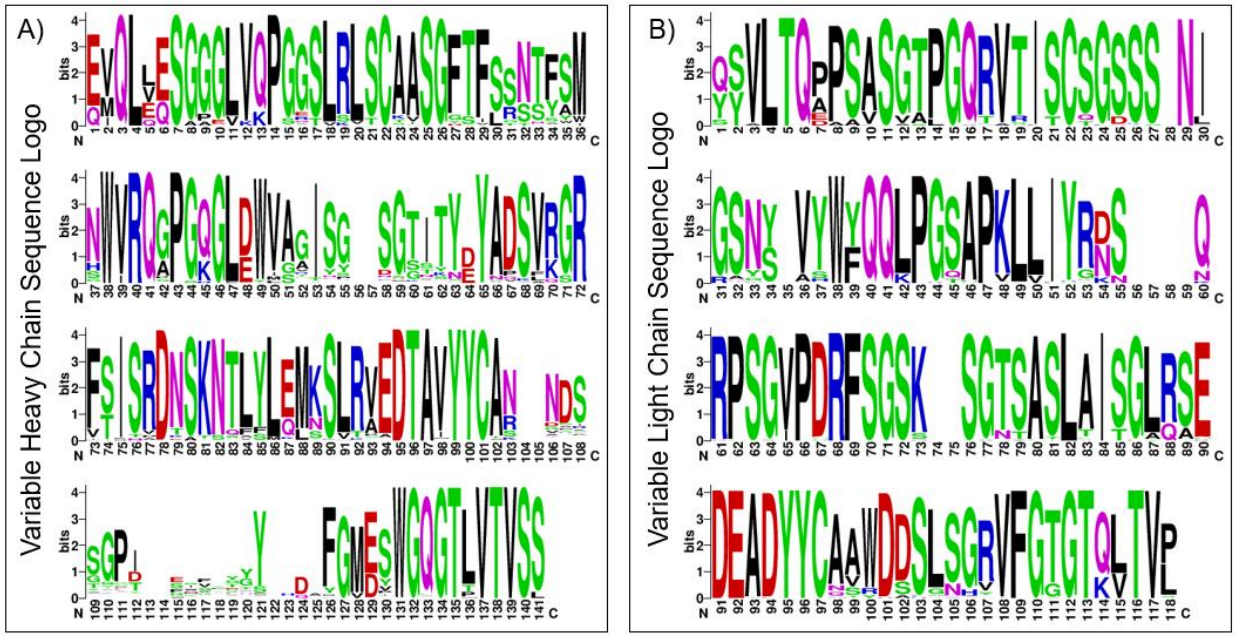

Figure 10: Sequence logo of the variable heavy and lambda light chains. Multiple sequence alignment of the amplicons was analyzed and translated by IMGT/HighV-QUEST and provided the consensus sequences of amino acids for (A) the variable heavy chain and (B) the variable lambda light chain where predominently the N-D-S glycosylation site is found in CDR3 of the variable heavy chain.

The heavy chain variable domain consensus sequence (E-V-Q-L-L-E-S-G-G-G-L-V-Q-P-G-G-S-L-R-L-S-C-A-A-S-G-F-T-F-N-T-F-S-M-N-W-V-R-Q-G-P-G-Q-G-L-D-W-V-A-G-I-S-G-S-G-T-I-T-Y-Y-A-D-S-V-R-G-R-F-S-I-S-R-D-N-S-K-N-T-L-Y-L-E-M-K-S-L-R-V-E-D-T-A-V-Y-

Y-C-A-N-**N-D-S**-S-G-P-I-Y-F-E-S-W-G-Q-G-T-L-V-T-V-S-S) possessing the glycosylation site within the CDR3 and the lambda light chain variable domain consensus sequence (Q-S-V-L-T-Q-P-P-S-A-S-G-T-P-G-Q-R-V-T-I-S-C-S-G-S-S-S-N-I-G-S-N-Y-V-Y-W-F-Q-Q-L-P-G-S-A-P-K-L-L-I-Y-R-D-S-Q-R-P-S-G-V-P-D-R-F-S-G-S-K-S-G-T-S-A-S-L-A-I-S-G-L-R-S-E-D-E-A-D-Y-Y-C-A-A-W-D-D-S-L-S-G-R-V-F-G-T-G-T-Q-L-T-V-L) were found to be in agreement among the clonotypes having among the most abundant reads for the heavy and light chains variable domains. These sequences were used to construct an antibody expression system to display the FL B cell derived variable domains on the membrane bound surface IgM for a novel engineered cell line.

2.3.2) Confirmation of engineered cell line stably expressing surface IgM derived from FL B cell. After construction of the expression vectors for the IgM heavy chain possessing a transmembrane domain and for the Ig lambda light chain, HEK293T cells were transfected followed by antibiotic selection. The given amount of antibiotics (blasticidin and zeocin) above the kill curve threshold for HEK293 were used for isolation of clones facilitating the successful selection of an engineered cell line (which we refer to as the BZ cell line) that provided stable expression of surface IgM. Expression of the heavy chain and light chain was confirmed by western blot as seen in Figure 11.

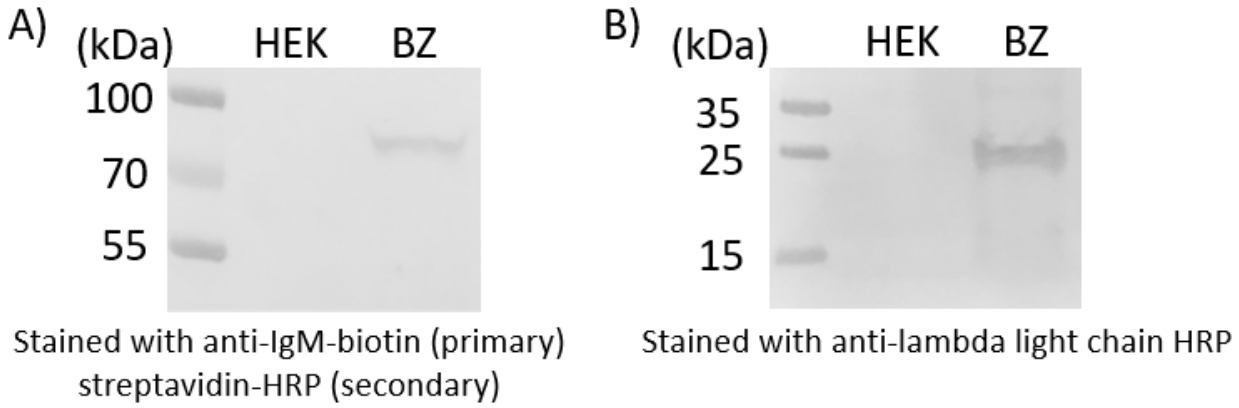

Figure 11: Immunoblotting of the engineered BZ and HEK background cell lysates resolved by SDS-PAGE. (A) Heavy chain anti-IgM staining and (B) light chain anti-lambda staining of the cell lysates from the engineered BZ cell line and the HEK background. BZ cell lysate reveals expression of IgM heavy chain and lambda light chain for the BZ engineered cell line but not detected for the HEK background. The light chain band appears at ~25kDa which is the expected size for the unglycoyslated light chain, whereas the heavy chain reveals larger than the unglycosylated molecular weight of ~66kDa proving that the heavy chain has indeed been glycosylated.

The expected size of the IgM heavy chain bearing transmembrane domain and the FL B cell derived variable domain consensus sequence was expected to have an unglycosylated molecular weight of ~66kDa while the lambda light chain was expected to have an unglycosylated molecular weight of ~25kDa. A band size for the heavy chain larger than 66kDa was seen by immunoblotting suggesting the IgM heavy chain was indeed glycosylated. In contrast, immunoblotting indicated the expected size for an unglycosylated light chain. The anti-IgM and anti-lambda bands in the immunoblotting were only observed for the case of the engineered BZ cell lysate and not for the HEK lysate control. This observation explains that the HEK background did not previously possess any cross-reactive proteins, and further confirms the expression of the full length heavy chain and lambda light chain in engineered BZ cell line.

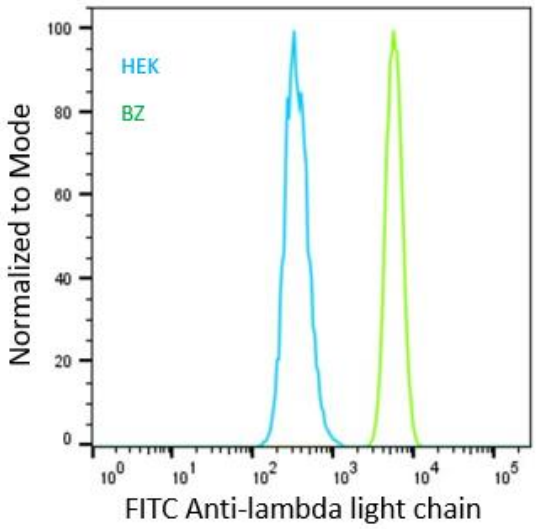

Figure 12: FACS analysis of HEK and BZ cell lines after incubation with FITC labeled anti-lambda light chain probe. The results show the BZ cells are positive for the display of surface antibody recognized by the FITC labeled anti-lambda light chain probe.

2.3.3) Examination for oligomannosylation of antibodies presented by the engineered BZ cells.

Here we investigated if the glycosylation site on antibody presented by our BZ cell line would result in the display of unusual high oligomannose as is observed on the surface antibodies of follicular lymphoma B cells. To confirm it, we conducted a series of high mannose specific glycosidase assays followed by western blot developing for the heavy and light chains. As shown in Figure 13, the assays using the BZ lysate revealed the appearance of unique band shifts compared to the untreated BZ lysate. This shift corresponds to the removing of glycans by the distinct glycosidases implemented in the assays. EndoH and Mannosidase enzymes have specificity in digesting that they only cut away glycans terminating in high oligomannose. This

allowed us to analyze immunoblotting results that high oligomannose was indeed presented by the heavy chain as observable by the band shifts. In contrast, the light chain showed no band shift suggesting no high oligomannosylation. It was expected to be given our knowledge of the location of the glycosylation site at the CDR3 of the heavy chain. No such glycosylation site was present in the light chain of the engineered BZ cell line and this is consistent with the immunoblotting results since either with or without EndoH glycosidase treatment the light chain band remains at the expected molecular weight of 25kDa.

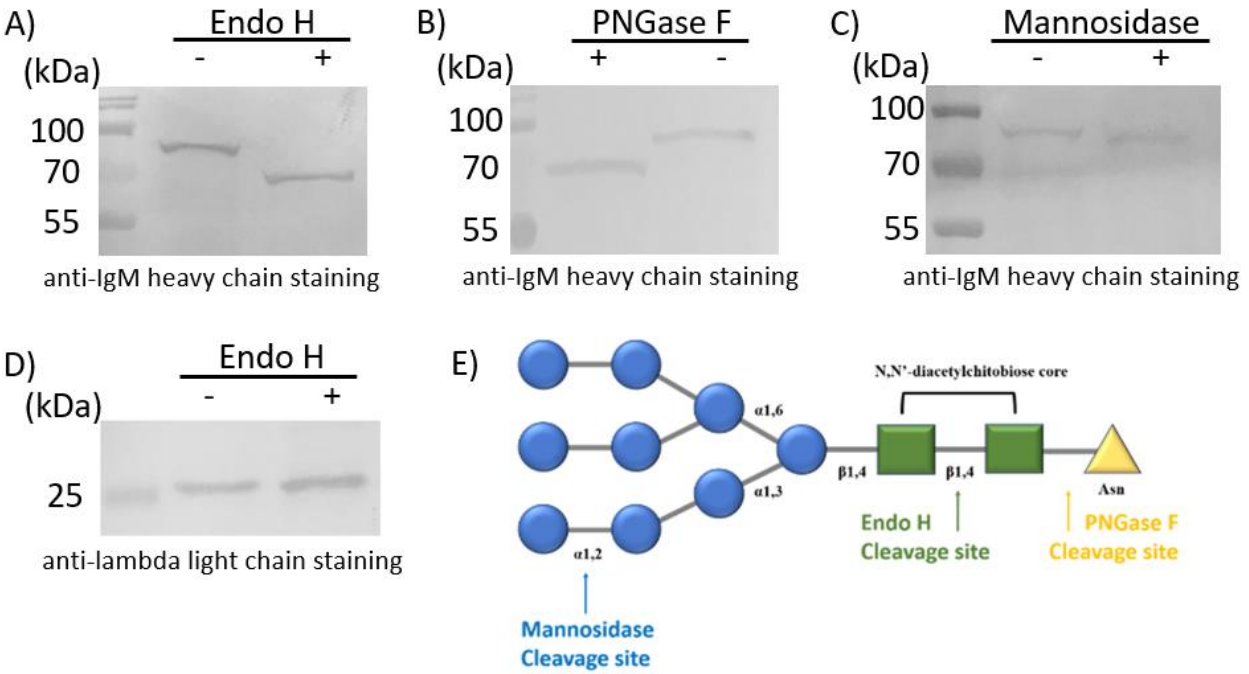

Figure 13: Immunoblotting of glycosidase assay. Cell lysates from engineered BZ cells were used for glycosidase assays using (A and D) EndoH, (B) PNGase F, or (C) Mannosidase and resolved by SDS-PAGE. Immunoblotting of the transferred each enzyme reactant and staining with (A, B, and C) anti-IgM heavy chain (primary) or (D) anti-lambda light chain (primary) revealed a shift in the size of the heavy chain caused by cleavage of the glycan while the size of light chain band was unchanged. A smaller band shift for cleavage by Mannosidase relative to EndoH or PNGase F is expected based on (E) the location of the cleavage sites in an oligomannose branch.

A predicted decrease in the molecular weight of the heavy chain after enzyme treatment was observed based on the specificity of the glycosidase to which it was exposed. For example, the EndoH cuts almost the entirety of high mannose glycan away by cleaving at the chitobiose core, thus showing a large decrease in the molecular weight of the IgM toward the expected

unglycoyslated size of ~66kDa. PNGase F will cleave the entire glycan, and it recognizes and cleaves between the innermost GlcNAc and asparagine residues of not only high mannose glycans but of all N-linked glycoproteins. As such PNGase F treatment showed the IgM size to again decrease to ~66kDa demonstrating the release of the N-linked glycan. In contrast, Mannosidase trims only the terminal mannose residues within high oligomannose and thus displayed a much lesser decrease in the molecular weight of the IgM as compared to the other glycosidases. The results validated that the surface IgM could be displayed on the engineered BZ cell line with the high oligomannose glycosylation as is presented by follicular lymphoma B cells where the variable segments had originated.

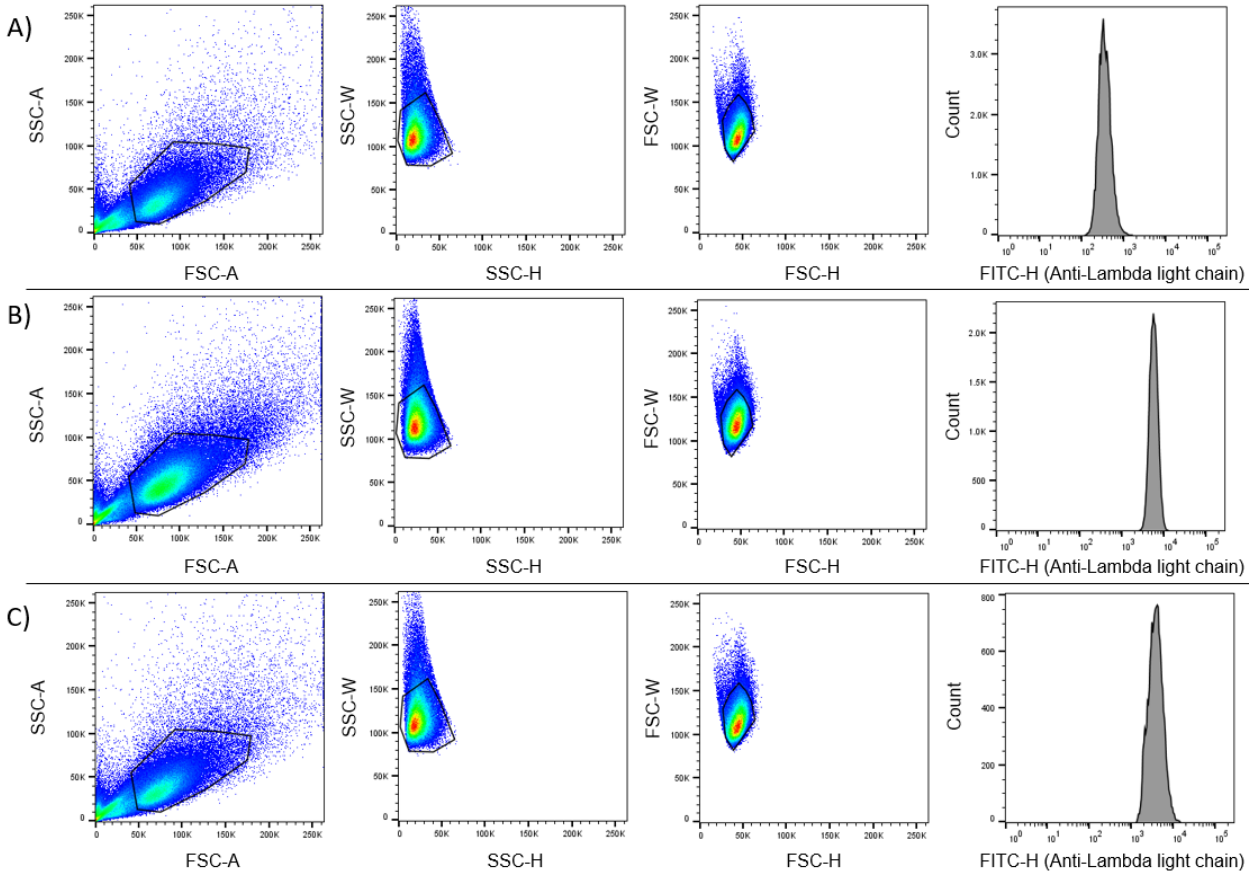

Figure 14: Gating strategy for cells exposed to FITC labeled anti-lambda light chain probe. Representative flow cytometry dot plots illustrate the gating strategy for examination of the presence of antibody on A) HEK293 cells, B) BZ cells, and C) BZ-mCherry cells. The results validate the BZ and BZ-mCherry cells are positive for the expression of surface antibody recognized by the FITC labeled anti-lambda light chain probe.

2.4) Discussion and Conclusion

It has recently been shown that oligomannose presented on the CDR of the immunoglobulin of follicular lymphoma B cells is a necessary characteristic for their survival, since it is this oligomannosylation that facilitates continual stimulatory interactions via the endogenous lectins in the surrounding tumor microenvironment(3,4). As an inherent result of this dependency, it has been historically difficult to examine isolated patient derived follicular lymphoma cells in vitro for any extended period of time and similarly is has been difficult to arrive at a realistic follicular lymphoma cell line (18,19). Here we worked toward the development of a reporter cell line that displays this characteristic high oligomannosylated surface antibody in the manner as presented by follicular lymphoma B cells via membrane bound immunoglobulins. As of yet there is a lack of oligomannose specific technologies and as such it is not yet possible to selectively target this biomarker, thus the intention of this work is to provide a possible tool for future development of suitable targeting moieties that could selectively bind the displayed oligomannose in order to facilitate targeted diagnostics. Similarly, such a targeting moiety would be useful for therapeutics that invoke disruption of the aforementioned lectin-oligomannose interactions. Initially, we pursue in this project the deep sequencing of the Ig variable regions of FL involved lymph node sections, where we identified a conserved glycosylation site presented at the third complementarity determining region (CDR3) of the variable heavy chain. Identification of a consensus variable heavy chain among the B lymphocyte showed there to be significant drift from the germline unlike other sequences found within the node indicating it had undergone significant somatic hypermutation. The sample was also found to be lambda light chain restricted and among the lambda light chains also exhibited a clear predominance for a consensus sequence. Using the consensus heavy and light chain variable sequences identified from the follicular lymphoma B cell sample, we genetically engineered a set of mammalian expression vectors incorporating the identified variable heavy and light chain sequences within a surface IgM and lambda IgL construct, respectively. Blasticidin and zeocin resistance within the heavy and light chain expression constructs, respectively, allowed us to carry out antibiotic selection of the transfected HEK cells and after continual growth we were able to isolate cell lines with stably integrated heavy and light chain constructs. The cell line was found to be very stable with no loss of expression or display of the IgM heavy chain or lambda light chain. Examination of the cells to determine if oligomannose was being presented by our engineered cell line was carried out using a series of glycosidase assays.

Specifically, we utilized Endoglycosidase H (Endo H) in order to cleave the internal GlcNAc core of high mannose structures, and we also made use of Mannosidase in order to trim only external mannose residues. These enzymatic assays were implemented in conjunction with Western blot analaysis in order to confirm the presence of high oligomannose terminating glycans presented by the antibody on the engineered BZ cell line. During the course of our study, we identified no oligomannose display by the lambda light chain. This was to be expected given the lack of any glycosylation site seqence at the variable lambda CDRs. In contrast, we did find oligomannose to be displayed on the FL B cell derived IgM heavy chain which we also expected given that a glycosylation sequences site was found at the CDRs of the variable heavy chain sequence. From our glycosidase assays, we confirmed the presence of high oligomannose, since the Endo H enzyme selectively cleaves high mannose terminating glycans, and immunoblotting revealed a corresponding large decrease in the size of the IgM after Endo H treatment. A slightly larger size shift was revealed for the use of PNGase F which is not high mannose specific but will more broadly cleave almost all N linked glycans. The fully deglycosylated heavy chain bands observed after PNGase F treatment were found to be in direct agreement with the expected unglycosylated molecular weight. The display of high oligomannose by the heavy chain was further validated by use of a third glycosidase assay using Mannosidase which has exoglycosidase specificity for only the terminal mannose residues. It is important to see that the Mannosidase treatment resulted in a much smaller decrease in the molecular weight observed for the heavy chain band as compared to that observed after EndoH treatment. This small shift was representative of the trimming of only the external mannose residues of high oligomannose that was presented on the IgM heavy chain. In addition, this decreased size after treatment with Mannosidase alone confirms the presence of the high oligomannose, but more importantly the smaller size shift relative to the band size found after cutting the entire glycan at the core GalNAc residues with EndoH and PNGase F suggests that the Mannosidase was indeed specific in trimming only the mannose from the high oligomannosylated IgM.

Chapter 3: Investigating Oligomannose-Specific Receptors

3.1) Introduction

The identification of molecular recognition elements for target oligomannose is approached from both an evolutionary screening approach to identify novel receptors as well as making use of naturally evolved receptors. In our evolutionary screening process, we utilized phage display as the screening modality to examine if we could identify a peptide based moiety with specificity for oligomannose. Phage display is a process which makes use of large libraries of bacteriophage (typically around 10^9 phage) each with a different receptor on their p3 tail coat protein. The power of the phage display process in combinatorial screening of potential receptors to bind with the oligomannose target of interest lies in the direct coupling of the genotype and phenotype in the small package of a bacteriophage virion. That is to say the instructional genetic information that can be easily utilized for selective amplification and determined from sequence analysis is in the same package that is decorated with a receptor that is possibly selective for binding a designated target. By introducing the library to a target of oligomannose coated beads, for instance, we aimed to identify only those phage that could remain stuck to the oligomannose beads while removing all other phage that could not bind. In doing so we could selectively capture only the phage which possessed receptors capable of binding to oligomannose. A receptor in this case is indicative of what is displayed by the phage, hence the name "phage display", and in the case of this work that library of receptors is a short sequence of 12 amino acids (referred to as a peptide). Selective amplification of only those phage that possess peptide based receptors capable of binding the target is provided by simple washing steps followed by transfection into *E. coli* with subsequent rounds conducted of "surviving" phage under more stringent binding conditions until a consensus sequence is identified. In addition to evolutionary screening, the examination of existing receptors with reported affinity for oligomannose were investigated, specifically with the lectins VIPL, GNA, and PFA as well as the antibody 2G12. In looking at the lectins we examined with reported oligomannose binding capabilities, VIPL represents a human L-type lectin which requires calcium for selective recognition of the trimannose unit in the D1 branch of oligomannose. Any glucosylation or mannose trimming of the D1 branch significantly weakens the affinity of VIPL binding while D2 and D3 trimming is well tolerated. The lectin GNA (*Galanthus nivalis* agglutinin) is a tertrameric protein with three carbohydrate binding motifs in each monomer with

specificity to Man alpha1,3 Man containing oligosaccharides, and has been reported to prevent the binding of HIV virions to DC-SIGN receptor by masking the oligomannosylated gp120 of HIV to block entry into dendritic cells(38). The lectin PFA (*Pseudomonas fluorescens* agglutinin) described extensively above has a further level of selectivity for oligomannose in reportedly recognizing not only the Man alpha(1-3) Man branch point but also the Man alpha(1-6) Man unit which resides at the core of oligomannose. Similarly the ability of the PFA lectin to bind oligomannose has also been recently exploited for inactivation of HIV transmission(28). In addition to lectin, antibodies with affinity for oligomannose have recently been identified. Reports of oligomannose specific antibodies in the sera of patients with high grade prostate cancer have been reported but none isolated. In contrast, an antibody discovered from a patient with HIV revealed high affinity for oligomannose and the sequence and structure have been well characterized. This antibody referred to as 2G12 is discussed in detail above but in brief it possess affinity for the Man alpha1-2 Man epitope of the D1 arm of oligomannose with particularly high affinity facilitated by its unique antibody architecture in which a heavy domain swap enable a high surface area abounding with acidic groups at the recognition site for oligomannose with reported nanomolar affinity (39).

Glycans have traditionally been complicated to study as their structural complexity allowing sugar building blocks to be linked at different sites and with different stereochemistries goes beyond the relatively simple linear template-driven synthesis of nucleic acids and proteins [1]. While the difficulty in their analysis, detection, and even synthesis continues, the key roles of glycans have become apparent within the full spectrum of biological processes and are a distinct requirement for life [2–4]. Tools for genetic and proteomic level testing are abundant but we have yet to possess sufficient glycan-related diagnostic tools that may be integrated into standard practice. Because of this bias in attention, there remains a lot to be understood regarding glycans in terms of not only basic science but also from the perspective of clinical diagnostics and is thus deserving of special consideration [5]. The objective of the following study is to assess a biotin mimetic peptide fusion to a well-known lectin as a proof-of-concept oligosaccharide probe that may be utilized with a variety of common clinical assay formats. Traditional glycan analysis techniques include chromatographic analysis of metabolically radio-labeled glycans, as well as capture with lectin affinity chromatography, and glycosidase treatment for chemical analysis of the constituent sugars [6–8]. Other techniques have included the use of sequential exoglycosidase

digestion coupled with methylation analysis utilizing chromatography, mass spectroscopy, and ^{1}H NMR [9–11]. Current analytical strategies for examining protein glycosylation include enrichment techniques prior to mass spectroscopy methods, where lectin chromatography [12,13] as well as chemical techniques, including the use of boronic acid [14] and hydrazide chemistry [15], have been applied to enrich glycoproteins. Enzymatic removal can facilitate the isolation of the glycans alone, which can have even more difficulty in separation as glycans have poor adsorption to reverse phase high performance liquid chromatography (HPLC) matrices. Glycan separation by HPLC thus requires derivatization by reductive amination [16], but this can be a source of artifacts [17]. A range of other options for glycan (either free or labeled) separation include capillary electrophoresis, tandem anion-exchange, porous graphitic carbon liquid chromatography, and hydrophilic interaction chromatography [4]. Assuming effective separation, analysis of which glycan structures are present requires the examination of mass spectral data or chromatographic/electromigratory assessment of the retention times given a definitive set of reference glycans. Since these aforementioned techniques are time consuming approaches, require multiple steps, and necessitate a high level of expertise, there have been recent groundbreaking works to simplify glycan analysis which have made the use of lectin-based arrays [18]. Lectins are natural glycan receptors that exist with specific recognition for a number of different glycan structures, and the use of lectin-based arrays as sensing modalities have been found to expedite the examination of protein glycosylation to under 6 hours [19]. Still, the number of possible combinations of glycans which exist far outweigh the number of currently known lectins for specific glycan structures, and as such lectin arrays must utilize classification techniques based on "fingerprinting" of glycan interactions with an array containing lectins with relatively broad specificities. An example includes an array of 24 plant lectins with overlapping specificities [18]. While individual lectins may have some promiscuity in their binding [20], the fact that an individual glycan can provide a unique fingerprint across the array still holds value in the analysis. Growing research efforts to identify and examine new lectins with distinct specificities as well as novel assay approaches utilizing lectins is still in demand, and with that we were motivated to pursue this research.

Serum level changes in glycan profiles as well as isolation of glycoproteins with irregular glycan structures have proven to be a distinguishing characteristic between cancer vs. control patients for a range of malignancies [21]. One form of irregular glycosylation type is high-mannose-type

glycans displayed on viruses (one such glycan is Man_9), including HIV and rotavirus [22], but also on the immunoglobulin of certain B cell lymphomas [23]. In addition to being displayed on subsets of B cell lymphomas, high-mannose-type glycans represent an interesting glycan-based biomarker found on a number of other cancer cells including the surface of human lung adenocarcinoma, colorectal cancer, as well as on the epidermal growth factor receptor of epidermoid carcinoma and gastric cancer cell lines [24]. In the context of healthy mammalian systems, mannose units are not a typical terminating moiety but rather are masked by other sugar moieties capped onto the end of mannose units after trimming [25]. This trimming of natural high mannose occurs as Man_9 is formed briefly and cleaved to Man_5 by mannosidases within the ER/early Golgi serving as the precursor internal core of more mature glycans [26]. Aberrant display of high mannose along the secretory pathway is handled by intracellular human lectins (like OS-9) that traffic such glycoproteins for proteasomal degradation by the ERAD (endoplasmic reticulum associated degradation) pathway [27]. Extracellular human C-type lectins, such as DC-SIGN (dendritic cell specific intercellular adhesion molecule-3 grabbing non-integrin) and MBL (mannose binding lectin), can bind aberrant oligomannosylation, requiring a calcium ion for coordination with the glycan, to facilitate their removal [28]. It has been reported that monosaccharide fucose units can also coordinate with the calcium ion in DC-SIGN and even manifest interaction with α1−α2 linked fucose as presented by histo blood group antigens, highlighting a prime example of the cross-specificity or promiscuity that exists in many lectins [29,30]. There are also several plant and microbe derived lectins that recognize oligomannose units in a calcium independent manner including *Pseudomonas fluorescens agglutinin* (PFA), which is a member of the *Oscillatoria agardhii agglutinin* homologue family of lectins capable of recognizing the Man alpha(1-3)-Man alpha(1-6)-Man core [31] present on high mannose and hybrid type glycans. Because PFA lectin has been found to recognize this core branch point, it provides broader selectivity for Man_6 to Man_9 variants as compared to other lectins [32,33]. This reported promiscuity for $Man_5GlcNAc_2$, $Man_6GlcNAc_2$, $Man_7GlcNAc_2$, $Man_8GlcNAc_2$, and $Man_9GlcNAc_2$ highlights that a single lectin may not be sufficient to distinguish glycan structure. Because these structural variants are all displayed by the HIV coat protein gp120 [34], the PFA lectins ability to bind the Man alpha(1-3)-Man alpha(1-6)-Man core has recently been exploited for inactivation of HIV transmission but has yet to be used as a sensing moiety [35].

3.2) Materials and Methods

For phage display experiments we utilized a 12mer linear peptide library comprising 10^9 distinct sequences as presented on the p3 coat protein of M13 bacteriophage. The library was commercially available as the PhD 12 Phage Display Kit from New England Biolabs and protocols followed were based on that provided by the manufacturer. The target utilized for our experiments was that of a biotinylated soy bean agglutinin which is known to possess oligomannose and was immobilized onto streptavidin magnetic beads for capture of M13 phage bound to the target. After incubating the library of phage with the target, the phage were washed to remove non-specific phage that would not interact with the target oligomannose. After washing the beads thoroughly, we could specifically elute only those phage from the beads that would have been bound to the oligomannose target by introduction of the GNA lectin which we had proved was capable of binding to the oligomannose of soy bean agglutinin. In doing so, the binding of GNA would displace the phage to elute them for isolation and amplification in *E. coli K12*. The amplification proceeded through 6 hour incubation with OD 0.4 E. coli K12 followed by centrifugation to remove all bacteria and retaining the supernatant containing the amplified numbers of virion clones based on the original phage eluate. To the supernatant was added PEG/NaCl for precipitation of the phage after 1hour incubation at 4°C and pelleting by centrifugation. The resulting phage represent the second round of input phage for rescreening against the target oligomannose which is conducted with the addition of higher

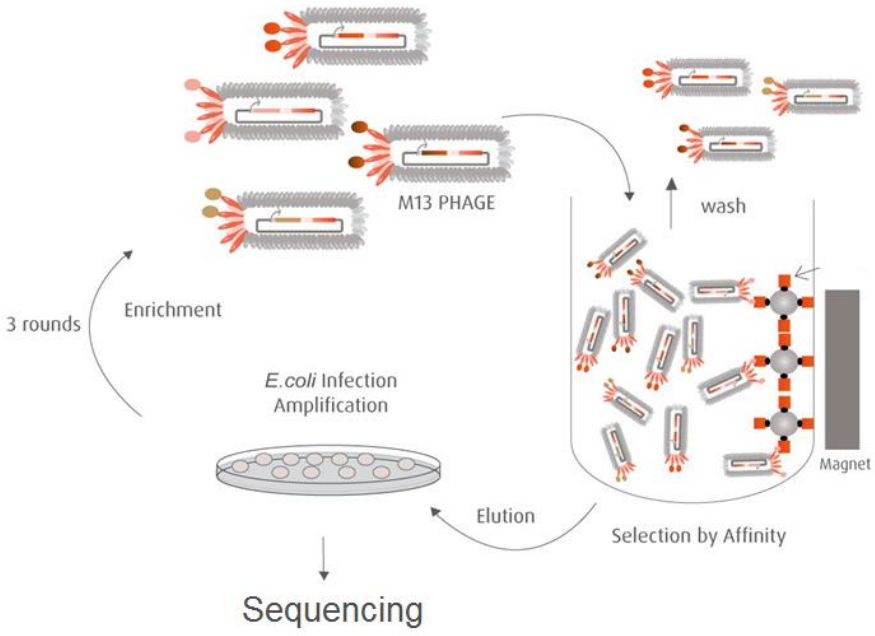

Figure 15: Schematic of phage display process in which library of M13 bacteriophage are introduced to suspension of magnetic beads possessing oligomannosylated target followed by washing away of non-specific binder and competitive elution for sequencing and amplification for additional rounds of selection.

concentrations of Tween 20 in the binding and washing buffers. After 3 rounds of screening the sequences of the resulting peptide-based receptors displayed by the phage were identified by PCR of the p3 region followed by Sanger sequencing. Phage ELISA was conducted to determine the affinity of the identified phage for the oligomannose target.

For production of reported oligomannose binding lectins and antibodies, pET14B bacterial expression vectors and pFUSE mammalian expression vectors were used respectively. PFA and VIPL were cloned into the pET14 vector for IPTG inducible expression within the BL21 DE3 expression system. Growth at room temperature in LB media proceeded until an optical density of 0.3 at which point cultures were place at 16^{o}C for 30 minutes followed by induction with IPTG and overnight growth at 16^{o}C. After collection of the cell pellet, lysis buffer was added followed by rocking incubation for 30 minutes on ice and then 10 minutes of probe sonication on ice (programmed at 1 second on and 1 second off at 60% power in 1 minute intervals). The lysate was centrifuged at 16,000 rpm for 1 hour and the supernatant was filtered prior to undergoing Nickel affinity chromatography at 1mL / min flow rate at 4^{o}C. After binding to the Ni column, the sample was washed for 1 hour and then subjected to an increasing gradient of imidazole for release from the column. The eluted fractions were assessed by SDS PAGE and fractions containing the pure protein of interest were pooled and dialyzed into the appropriate storage buffer. Initial testing of 2G12 proceeded with procured samples while we are currently in the process of cloning the 2G12 variable heavy domain into IgG_3.

To provide the source of materials in this study, gBlocks were obtained from Integrated DNA Technologies for cloning of the PFA fusion protein. The oligomannose bearing gp120 was purchased from Sigma Aldrich and confirmed for the presence of oligomannose using known commercial probes capable of binding to oligomannose (Figure 16), specifically the anti-oligomannose antibody 2G12 obtained from Polymun and the Man alpha(1-3)-Man binding lectin GNA (*galanthus nivalis agglutinin*) obtained from Vector Laboratories as well as fluorescein labeled GNA from the same source. In these validation assays, glycosidase treatment with Endo H (endoglycosidase H obtained from New England Biolabs) was used to remove oligomannose from glycoproteins by cleaving the chitobiose (GlcNAc2) core to confirm the specificity of the 2G12 and GNA for oligomannose. DC-SIGN/Fc (dendritic cell-specific intercellular adhesion molecule-3 grabbing non-integrin fused to fragment crystallizable domain) and DC-SIGNR/Fc (DC-SIGN related protein fused to fragment crystallizable domain) were purchased from R&D

Systems. Unless otherwise specified, all reagents used for cloning were obtained from New England Biolabs and all reagents used for expression, purification, and analysis were obtained from Sigma Aldrich.

For production of the engineered PFA lectin, a pET14b bacterial expression vectors was used. A custom double stranded DNA gBlock possessing the open reading from the PFA gene was purchase from Integrated DNA Technologies. The gBlock underwent PCR with the following primers to produce restriction sites of BamHI and NdeI for cloning into the pET14b expression vector: For PFA (CTAAACATATGATGTCCAAATACGCGGTCGCAAATCAATG); Rev PFA (GATTGGTTTTCGCGGACAGATTGAGTAGGGATCCATAACA). Generation of the engineering VSHPQAPF fusion to PFA was carried out by using the following primers: BiotinMim1 (CTGTGGGTGCGAGACCTCAATCTGTCCGCGAAAACC) and BiotinMim2 (ATACGGGATCCCTAAAAAGGTGCCTGTGGGTGCGAG). After confirmation of the clones and expression testing for IPTG inducible expression within the *E. coli* BL21 DE3 expression system, larger scale 1 L cultures were grown at room temperature in LB media proceeded until an optical density of 0.3 at which point cultures were placed at 16 °C for 30 minutes, followed by induction with IPTG (isopropyl thiogalacto pyranoside) and overnight growth at 16 °C. After collection of the cell pellet, lysis buffer was added followed by rocking incubation for 30 minutes on ice and then, 10 minutes of probe sonication on ice (programmed at 1 second on and 1 second off at 60% power in 1 minute intervals). The lysate was centrifuged at 16,000 rpm for 1 hour and the supernatant was filtered prior to undergoing nickel affinity chromatography at 1 mL/min flow rate at 4 °C. After binding to the Ni column, the sample was washed for 1 hour and then subjected to an increasing gradient of imidazole for release from the column. The eluted fractions were assessed by SDS PAGE (sodium dodecyl sulfate polyacrylamide gel electrophoresis) and fractions containing the pure protein of interest were pooled and dialyzed into the appropriate storage buffer.

Amine-reactive protein labeling kit (NT-647-NHS) was used for PFA labeling. Labeling buffer was prepared by adding 3 mL distilled water to labeling buffer salt (included in the kit). Zeba spin columns (included in the kit) were prepared according to manufacturer's protocol. Briefly, the bottom cap was removed, and upper cap was loosened followed by centrifugation at 1500 g for 1 minute to remove storage liquid. Column was equilibrated by washing with 300 µL of labeling buffer three times. Then, 125 µL of PFA solution was placed and buffer exchanged PFA was collected in a microcentrifuge tube after centrifugation at 1500 g for 2 minutes. NT-647 dye was

reconstituted by adding 30 µL of 100% DMSO (dimethyl sulfoxide) yielding approximately 470 µM and diluted further to achieve 11 µM. This concentration is about three times more than that of the PFA protein that was to be labeled (3.88 µM). Using 250 µL of PFA and NT-647 dye, each were mixed in a 1:1 volume ratio and incubated for 30 minutes at room temperature in the dark. During that time, a PD minitrap desalting column was prepared according to the manufacturer's manual. After equilibrating the column three times with PBS (1X phosphate buffered solution), 500 µL of labeling reaction was loaded to the center of desalting column followed by the addition of 600 µL of PBS. Finally, 100 to 150 µL fractions of the eluate were collected and measured for their concentration by Bradford assay where the final PFA-NT-647 concentration was 11 µg/mL, which was equivalent to 392 nM.

For competitive binding assays, a total of 100 µL of 1 mg/L gp120 was absorbed to 96-well immunoplates overnight at 4 °C and each well was washed with 300 µL of PBS once. The plate surface was blocked with 1% BSA (bovine serum albumin) in PBS (phosphate buffered solution) for 2 hours at room temperature with horizontal shaking at 50 rpm. After discarding the blocking solution, 100 µL of 400 nM PFA was added to the wells and incubate for 10 minutes with shaking. After PFA binding, 100 µL of 40 nM biotinylated GNA was directly added to the wells and incubated for 1 hour then each well was washed with 300 µL of washing buffer (1% BSA in 1X PBST (phosphate buffer solution containing tween-20). Then, 100 µL of 1 µg/mL streptavidin-HRP in washing buffer was added to each well and incubated for 30 minutes. After washing unbound streptavidin-HRP with 300 µL of washing buffer, 100 µL of TMB solution was added and the signal was recorded at 450 nm using an Epoch2 microplate spectrophotometer (BioTek Inc., Winooski, Vermont, USA) after 2 minutes development and stopping the TMB-peroxide reaction by adding 100 µL of 0.16 M sulfuric acid. To examine if PFA was binding to oligomannose, we carried out an experiment to see if the PFA would inhibit the GNA binding. This experiment was conducted as above but with the addition of 100 uL of 400 nM PFA (non-biotinylated) to the wells prior to addition of the biotinylated GNA. After confirming the ability of PFA to bind to the glycans of gp120, we utilized soluble mannose in another competitive binding assay wherein 100 µL of 1 mg/L gp120 was absorbed overnight to a 96-well immunoplate, incubated at4 °C, and each well was washed with 300 µL of PBS once. Again, the plate surface was blocked with 1% BSA in PBS for 2 hours at room temperature with horizontal shaking at 50 rpm. After discarding the blocking solution, 100 µL of 400 nM PFA was added to the wells, along

with 0–2000 mM soluble mannose directly added to the wells. After shaking and incubating for 1 hour, each well was washed with 300 µL of washing buffer (1% BSA in PBST) and again ELISA was carried out with 100 µL of TMB solution to observe the remaining PFA with the signal recorded at 450 nm using the Epoch2 microplate spectrophotometer (BioTek Inc.) after 10 minute development with the TMB-peroxide reaction was stopped by adding 100 µL of 0.16 M sulfuric acid.

As part of SDS-PAGE and Western-blot studies, proteins to be separated were treated as follows: 3 µL sample loading buffer (containing SDS, glycerol, Tris-HCl, β-mercaptoethanol, and bromophenol blue) was added to 9 µL of protein and the mixture was heated for 10 minutes at 95 °C to be denatured. The 12%/4% separating/stacking gel was made for electrophoresis. Samples were loaded onto the gel and run using SDS-PAGE running buffer (containing SDS and Tris-HCl, pH 8.3) for the first 30 minutes at 80 V, then an additional 1 hour at 120 V until maximally resolved. Separated protein was transferred to the nitrocellulose membrane using a Bio-Rad mini-trans blot system as follows: nitrocellulose membrane was presoaked in 1X transfer buffer (containing Tris-HCl, Glycine and methanol, pH 8.3) after assembling a blot sandwich, followed by wet blotting for 16 hours at 4 °C. The membrane was then blocked in 1% BSA 1X PBS overnight at 4 °C in a humid chamber. For staining, to identify the ability of PFA to serve in affinity to oligomannosylated proteins, we first conducted incubation of 12 µL of 10 µM PFA-HPQ (PFA bearing the VSHPQAPF fusion) with 4 µL of 1 mg/mL strep-HRP for 30 minutes at room temperature in 4 mL of washing buffer. These mixtures were then directly added to the blocked membrane for 1 hour at room temperature with shaking, followed by washing three times with washing buffer (containing 1% BSA and 0.5% Tween-20 in 1X PBS). The membrane was developed in 2 mL of 1X AEC solution (0.02% 3-amino-9-ethylcarbazole in N, N Dimethylformamide, 0.015% hydrogen peroxide in acetate buffer pH 5.5) for 20 minutes. An identical staining technique was used for DC-SIGNR/Fc and DC-SIGN/Fc primary using HRP conjugated anti-IgH as secondary. For the Western blot, samples of gp120 were added with or without prior glycosidase treatment. EndoH and a1-2,3,6 Mannosidase obtained from New England Biolabs were used for the gp120 samples in the right and left lane, respectively, using the manufactures recommended reaction conditions. After transfer to nitrocellulose membrane and blocking with BSA, staining was carried out as described above but using a 1:1 premix of strep-HRP and PFA-HPQ.

For bead-based agglutination assays, a total of 30 µL of 4 mg/mL streptavidin beads (streptavidin covalently coupled with <1 µm super paramagnetic particles) was suspended in 1 mL of binding buffer (20 mM Tris-HCl, 0.5 M NaCl, 1 mM EDTA pH 7.5). Coating of the beads with our engineered PFA bearing the VSHPQAPF fusion (termed PFA-HPQ for short as the HPQ motif is the widely found consensus region of streptavidin binder) was carried out with the addition of 5 µL of 435 µg/mL PFA-HPQ protein, followed by shaking at 80 rpm for 1 hour at room temperature. Beads were removed and washed with 1 mL of binding buffer three times using magnetic capture for isolation during washing. The beads were then blocked with 1 mL of blocking buffer (1% BSA in PBS) for 1 hour. The beads were then diluted with two volumes of washing buffer (0.5% Tween 20, 1% BSA, 1X PBS). Then, 100 µL of diluted beads were used for each group either with or without the incorporation of PFA-HPQ. After adding an additional 5 µL of either 100 µg/mL of gp120 as the oligomannosylated target or BSA as the target without oligomannose. Microscopy images (acquired using a Nikon Ti-2) of the samples were captured at zero minutes, 40 minutes, and 80 minutes to assess the extent of agglutination.

3.3) Results

Examination of the output sequences from our phage display process are seen below. In looking for a consensus among the result however we did not find any homology with only weak relation among sequences based on phylogenetic analysis. In addition, we examined each of these sequences by phage ELISA to determine if they had any specific binding capability to the oligomannose target; however, we found none of the clones to have any higher binding above baseline of our negative control indicating that our phage display results did not provide any candidate binders. In looking to move forward, we then examined the expression of existing oligomannose receptors that evolved naturally and that have been reported in literature, specifically lectins and the 2G12 antibody.

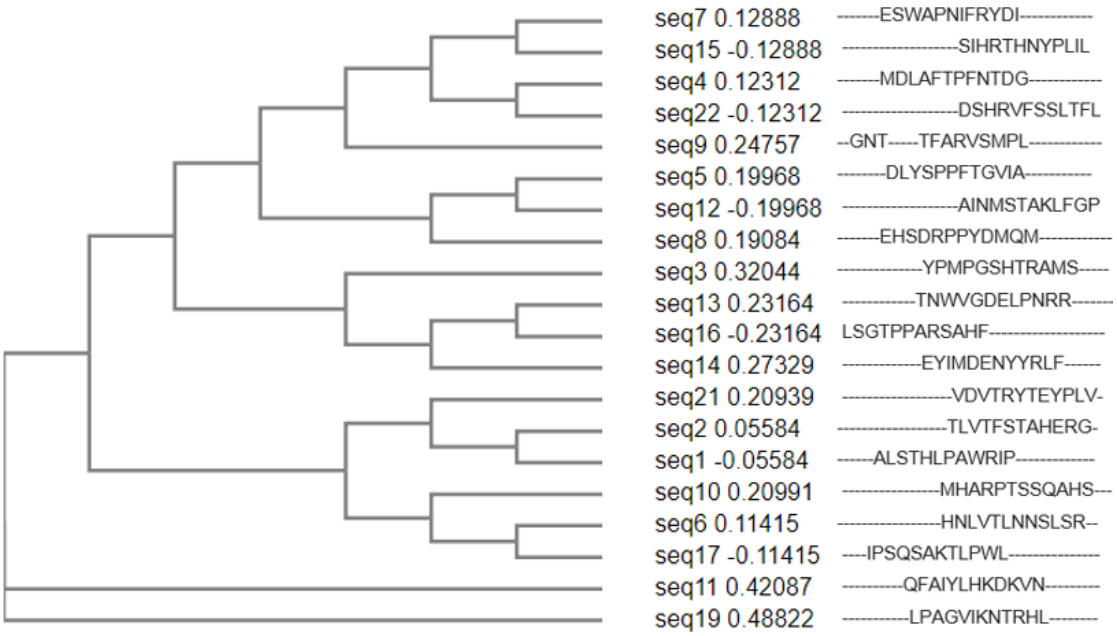

Figure 15: Tree showing evolutionary distance in identified phage display sequences after panning against oligomannose target showing no clear consensus across the observed sample space.

Examination of the commercially available 2G12 antibody and its ability to recognize oligomannose was also validated before moving on with exploring this as a possible receptor moiety for further diagnostic development. Specifically we confirmed that the 2G12 could indeed selectively recognize the oligomannose of gp120 by western blot. Confirmation of the reported ability of the 2G12 antibody to selectively recognize oligomannose also warranted further development of this antibody based receptor for use as part of a diagnostic tool for follicular lymphoma and as outlined in subsequent sections.

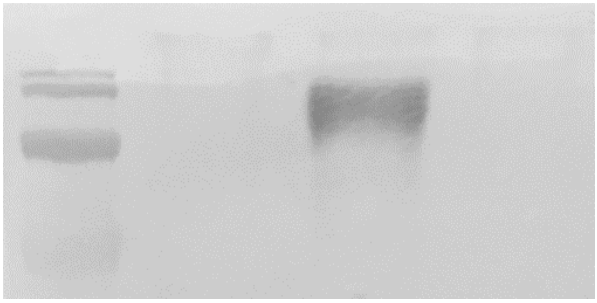

Figure 16: Western blot of gp120 using anti-oligomannose antibody 2G12 staining.

The first lectin we examine was VIPL which is a membrane protein that resides in the endoplasmic reticulum and is reported to have an affinity for oligomannose of around 40uM at pH 7 representing relatively weak binding(40) that may not have value as a diagnostic. Nonetheless, we examined how well we could express and purify the oligomannose binding cytoplasmic domain. Expression tests of VIPL revealed it to exist as an inclusion body with denaturing and refolding being unsuccessful in yielding the protein despite multiple attempts. Given the relatively weak affinity reported as compared to PFA we examined the expression of PFA which we found to be successful in yielding a large quantity of soluble protein.

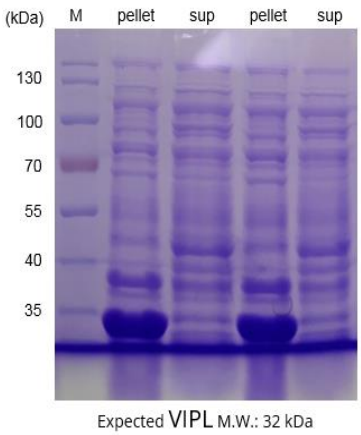

Figure 17: SDS-PAGE of expression test of VIPL in pET14 BL21 showing the formation of inclusion bodies.

Having more readily purified the lectin *Pseudomonas fluorescens* agglutinin, we examined its ability to bind to oligomannose as compared to GNA. From two 1 L cultures of *E. coli* BL21 DE3 harboring the pET14b expression vector, we obtained 8 fractions of different purity of the PFA, where the purest fractions E13 and E14 were combined and used for our studies yielding 14 mL of 435 µg/mL of PFA as determined by Bradford assay. Having purified the lectin *Pseudomonas fluorescens agglutinin* (Figure 18), we initially examined its ability to bind to the glycans of gp120

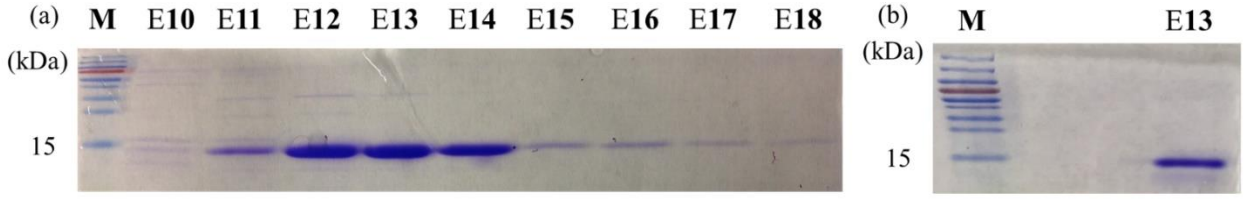

Figure 18: SDS-PAGE of PFA fractions after affinity chromatography (a) before and (b) after dialysis showing pure PFA protein isolated with expected molecular weight of 14kDa.

as compared to GNA (*Galanthus nivalis agglutinin*) which is known to bind glycans with (α-1,3)-linked mannose residues. We determined the GNA was capable of binding to the glycans presented by the HIV glycoprotein gp120, which we then used as one of two glycan bearing targets in this study (Figure 19a). A competitive binding assay was initially used to examine the ability of our PFA product to bind the glycans displayed on gp120. From Figure 19b, we can see that by pre-incubating the gp120 with PFA, we could significantly reduce the binding ability of the GNA which provided an indication that PFA could bind and mask a portion of glycan sites of the gp120. While we were not interested in confirming the exact specificity of the lectins given the likelihood

that GNA and PFA could have occupied different sites, (despite reports that these lectins both recognize the mannose branch point), we merely used the initial results to justify moving forward to conducted further binding assessment of the PFA. Examination of GNA also revealed it to bind the oligomannose target; however comparison of PFA and GNA binding ability by competitive elution revealed the PFA was able to displace GNA bound to oligomannose indicative of a higher affinity binding. We therefore examined PFA for its binding affinity by ELISA and microscale thermophoresis.

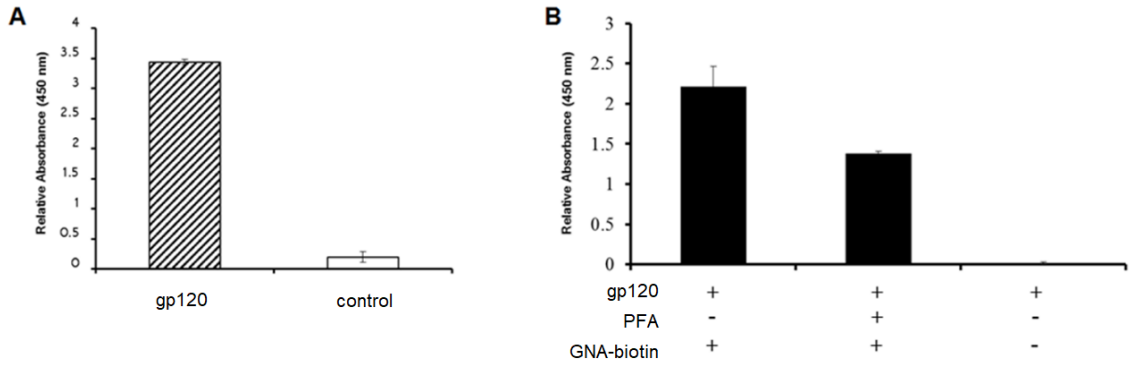

Figure 19: ELISA signals showing binding of (A) GNA (galanthus nivalis agglutinin) lectin to immobilized gp120 target and (B) competitive elution of GNA lectin when in the presence of PFA lectin.

In looking at the binding ability of PFA to oligomannose we examined if it could be competitively inhibited by mannose alone. We found that no inhibition to occur for PFA binding to oligomannose for physiologically relevant levels of added mannose which supports that PFA may hold value as a diagnostic tool in biologically relevant fluids. The use of free mannose to inhibit binding of PFA to oligomannose was not effective until at least 200mM of free mannose was added. Looking to assess the binding affinity of PFA we utilized known glycoproteins that possess high oligomannose as targets, for example gp120. Gp120 is the envelope glycyoprotein of HIV that displays oligomannose for binding to DC-SIGN for infection of dendritic cells. Examination of oligomannose binding by PFA using both ELISA and microscale thermophoresis reveal similar binding affinities of approximately 4nm. Such a strong affinity warranted us to explore this lectin as one of our lead recognition moieties for development in a diagnostic tool for the oligomannose presented by certain subsets of non-Hodgkin lymphoma.

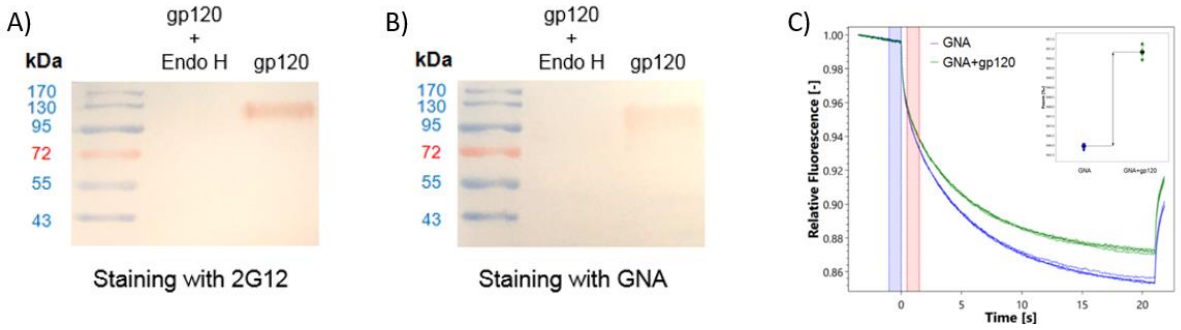

*Figure 20: Validation of gp120 display of oligomannose and binding of GNA to oligomannose by (**A**) western blot of gp120 with and without EndoH glycosidase treatment using the anti-oligomannose antibody (2G12) for staining or (**B**) using the lectin GNA for staining. (**C**) Microscale thermophoresis (MST) experiments using gp120 (208.5 nM) and fluorescein labeled GNA (20 nM) were carried confirm by the MST traces showing a distinct shift in the thermophoretic mobility of the GNA alone (blue) as compared to GNA with addition of gp120 (green) (inset showing the shift in normalized fluorescence based on the readings taken in the red column (hot) and blue column (cold) time frame representing after and before onset of the thermal gradient).*

In order to demonstrate if the PFA ability to recognize the glycans was displayed by gp120, wells coated with gp120 were exposed to PFA in the presence of increasing concentrations of soluble mannose. As seen if Figure 21, when labeling the remaining PFA with an enzymatic probe, the colorimetric signal remained consistent up to the condition of nearly 200 mM of free mannose. From this assessment of the binding ability of PFA to the glycans of gp120, we see that there was no significant inhibition by mannose in preventing PFA binding to oligomannose for physiologically relevant levels of added mannose, which supports that PFA may hold value as a diagnostic tool in biologically relevant fluids where free mannose would not exist beyond the 200 mM concentration needed to begin inhibit binding of PFA to the glycans of gp120.

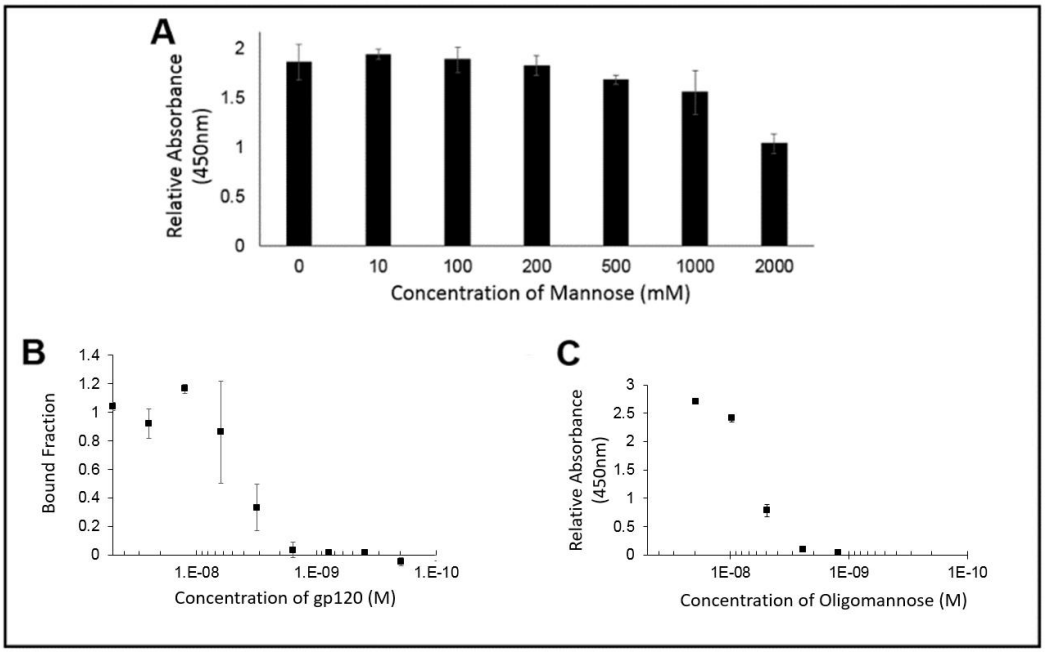

Figure 21: (A) ELISA signal of PFA against an immobilized gp120 target in the presence of increasing amount of soluble mannose showed no substantial inhibition in PFA binding until greater than 200 mM of soluble mannose was added; (B) Microscale thermophoresis and (C) ELISA of PFA against gp120 target showing similar binding constants, K_d ~4 nM.

To provide direct evidence for the ability of PFA to bind to glycans possessing the Man alpha(1-3)-Man alpha(1-6)-Man core unit, we utilized the technique of microscale thermophoresis for quantitative assessment of binding affinity. Having prepared the fluorescently labeled PFA possessing the NT-647 fluorophore and confirmed its labeling efficiency, we setup a series of experiments to first identify the relative extent of binding ability of PFA for gp120 to properly choose the dilution range for quantitative examination of the binding affinity of PFA for the Man alpha(1-3)-Man alpha(1-6)-Man bearing target. Using the NT-647 labeled PFA samples with or without gp120 in 0.1% PBST, we could see a clear shift in the thermophoretic mobility and thus, conducted a full serial dilution of the gp120 ligand concentration as shown in Figure 21. The measured decrease in the bound fraction with decreasing amounts of gp120 revealed an effective binding affinity of 4.1 ± 1.4 nM. To validate these results, we utilized a conventional ELISA approach in which another Man alpha(1-3)-Man alpha(1-6)-Man glycan unit displaying protein target (soy bean agglutinin conjugated to HRP) was exposed to serial dilutions of PFA to identify

via the colorimetric signal generated by TMB the binding signal against PFA, as shown in Figure 21. Examining the PFA for its binding affinity to oligomannose by ELISA and microscale thermophoresis confirmed a similar value of approximately 4 nM. Having validated the binding capability of PFA for Man alpha(1-3)-Man alpha(1-6)-Man displaying glycans, we then examined how modification of an engineered PFA to display the biotin-mimetic HPQ tag could make this receptor adaptable to common sensor modalities such that we may detect the presence of oligomannose as shown in the following section.

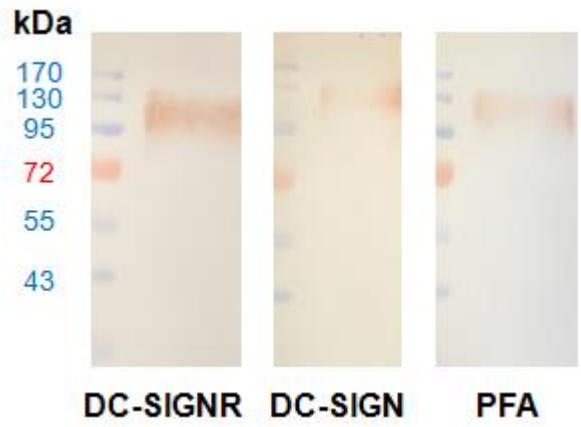

*Figure 22: Western blot with ladder in lane 1 and glycan displaying gp120 in lane 2 utilizing primary receptors of DC-SIGNR/Fc (**left**), DC-SIGN/Fc (**middle**), and PFA-HPQ (**right**). Secondary incubation was carried out with HRP conjugated anti-IgH for DC-SIGNR and DC-SIGN, while the use of Strep-HRP was used for PFA. The presence of gp120 target could be identified using the experimental PFA-HPQ to the same extent as that of the positive controls of DC-SIGNR and DC-SIGN, natural receptors for HIV transfection.*

After assessing the binding affinity of PFA, we utilized the engineered PFA fusion which bears the biotin mimetic tag VSHPQAPF known to have high affinity to streptavidin in order to facilitate its implementation with standard pathology lab analysis techniques including Western blot and agglutination assays. In conducting these experiments, we utilized the gp120 envelope glycoprotein of HIV that displays glycans that natively bind to DC-SIGN and DC-SIGNR for infection of dendritic cells and endothelial cell, respectively [39]. As positive controls for our Western blot experiments, we thus utilized DC-SIGN and DC-SIGNR as natural receptors for the glycans displayed by gp120 to compare our engineered PFA-based probe. From Figure 23 showing gp120 transferred to a nitrocellulose membrane, we can clearly see the AEC stained signal using PFA-HPQ (PFA bearing the biotin mimetic VSHPQAPF tag)

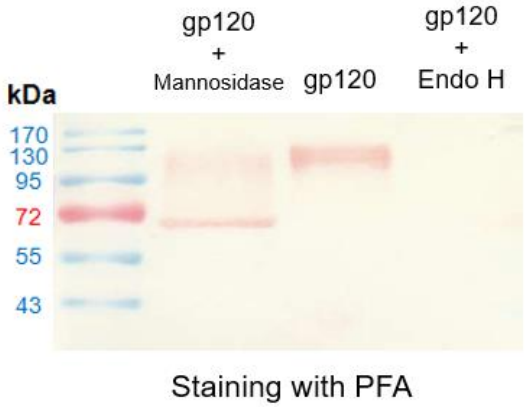

*Figure 23: Experiment of PFA fusion probe staining against gp120 with and without glycosidase treatment. Western blot of gp120 that had undergone Mannosidase treatment (**left**), gp120 without glycosidase treatment (**middle**), and gp120 that had undergone Endo H treatment (**right**).*

primary and strep-HRP (streptavidin conjugated to horseradish peroxidase) secondary. In fact, the PFA-HPQ signal against gp120 was comparable to that of the positive control signals determined for DC-SIGN and DC-SIGNR. The results were obtained after incubation of the membrane with the bound biotin mimetic peptide fusion PFA and strep-HRP (1:1 premix) for staining. No observed probe signal was seen for the right lane containing the Endo H treated gp120 as the glycans were removed. The middle lane reveals the approximate 120 kDa band for gp120 which was recognized by the PFA fusion probe. The left lane provides a weaker signal for the gp120 and at a slightly smaller molecular weight due to incubation with alpha-Mannosidase from jack bean resulting in cleavage of the terminal mannose residues from the gp120. This is expected as hybrid type glycans have been reportedly displayed by gp120 [1] that would be unaffected by the mannosidase and would thereby still provide the Man alpha(1-3)-Man alpha(1-6)-Man core to which the PFA has been reported to bind. The weaker signal would thus be representative of the reduction in the number of binding sites resulting from the Mannosidase cleavage of the Man alpha(1-3)-Man alpha(1-6)-Man core of high-mannose. In addition, a distinct band can be seen at the ~66 kDa size representative of the large subunit of the alpha-Mannosidase which from literature is known to possess a glucose-containing high-mannose-type glycan ($Glc_1Man_9GlcNAc_2$) and a small xylose- and fucose-containing complex-type glycan ($Xyl_1Man_1Fuc_1GlcNAc_2$) [2]. Note that the small 44 kDa subunit of the alpha-Mannosidase is not glycosylated and thus a band at 44 kDa could not be observed as there was no glycan for the PFA probe to bind.

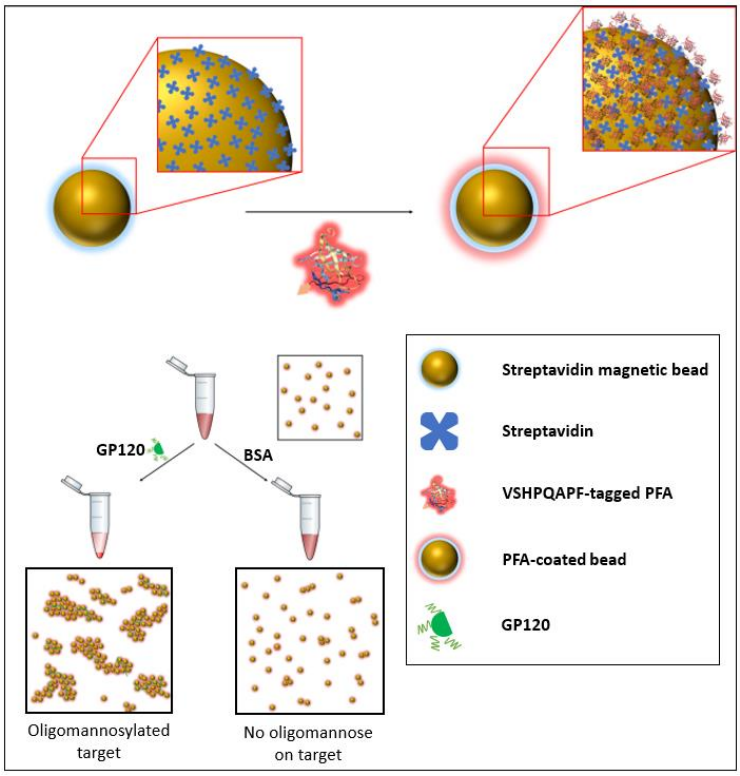

Figure 24: Schematic of one of the sensing modalities (specifically an agglutination assay) in which the PFA engineered with a biotin mimetic fusion peptide of the sequence VSHPQAPF may be implemented to provide detection of the presence of oligomannosylation.

The engineered PFA-HPQ fusion did well in the common Western blot assay format for recognizing the presence of glycans displayed on the gp120. To examine the PFA-HPQ performance with another typical detection modality, we carried out immobilization of the PFA-HPQ onto streptavidin beads (<1 µm diameter super paramagnetic iron oxide particles) in order to determine its adaptability to agglutination assays. In the course of conducting the agglutination assays against glycosylated gp120 target and control for both the streptavidin bead as well as the PFA-HPQ coated streptavidin bead, we find the onset of a distinct agglutination event for the PFA-HPQ coated beads when exposed to the gp120 target. This qualitative binding signal occurs with increasing relative aggregation compared to the control samples as time progresses. This format provides an easy to understand assay for the presence or absence of glycans such as in this case glycans possessing Man alpha(1-3)-Man alpha(1-6)-Man core units as was shown here in Figure 25 for the case of gp120. Having assessed the binding affinity of PFA and incorporating the VSHPQAPF biotin mimetic tag, the engineered PFA has shown to offer a useful component for a variety of assay formats to detect oligomannosylation.

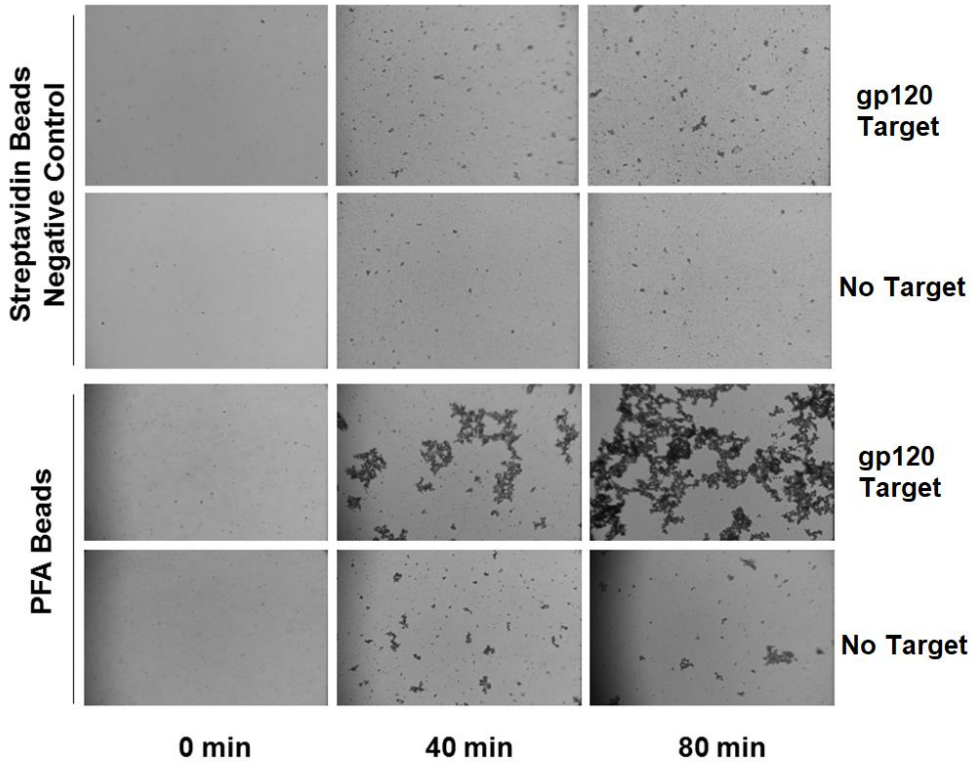

Figure 25: (A) ELISA signal of PFA against an immobilized gp120 target in the presence of increasing amount of soluble mannose showed no substantial inhibition in PFA binding until greater than 200 mM of soluble mannose was added; (B) Microscale thermophoresis and (C) ELISA of PFA against gp120 target showing similar binding constants, K_d ~4 nM.

3.4) Discussion and Conclusion

This biotin mimetic peptide fusion to a glycan receptive moiety could provide an oligosaccharide probe development strategy which may be useful to various assay formats relevant to clinical pathology labs. We selected the lectin PFA as our glycan receptive moiety based on reports of its high yield in bacterial expression along with the extensive literature reporting the ability of PFA to bind the glycans of the HIV coat protein gp120 which we could use as a model target for our proof of concept study [32,33,35]. While endogenous human lectins, DC-SIGN and DC-SIGNR, are known to be capable of recognizing oligomannose, we examined a bacterial derived lectin that may be produced in high yield in our bacterial expression system. Indeed, we find that expression proceeded well in our *E. coli* BL21 DE3 system, given the nature of the protein and after purification by nickel affinity chromatography afforded approximately 6 mg of pure protein from 2 liters of culture. Before proceeding with examining the PFA, we first confirmed our assays using positive controls of GNA lectin, DC-SIGN, and DC-SIGNR used throughout this study. To assure that our receptive lectin moiety was indeed undergoing glycan binding, we conducted competitive binding experiments, Western blots of gp120 under various glycosidase treatments, as well as quantitative binding assays. GNA is reported to recognize the Man alpha(1-3)-Man unit and through lectin frontier database [40], the interaction graph reveals GNA to bind to those such glycans which possess (α-1,3)-linked mannose residues with high affinity for Man_3 [40]. We hence utilized it as our competitive binder and in doing so found that PFA reduced the extent of GNA binding to gp120 by virtue of masking a proportion of the glycan binding site. This offered an initial promising result that our engineered PFA could bind to glycans presented by gp120 and we assessed that free mannose up to 200 mM had no inhibitory effect on the PFA binding. To provide assessment of the glycan binding capability of the engineered PFA, we carried out two distinct binding affinity assays to cross-validate our quantitative assessment. We confirmed, by both ELISA and microscale thermophoresis, a similar glycan binding affinity of the PFA lectin to be approximately 4 nM.

The strong glycan binding affinity seen for the engineered PFA could be considered sufficient for a receptive moiety for in vitro diagnostic applications, but to adopt this receptor for common clinical workflows we needed to engineer the PFA for both Western blot and agglutination assays. We have previously used the well-known VSHPQAPF peptide as a biotin mimetic motif capable of high affinity binding to streptavidin [36]. Because of the wide commercial availability of

streptavidin conjugated products, including fluorescent molecules, horseradish peroxidase (HRP), and magnetic beads for clinical assays, the engineered PFA-HPQ fusion can now be utilized in a variety of detection platforms. Here, we have incorporated the VSHPQAPF as a fusion onto the PFA to specifically facilitate its implementation with strep-HRP secondary reporters for Western blot, as well as for capture onto coatings of streptavidin beads for use in agglutination assays. Specifically utilizing the glycan bearing target gp120 as the analyte for detection, we see that the PFA-HPQ receptor conjugated with strep-HRP performed well as a glycan probe in providing a visually detectable signal by Western blot. In fact, this signal was comparable to that of natural receptors for the gp120 glycans, namely DC-SIGN and DC-SIGNR, which are receptors present on dendritic cells and endothelial cells that act as virion binding sites during HIV transfection.

In looking at an agglutination assay platform, typical manifestations utilize latex beads coated with antigen and are used to identify the presence of specific antibodies, or conversely coated with antibodies and used to identify the presence of antigens. In this demonstration, we utilized streptavidin coated magnetic beads having a diameter of less than one micron to serve as the solid phase component. As these particles are super paramagnetic iron oxide, they will not aggregate unless exposed to an external magnetic field of sufficient strength which allowed us to easily wash, collect, and re-suspend the beads during coating with the engineered PFA-HPQ lectin. The success of our probe in this agglutination assay to detect glycans of gp120 possessing the Man alpha(1-3)-Man alpha(1-6)-Man core unit in a sample was confirmed using these PFA-HPQ coated streptavidin beads, where the positive signal became apparent at the 40 minute time point post-introduction of the glycan bearing gp120 sample, and to a much greater extent at the 80 minute time point. With this proof-of-concept aggregation confirmed for the PFA coated beads in the presence of glycan bearing gp120 target, we show that our strategy of using an engineered lectin fusion is successful in providing a detectable signal for future development or potential incorporation with existing agglutination assay platforms. Different formats of agglutination assays have been used commercially and in literature to generate a variety of visual feedbacks to the user as a result of the aggregation of the bead sample and can even provide, in some cases, a color change or optical signal to confirm a positive result in the sample [41,42]. The importance of this work in showing that this proof-of-concept engineered lectin fusion may be incorporated into a variety of detection modalities highlights the possibility of this serving as a robust strategy, and we hope to continue to develop a series of related lectin-based receptors for other glycans that

may provide a toolkit/panel to begin assessing the vast repertoires of glycosylation motifs of clinical interest.

Chapter 4: Generating In Vivo Model of Oligomannose Displaying Tumor

4.1) Introduction

The objective of this research is to determine if cancer cells that are displaying unique sugars on their surface can be injected into mice to form tumors that will still possess that unique sugar or if the cells change the sugar moieties or the sugar is not displayed over time. The significance is to develop an animal model that can present the mock oligomannose displaying in an ectopic xenograft as those that are displayed by follicular lymphoma. If this sugar persists to be displayed by the tumor in these animals, we may utilize them in future studies for introducing diagnostics and therapies for this form of lymphoma, particularly not only injected antibodies in this models can be tracked to see if they will localize to the tumor site which displays oligomannose but also the efficacy of targeted diagnostic imaging probes or therapeutics can be proved. A secondary goal of this study is to examine the tumor growth rate for different concentrations of non-condition versus conditioned xenograft cells which display the follicular lymphoma biomarker, oligomannose, and to further determine the extent of sustained oligomannose display throughout the tumor. Generating a tumor model that can sustain the display of the oligomannose biomarker is critical in follicular lymphoma research for developing new targeting moieties used in diagnostics and therapeutics to overcome currently incurable nature of this form of cancer. Moreover it is important to identify if the subcutaneous injections of these cells which display oligomannose in vitro can still maintain that display of oligomannose in vivo since different media and culture conditions have been known to affect (and in some cases restrict) the display of certain oligosaccharides. Validation of the sustained oligomannose display in the ectopic xenograft tumor model will advance the next phase of pre-clinical studies for determining the selectivity of oligomannose targeting receptor moieties. The establishment of an in vivo tumor model which displays oligomannose on a membrane B cell receptor (BCR) provides a critical step toward examining sensitivity and specificity of in vivo probes for this glycan biomarker. Since commercially validated cell lines that display oligomannose on the BCR are limited, the engineered cells we have developed are potentially very promising to recapitulate the glycan display profile of follicular lymphoma and other distinct lymphoma subtypes. The development of a xenograft model which possesses a stable engraftment of oligomannose displaying cells is expected to be useful for future work particularly in targeting the unusual glycosylation displayed as oligomannose in the ectopic xenograft. Specific targeting to this biomarker will impact the

development of targeted therapeutics which can be used to treat this as of yet incurable form of cancer. Patient derived xenografts of follicular lymphoma are mostly unable to find stable engraftment since the follicular lymphoma is highly subject to the local tumor microenvironment for survival. In this study, we can examine the first stable tumor models for display of the follicular lymphoma biomarker of oligomannose displaying B cell receptor. We may examine the stability of the biomarker display and utilize this model in the future for developing targeted interventions and diagnostics. The understanding of a tumor model which displays the recently validated follicular lymphoma biomarker, oligomannose, could allow for new therapies and diagnostics to be tested as regard to in vivo selectivity/specificity for targeting moieties including antibodies.

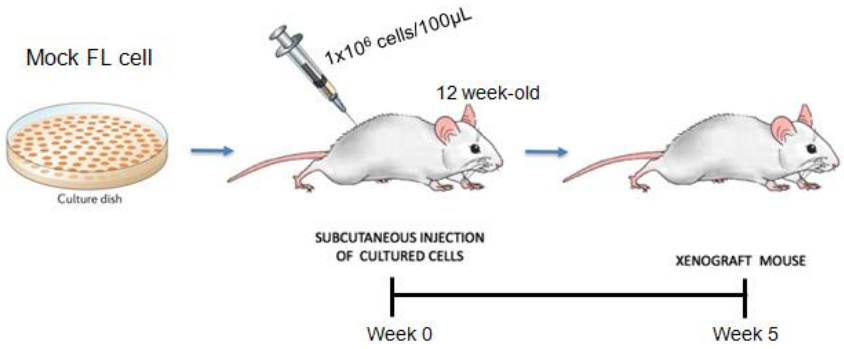

Figure 26: Schematic of strategy for engraftment of mock follicular lymphoma to generate ectopic tissue specimens for presentation of oligomannose in vivo.

4.2) Materials and Methods

To generate ectopic tumors in mice, 6 NOD-scid (NOD.CB17-Prkdc<scid>/J) mice at 9 weeks of age were obtained from The Jackson Laboratories (ME, USA). All animal experiments were authorized by the Institutional Animal Care and Use Committee (IACUC) of the University of Texas at Arlington and were conducted in accordance with the approved standards of humane animal care. The mice were fed standard chow and water *ad lib* and housed in the UT Arlington IACUC approved barrier facility under a 12-hour light cycle. Non-murine HEK293 background, BZ, and BZ-mCherry derived tumors were used as each group of mice (one male and one female in a group) for the growth each cell type. particularly, after one week of adaptation to the barrier facility, the mice were anesthetized with 2% isoflurane followed by subcutaneous injection in the flank with $6x10^6$ cells per 100uL PBS of either HEK293, BZ, or the BZ-mCherry cell line. The mice were sent to their cage and tracked weekly for tumor growth at the area of the injection. Once a palpable tumor had formed, the animal was either euthanized to collect the tumor sample along with surround tissue for further examination or instead anesthetized, shaved, and exposed to

fluorescence *in vivo* imaging using a Perkin Elmer IVIS Lumina XRMS Series III after which the mouse was euthanized for tissue collection. Imaging was processed with the following parameters: Emission=620, Excitation=580, Bin=4/4, Fnumber=f2, exposure=0.5s.

After euthanizing the mice by CO_2 and cervical dislocation, we made a small incision on the abdomen and the separated skin of mice to expose the underneath engrafted tumors. The tumor was excised, measured, and either placed in PBS for resuspension and lysis (as described above for glycosidase assay or immunoblotting) or settled in OCT for flash freezing and cryosectioned on polylysine slides at 5um using a cryotome stored at -80^{o}C. For immunohistochemistry, the sections were first blocked overnight using 1% bovine serum albumin (BSA) in 10 mM PBS buffer. Every 1 µL of primary antibody (either anti-IgM heavy chain or anti-lambda light chain) was diluted with 1 mL of washing buffer (1 % BSA and 0.5% Tween-20 in 10 mM PBS) and incubated overnight with slow horizontal agitation (50 rpm). The slides were washed at room temperature with 10 mL of washing buffer for 10 minutes, three times with horizontal agitation. 1 µL of secondary antibody conjugated with HRP was diluted to 2 mL and incubated for 30 minutes at room temperature with agitation followed by three times washing. Colorimetric reagent (10 mL of 0.05% AEC and 0.015% H_2O_2 in 50 mM acetate buffer pH 5.5) was added to develop the sections.

FACS analysis of the HEK293, BZ, and BZ-mCherry cells was carried out using a BD FACS Melody flow cytometer. Prior to analysis, cells were fixed by 4% paraformaldehyde (PFA) for 20 minutes at room temperature and stored in 1% BSA in PBS. FITC labeled anti-lambda antibody was diluted 1:2000 ratio and blocked with 1% BSA in PBS buffer for 1 hour in the dark at room temperature with rocking (50rpm). 1 mL of blocked antibody was then incubated with fixed cells for an hour with rocking. Cells were washed with 1 mL of blocking buffer, pelleted by centrifugation at 500 rpm for 3 minutes and resuspended in 1 mL 0.1% BSA in PBS buffer and filtered through a cell strainer prior to analysis. Details of the gating strategies used for FACS are presented in the Supplementary Information.

4.3) Results and Discussion

A palpable tumor could be formed in NOD-scid mice injected with at least $5x10^5$ BZ cells / 0.1 mL after 5 weeks. Moreover, the higher concentration of $2x10^6$ cells/ 0.1mL was able to yield fast engraftment of palpable tumor. Vascularization was observed in the excision of the tumors and resuspended cells from engraftment subjected to cell based ELISA using anti-lambda HRP

conjugate antibody proved surface IgM presentation in the excised tumor cells as confirmed by the blue color afforded after TMB colorimetric assay. The positive signal was seen only in the resuspended BZ tumor cells and not for the resuspended HEK background cells.

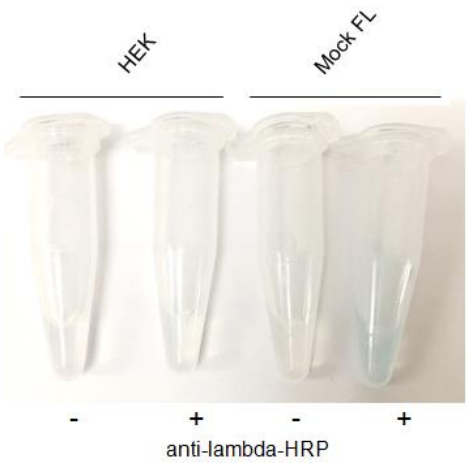

Figure 27: Cell based ELISA of HEK and BZ harvested from mice showing the presence of surface lambda light chain of the mock FL cells (BZ cells).

For examination whether tumors originated from the engineered BZ cell line could be engrafted and still express the surface IgM, we introduced ectopic murine tumors in NOD-SCID mice using the BZ cell line as compared to the HEK293 background. The appearance of tumors was confirmed after 4-5 weeks with an approximate size of 9 mm. Tumors were excised and were subjected to either lysis for testing by glycosidase assay and western blot or flash frozen in OCT for cryosectioning. From Figure 28, glycosidase assays specific for high oligomannose catalyzed for tumor lysate samples confirmed high oligomannose display only on the IgM heavy chain of BZ tumors but not HEK tumors. Furthermore, we see that IHC staining revealed the positive signal of heavy and light chain for the engineered BZ tumor sections but was not seen for the control HEK tumor sections which confirm *in vivo* antibody expression by BZ derived tumors (Figure 29).

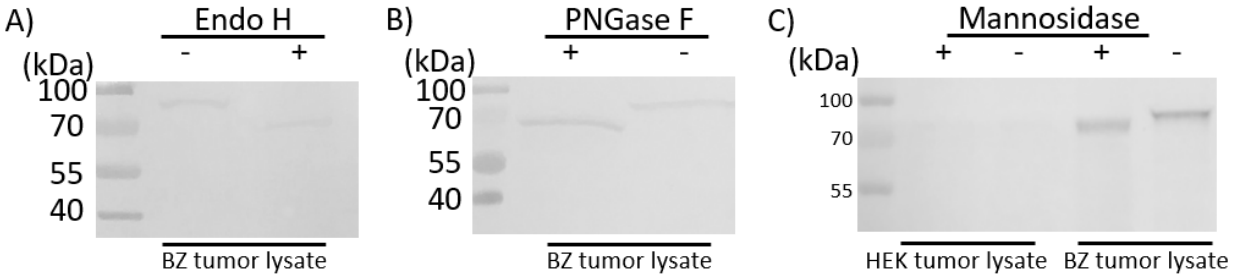

Figure 28: Immunoblotting of glycosidase assay results from tumor lysate. Tumor lysates from 4-5 week palpable tumors originated from BZ cells or HEK cells were used for glycosidase assays using (A) EndoH, (B) PNGase F, or (C) Mannosidase and separated by SDS-PAGE. Immunoblotting of the protein lysates and staining with anti-IgM heavy chain (primary) revealed a shift in the size of the heavy chain resulting from cleavage of the glycan. Only a very small band shift for cleavage by Mannosidase is seen as compared to EndoH or PNGase F. This is to be expected since the specificity of Mannosidase trims only the terminal mannose groups.

The reporter cell line BZ-mCherry was explored for its capability to be used as a tool for some of the more conventional *in vitro* and *in vivo* targeting techniques of FACS and fluorescence *in*

vivo imaging, respectively. From Figure 30, the BZ-mCherry cell line is observed to provide a bright red fluorescence that is a readily observable by fluorescence microscopy, and ectopic tumors originated from BZ-mCherry are also clearly visible with fluorescence in vivo imaging systems. Moreover, the reporter BZ-mCherry cell line holds the potential for being implemented in FACS studies as seen in Figure 30c by the high mean fluorescence intensity (MFI) through the red channel relative to the original BZ cell line. When incubating the BZ, BZ-mCherry, and HEK cell lines with FITC-labeled anti-lambda light chain probe, we also found a clear increase in MFI was detected from FACS analysis (Figure 30d) for the BZ-mCherry relative to the HEK control indicating the presence of surface antibody, where this can similarly be seen (Figure 14) for the BZ cell line. The ability for the reporter cell line to be readily identified from the non-reporter BZ cell line and HEK293 background cells by the red fluorescence in FACS system suggests it to have potential utility for screening. Moreover, the ability to detect the reporter BZ-mCherry cells within an *in vivo* context when examining fluorescent *in vivo* imaging of ectopic murine BZ-mCherry tumors suggests that this engineered reporter cell line may demonstrate its effectiveness since it is bright in red fluorescence and at the same time displays the oligomannosylated antibody.

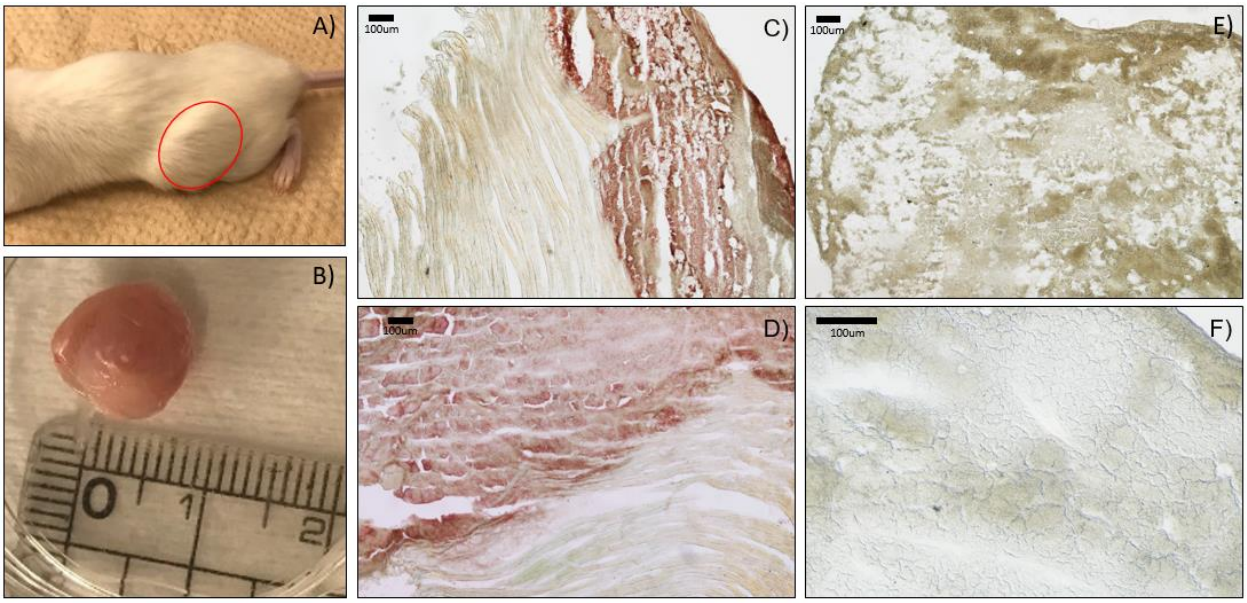

Figure 29: Tumor engraftment and immunohistochemistry. (A-D) After subcutaneous injection of BZ cells into the flank of NOD-scid mice, (A) Palpable tumors were formed at 4-5 weeks, (B) removed and (C and D) cryosectioned for immunohistochemistry. (E and F) HEK cell derived tumor were similarly engrafted, removed, and sectioned. IHC staining of tumors with (C and E) anti-lambda light chain and with (D and F) anti-IgM heavy chain showed positive signal at the location of the tumor but not in the adjacent muscle tissue in the BZ tumor sections (middle column) while HEK derived tumors exhibited negative signs for both staining (right column).

IHC of crysosectioned BZ tumor indicated the expression of the membrane bound Ig which was also confirmed by flow cytometry with FITC labeled anti-lambda. Confirmation of presence of oligomannose on the tumor derived BZ cells was provided by culturing the tumor cells followed by fixation where the cells then carried out immunohistochemical staining with 2G12 as the primary anti-oligomannose antibody. Further validation of the oligomannose displayed by the BZ tumor cells was proved by analysis of the lysate by western blot. Distinctively, we found that the lysate of the BZ tumor cells representing the mock FL incubated with an anti-oligomannose primary antibody (2G12) revealed a distinct band for the oligomannosylated heavy chain but was not seen for the HEK control cell lysate. As we examined the lysate of the resuspended BZ tumor cells, we utilized clipping of the mannose residues by glycosidases to observe an apparent shift in the molecular weight of the IgM heavy chain.

Given the successful display of the oligomannose biomarker on the surface IgM of our engineered cell line *in vitro*, we then moved to investigating the cells in vivo using NOD-scid mice. We identified that when our engineered BZ cell line was injected subcutaneously into the flanks of the mice at $5x10^6$ cells per 100uL PBS it could lead to a palpable tumor formation after 4-5 weeks. Excision of the tumors and immunohistochemical staining with anti-lambda and anti-IgM antibodies confirmed the presence of the surface antibody expression throughout the tumor mass. The presence of the oligomannose retained on the heavy chain was also indicated by western blot analysis of the tumor tissue lysate as confirmed by endoglycosidase assay and the result demonstrates that the glycan display was not affected by the *in vivo* microenvironment. We next turned to further developing a second cell line which holds an additional element of an internal mCherry fluorescence reporter fused to the cytoplasmic side of the membrane anchored IgM. The efficacy of this BZ-mCherry cell lines as a potential tool for screening of moiety that can bind the high oligomannose target may be significantly valuable in development of future therapeutics and pre-clinical screening. One observed feature of the surface IgM expressing cells relative to the HEK background was a decrease in the adhesion capabilities of the BZ and BZ-mCherry cells as compared to the HEK293 background from which they were derived for *in vitro* culture. This may be attributed to the display of surface immunoglobulin presented by the engineered BZ and BZ-mCherry cell lines in some manner hindering interaction of integrins with the surface of flasks but was not explored as it was out of the scope of this study. The HEK, BZ, and BZ-mCherry cell lines were also utilized for generating ectopic xenograft tumors in NOD-scid mice where it was shown

that the display of oligomannose on the heavy chain was conserved during *in vivo* growth in the BZ and BZ-mCherry tumor lysates analysis.

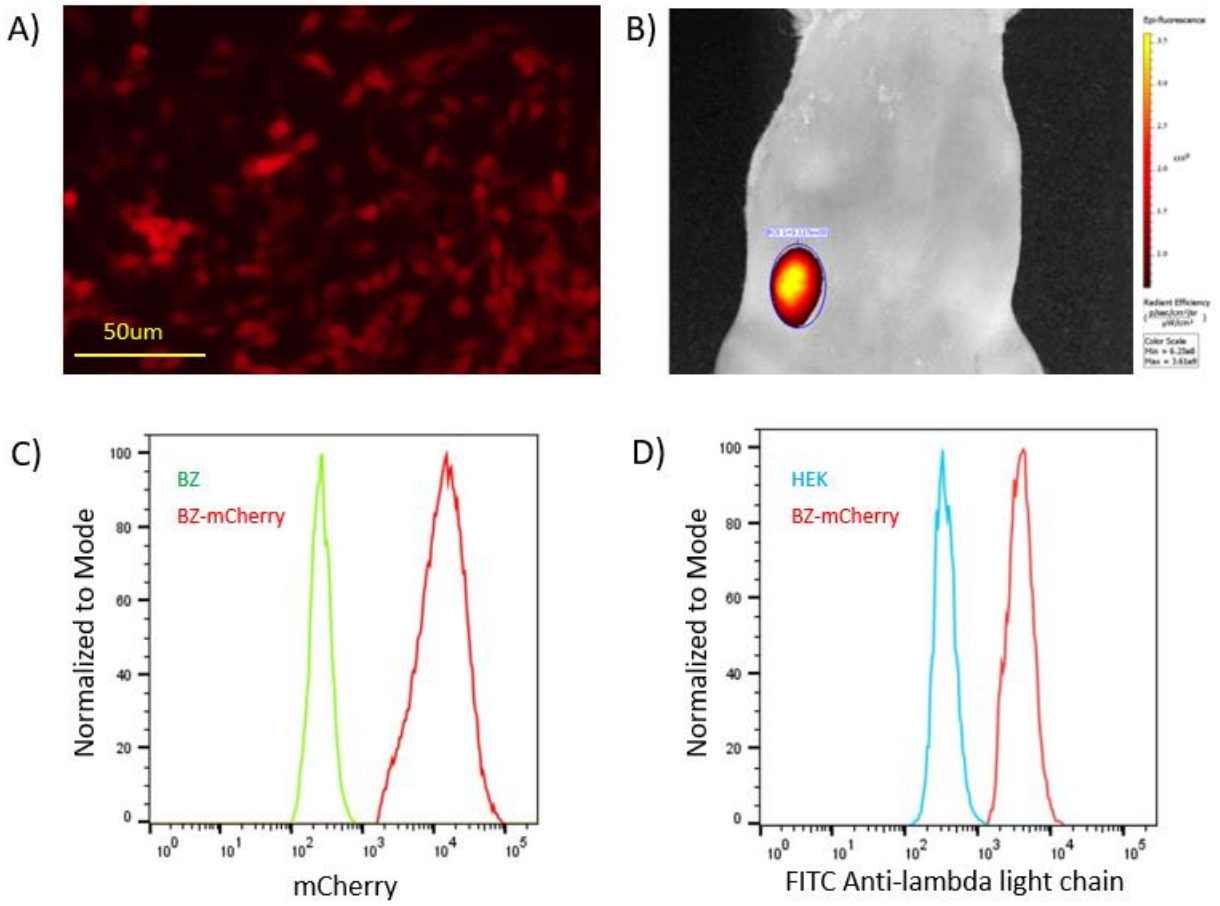

Figure 30: Fluorescence in vivo imaging and FACS analysis. (A) Fluorescent microscopy image of engineered BZ-mCherry cell line indicates the clear red fluorescence of the reporter cell line (scale bar=50um). (B) Ectopic murine BZ-mCherrry tumors are easily observable by fluorescence in vivo imaging taken at Em=620, Ex=580, Bin=4/4, Fnumber=f2, exposure=0.5s. (C) The potential use of the BZ-mCherry cell line for FACS based screening is also evident by the bright red fluorescence. (D) Distinct shift in the mean fluorescent intensity was observed for the BZ-mCherry cells compared to HEK when incubated with FITC conjugated anti-lambda probe.

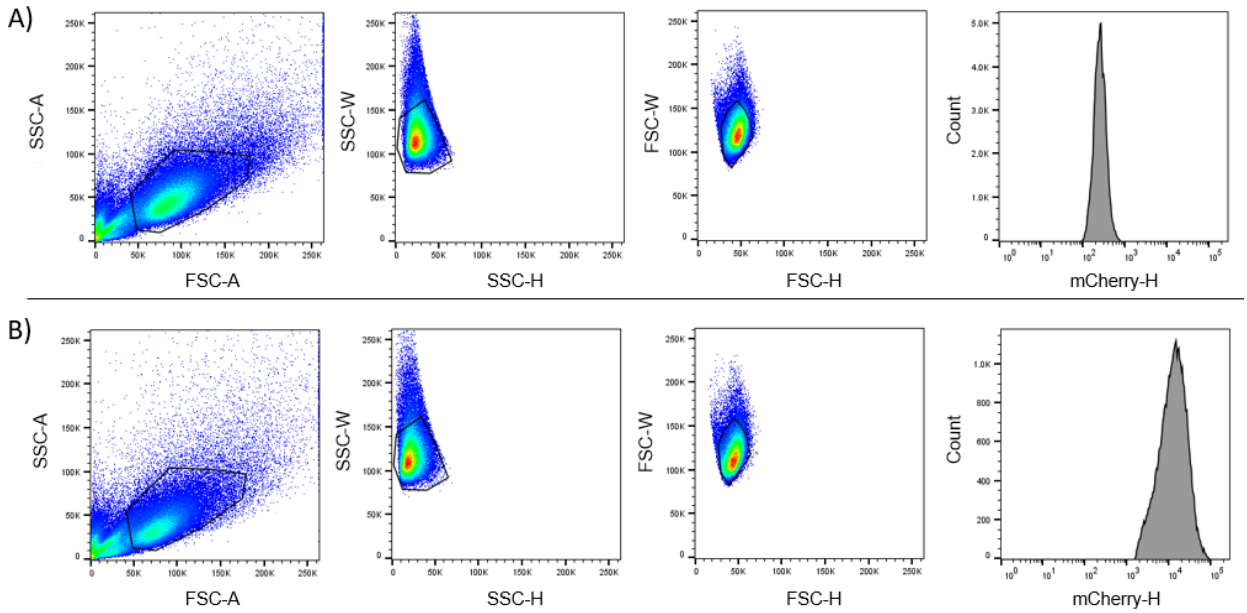

Figure 31: Gating strategy for engineered cells to examine fluorescence reporter. Representative flow cytometry dot plots illustrating the gating strategy for analysis of the presence of red fluorescence reporter within A) BZ cells and B) BZ-mCherry cells. The results prove the BZ-mCherry cells as emitting a high fluorescence signals from the expressed cytosolic mCherry reporter.

To summarize, in this section we describe our production of an engineered fluorescent reporter cell line that presents high oligomannose as displayed on the complementarity determining region of a membrane bound surface IgM as to mimic that displayed by follicular lymphoma B cells. Beginning from formalin fixed paraffin embedded tissue slides of FL involved lymph nodes, we identified the dominant subclones presenting glycosylation sites on the CDR by deep sequencing. Next, we cloned the consensus variable domain sequences for the FL derived heavy and light chains into an expression vector and after transfection we confirmed the stable expression of the surface antibody both in vitro and in vivo. Western blot following glycosidase assays was used to validated the oligomannosylation of the heavy chain. Finally, a reporter was integrated with the oligomannosylated antibody presenting cell line to provide a tool that may be utilized as a potential screening tool. In this work, we provide this cell line which displays oligomannosylated surface immunoglobulin in hopes that it will serve as a mimetic target for in vitro or in vivo development and testing of high oligomannose binding moieties. Such oligomannose specific targeting moieties are not yet available for recognizing follicular lymphoma B cells. Unlike previous reports that have sought to create follicular lymphoma cell lines for in vitro studies, it is important to note that our approach does not try to incorporate the cell signaling features of

follicular lymphoma B cells. In contrast, our work in generating the BZ cell lines solely focused on providing the key mimetic surface feature of a uniquely oligomannosylated antibody. We anticipate that this cell line may be used as a screening tool for future identification of a receptive moiety that can properly bind to the unique high oligomannose target presented by the Ig of certain B cell lymphomas. Since this target has been suggested to be a critical element for not only diagnostic but also potential therapeutic purposes, we hope this work will serve as the starting point for opening the way to future work in developing clinically relevant technologies that may bind to high oligomannose.

Chapter 5: Developing & Testing Diagnostics for Oligomannose Presenting Cells

5.1) Introduction

While in depth genetic analysis to identify glycosylation site sequences in the CDR of human immune repertoires and confirmation of those glycan structures by complex chromatographic techniques has proven successful in the realm of dedicated research laboratories,[3, 12] it is important to understand that deep sequencing and UHPLC are not currently employed clinical diagnostic approaches for routine workup. Instead, direct detection of oligomannose requires an approach more relevant to common workflow used in a clinical pathology lab. There are several clinically relevant immunophenotyping techniques common across pathology laboratories, but we and other have found that the extensive cross-linking of glycans in FFPE (formallin-fixed paraffin embedded) tissue biopsy samples can be problematic for accurate immunophenotyping particularly for glycans where antigen retrieval is poor. Because follicular lymphoma and DLBCL are heterogeneously categorized despite the existence of a known subset which displays a unique glycosylation marker of high oligomannose on their immunoglobulin. A clinical assay for determining the number of circulating malignant B cells with this distinct glycosylation from patient blood samples is not yet available and the prognostic significance has yet to be addressed. One of the goals of this aim is to create a novel diagnostic platform that can selectively capture, release, and quantify follicular lymphoma (FL) B cells present in patient collected specimens by virtue of the fact that these FL B cells display a unique oligomannose glycosylation on their immunoglobulin. We hypothesize that the number of follicular lymphoma B cells in a patient collected specimen can be quantified utilizing a lectin coated magnetic bead assay as a diagnostic for early detection and assessment of reoccurrence based on our prior results that the lectin (Pseudomonas fluorescens agglutinin) may bind to the oligomannose presented by follicular lymphoma B cells. We have demonstrated a protein fusion in which a lectin (Pseudomonas fluorescens agglutinin) is linked to a His-tag can be purified in high yield after expression BL21 DE3 using a pET expression system as purified by nickel affinity chromatography. We have also previously examined that a biotin mimetic domain (VSHPQAPF) which revealed that it can be effectively captured by streptavidin and fully released by addition of native biotin via competitive elution (41). While in this work we are primarily examining our diagnostic system for counting of follicular lymphoma cells as a proof of concept, we aim to expand this to DLBCL to provide a

means for clinicians to assess the presence of high oligomannose display in a B cell population. This will provide a new way in which patients that have been diagnosed as having DLBCL by patient biopsy may be further categorized into subsets based on the display of high-mannose on the membrane Ig. As such this diagnostic will facilitate a means for discerning those with high oligomannose positive lymphomas in order to more accurately define the patient population. This could prove to be a distinct benefit should future research reveal this as an effective prognostic indicator and similarly could benefit the design of more accurate clinical trials in lymphoma research by providing the means for obtaining a more well defined and homogenous DLBCL cohort.

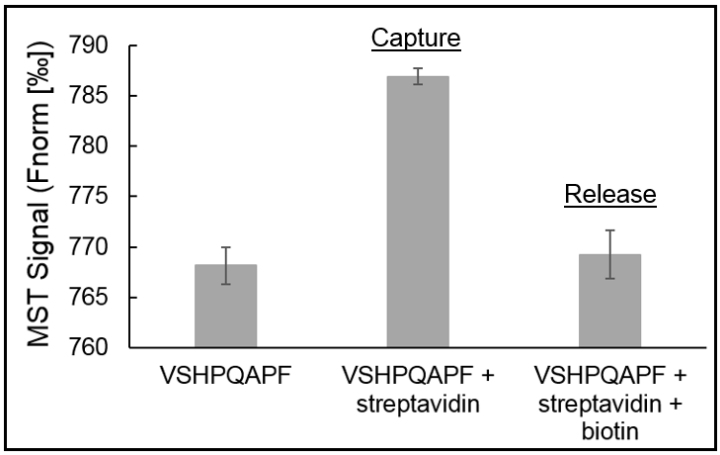

Figure 32: Biotin mimetic peptide (VSHPQAPF) showed reversible binding to streptavidin and release by addition of biotin as confirmed by microscale thermophoresis.

Our initial approach explores the use of a capture and release technique utilized in our assay as streptavidin magnetic beads can be used to display the lectin for agglutination and separation of only the follicular lymphoma (FL) B cells. After washing away of the normal B cell population, we will subsequently release the FL B cells by addition of biotin for quantification initially by hemocytometer for this study but eventual adaptation of this approach for automated analyzers. From our prior assessment, this lectin demonstrates high affinity for oligomannose and is an ideal component for this diagnostic assay. We utilized our previously developed cell line which we engineered to express an IgM bearing a patient derived variable heavy chain possessing the oligomannose

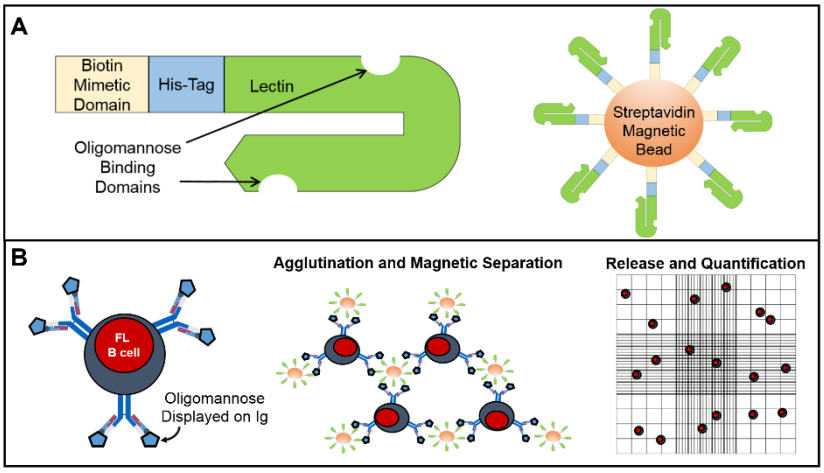

Figure 33: Schematic overview of A) PFA lectin fusion protein and labeled bead as well as B) general outline of lectin coated bead assay for quantifying the number of follicular lymphoma B cells.

glycosylation site. These engineered oligomannose displaying cells are used to tune the number of target positive cells in a normal human blood sample such that we may optimize our system and also determine the linearity and reproducibility. A schematic of the fusion protein is provided where the His tag facilitates purification by nickel affinity chromatography and the biotin mimetic domain (VSHPQAPF) provides for directional capture of the lectin onto streptavidin magnetic beads. The biotin mimetic domain facilitates a strong but non-covalent linkage between the magnetic support and the lectin that may be released upon addition of native biotin which will be used in this assay via competitive elution for de-agglutination and release of any bound oligomannose positives B cells after magnetic separation and washing away of normal B cells.

In addition, flow cytometry offers a sensitive and routinely applied technique in clinical pathology labs for quantitative assessment of cellular biomarkers and is considered to be one of the key immunophenotyping tools. Immunophenotyping by flow cytometry would offer an effective approach if a probe were available for oligomannose. As no such probe exists, we aimed to develop a flow cytometry probe using an engineered oligomannose-binding lectin conjugated to a magnetic bead for selection and validate its ability to distinguish cells in a population based on the display of oligomannose. Because flow cytometry allows identification of cell populations possessing different characteristic biomarkers as afforded by attachment by fluorescent probes, the use of fluorescent small molecules, proteins, and even inorganic nanoparticles (i.e., quantum dots) as reporters have been successfully utilized within clinical flow cytometry probe panels. Here we utilize magnetic separation of oligomannose specific PFA-labeled magnetic beads as the capture element. For glycan recognition, this ability to couple high avidity (i.e., multi-site binding to oligomannose units on both CDRs and across multiple surface sites) is critical in enhancing the effective binding capabilities for the probe as compared to the more traditional approach of using a single receptive moiety coupled to a single reporter.

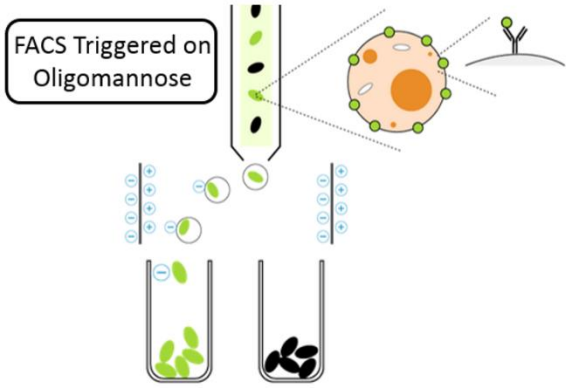

Figure 34: Overview of strategy in which cell mixtures containing follicular lymphoma are first incubated with magnetic beads displaying PFA, separated magnetically, and assessed by FACS.

Here we utilize our validated lectin in contrast to the 2G12 oligomannose antibody. Oligomannose antibodies have been historically difficult to develop, so our choice of using an engineered lectin over a traditional antibody based receptive moiety as typically seen for flow cytometry probes is due to the fact that the oligomannose displayed by a subset of B cell lymphomas is not restricted to a single oligomannose structure while the only existing anti-oligomannose antibody 2G12 has preferential specificity of the structure presented by HIV. Several research groups have verified by UHPLC that the oligomannose displayed on the CDR of follicular lymphoma present as Man5, Man6, Man7, Man8, and Man9 variant structures of oligomannose. The pursuit of high-mannose specific antibodies had been of interest but was largely unsuccessful with the exception of a serendipitous discovery of a monoclonal derived from an HIV patient having a peculiar configuration of a non-canonical heavy domain cross-over to provide a high-surface area combined CDR for binding to the Man9 displayed on the HIV capsid, gp120. In our examination of the 2G12 antibody that is a specific monoclonal against gp120, we found it to be insufficient in recognizing the high mannose on follicular lymphoma, we found the specificity to be insufficient. As such, we examined a range of natural lectins with broader specificity for the high mannose variants of Man6, Man7, Man8, and Man9. When examining a recently identified Pseudomonas Fluorescence Agglutinin (PFA) which was reported to recognize the Man alpha(1-3)-Man alpha(1-6)-Man core of oligomannose, we found that the PFA lectin was capable of not only recognizing the Man9 of gp120 but also because it recognized the core oligomannose branchpoint, it provided broader selectivity for the high mannose variants Man6, Man7, Man8, and Man9 as found on follicular lymphoma B cells surface immunoglobulin. The scientific premise for utilizing an engineered lectin based on the PFA backbone as the oligomannose receptor is thus based on strong literature support, protein crystal structures of the homologous Osciallatoriaagardhii agglutinin lectins in complex with high mannose variants, and our own validation of our engineered PFA lectin with specificity for high mannose variants including binding measurements against Man9 showing nanomolar affinity and western blot analysis showing the ability of the engineered PFA to bind the high-mannose displayed on follicular lymphoma patient derived surface Ig.

5.2) Methods and Materials

As a mock follicular lymphoma cell line, we utilized our engineered HEK293 cells (referred to as BZ) which express a lymphoma patient derived VH/VLλ pair as a membrane bound IgM possessing the glycosylation site on the VH chain. For initial agglutination assay experiments, we utilized the aforementioned BZ cell line, BZ-mcherry cell line and the control HEK293 background as control. A mixture of mCherry expression target cells displaying the high oligomannose marker in combination with the control HEK293 were used for FACS measurements in order to identify if we could determine distinct enrichment and quantification of the mock FL cells within the lectin coated magnetic bead tandem FACS assay. We also assessed the selectivity of recovery via fluorescence presented that was provided by our engineered target BZ-mCherry cells as compared to the non-fluorescent normal HEK background.

Optimization of the surface density of the oligomannose specific lectin (Pseudomonas fluorescens agglutinin) coating on the magnetic beads was be carried out in conjunction with western blot analysis. Tuning the surface density of the displayed recognition moiety (PFA lectin) was be done by varying the amount of lectin relative to the concentration of magnetic beads. Confirmation of this labeling approach was carried out by an enzymatic colorimetric assay using biotinylated horseradish peroxidase. Based on experience with the streptavidin magnetic beads in the past, we optimized the blocking and washing strategy with BSA. Selectivity in recovery of only target B cells displaying the oligomannose marker and initial experiment examining the capability of this process against the display of anti-lambda surface marker were carried out with a BD FACSMelody. We initially used a concentration of $1x10^5$ cells per mL. To determine this dynamic range and detection limit of our lectin coated magnetic bead assay. The ratio of the number of magnetic beads to total number of cells was tuned in order to improve the sensitivity and dynamic range. In order to determine the selectivity of only target mock FL cell recovery, we assessed the captured and released cell for fluorescence present on the engineered target cells as compared to the non-fluorescent HEK cells. An inverted microscope was utilized for discerning the agglutination ability of the distinct bead formulations for both HEK control as well as the BZ cell line expressing the oligomannosylated target. Experiments were conducted in at least triplicate with consistent FACS gating used across experiments.

In order to translate our engineered lectin into a useful diagnostic tool, we first determined the appropriate optimization of the labeling and flow cytometry assay conditions. Aspects including

the consistency in labeling are important metrics that must be assessed to appropriately design a high performance flow cytometry probe for oligomannose. Thus, we began our experiments utilizing two distinct magnetic bead systems with an anti-lambda capturing moiety to validate our assay, specifically streptavidin magnetic beads coupled with biotinylated anti-lambda and proteinA magnetic beads coupled with anti-lambda. As to initially design our probe for maximal reproducibility, we examined this labeling approach based on an integrated biotin mimetic tag that we have displayed on the PFA lectin. The outcomes of these experiments inform us of the appropriate labeling conditions to begin moving toward conducting the flow cytometry experiments in the context of selective determination of oligomannosylated cells.

For initial testing, we will utilize our oligomannose positive BZ cell line confirmed to display oligomannose and compare this to our HEK control on the same cell background that does not express the IgM. Cultured cells will be washed in PBS, pelleted, and resuspended in PBS with 3%BSA at a concentration of 0.1 million cells/mL. Holding the number of cells constant, we examined the probe titer with respect to enrichment of the oligomannose positive cell population as to try to minimize nonspecific binding. For data analysis and proper interpretation we ensured a consistent gating strategy was employed between samples. Before running samples, we first examined the response of our flow cytometer with a set of labeled CS&T microbeads for calibration of each fluorescence channel to ensure consistency in the performance parameters of detection threshold to see the lowest level of fluorochrome detectable, the dynamic range of the detector, and the fit of the calibration line. During sample acquisition, we initially used the control sample of unlabeled cells to adjust for the optimal voltages for electronic noises for the each channel to be under the second decade in intensity. Examining the anti-lambda bead or PFA-bead selected samples for positive and negative oligomannose populations independently, we were able to identify the mean fluorescent intensity (MFI) representative of high MFI for the positive oligomannose cell population BZ-mCherry and low MFI for the negative oligomannose cell population HEK. Using the MFI and appropriate gating we were able to distinguish the number of counts for the beads, BZ-mCherry, and HEK cells

5.3) Results and Discussion

In looking at the agglutination response of the HEK control as compared to the oligomannosylated BZ cell line, we examined the cells natural agglutination without beads, with streptavidin beads,

with biotin-blocked streptavidin beads, with anti-lambda labeled beads, and with PFA labeled beads as shown below. After extended incubation we could not identify any significant cellular aggregation for the PFA beads relative to the control beads or in comparing BZ to HEK. Our suspicion was that the PFA beads would have provided aggregation as we had seen previously for our examination of the free soluble oligomannoyslated target, but this was not the case as we presume to be a result of the much larger size of the cells relative to the molecular suspension. The forces needed to maintain a clusters of were suspected to be much higher than that of a cluster of beads. We could visually observe the capture of magnetic beads on the cell surface but only a slight indication of cell clustering was observed for the anti-lambda or PFA beads with BZ; thus, we moved forward instead to the prospect of selective magnetic cell capture and subsequent quantification by FACS.

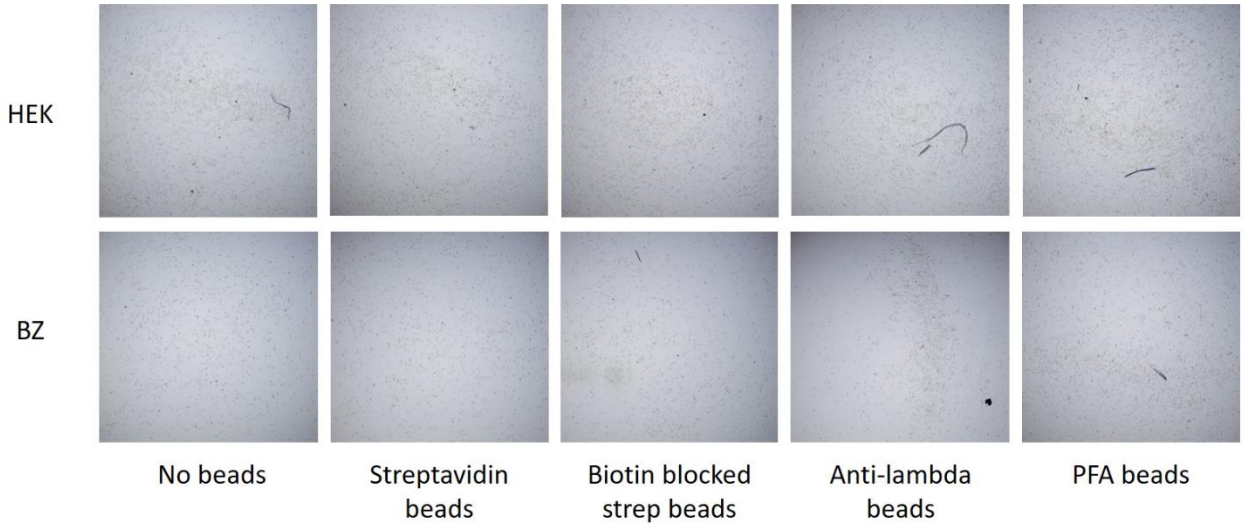

Figure 35: Agglutination assay of oligomannose negative (HEK) cells and oligomannose positive (BZ) cells using various bead conditions.

Before examining the ability of our oligomannose specific magnetic beads to providing meaningful selection as assessed by flow cytometry, we first examined the ability of a known anti-lambda antibody which was labeled onto the beads to provide selective enrichment for optimization of our assay conditions. Examination of streptavidin magnetic beads after the capture assay was conducted on the BD FACSMelody system and the results can be seen as displayed below to reveal how we setup our gating strategy. The bead signal alone (shown as the image on the left in Figure 36) was seen to not provide an mCherry fluorescence intensity above 10^3 and only minimal forward scattering (FSC-A) above 50,000. Using a cell only mixture (Figure 36b) we could see the same unwanted signal below for FSC-A below 50,000 and thus we used a gating

strategy like that demonstrated by the red ellipses for discerning our cell populations. In Figure 36, the image on the right reveals a sample after incubation with streptavidin magnetic beads and collection wherein the red ellipse regions of interest are the designated HEK (low mCherry intensity) and BZ-mCherry (high mCherry intensity cell lines. The cells determined to be positive or negative for oligomannose based on our probe were collected separately and examined.

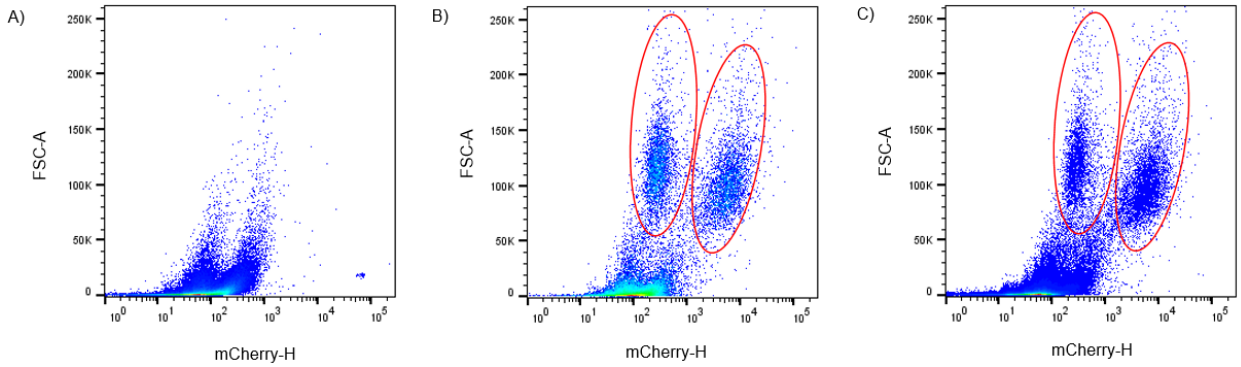

Figure 36: Overview of gating strategy as shown by dot plots of A) streptavidin beads, B) cell only mixture of HEK and BZ-mCherry, and C) mixture of HEK and BZ-mCherry cells after capture with streptavidin beads.

The use of this internal mCherry signal to distinguish between control cells and oligomannose positive cells permitted us to easily examine the ability of the anti-lambda and lectin beads to be able to distinguish positivity and also afford absolute counting of positive cells and negative cells within a mixed population. Using an almost equal mixture of positive (mCherry) and negative (HEK) cell populations, we carried out cell counting of the respective numbers of the captured populations after exposure to different bead formulations. Based on gating determined from the prior experiment, we were able to determine the enrichment in the ratio of mCherry (oligomannose positive cells) relative to HEK (oligomannose negative cells).

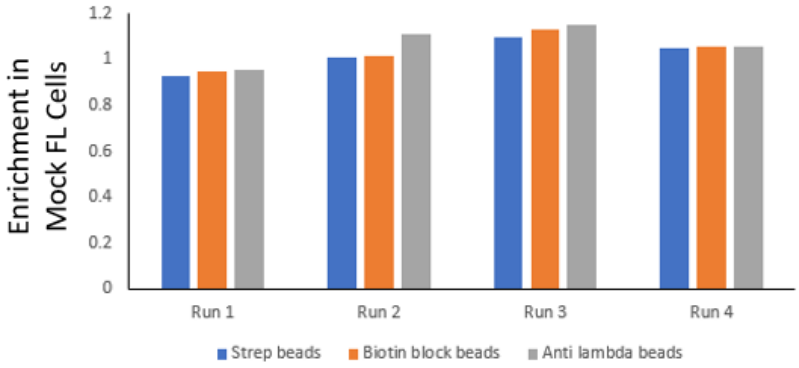

Figure 37: Enrichment level of mock FL cells (BZ-mCherry) relative to HEK cells as determined from FACS after selection using streptavidin beads, biotin blocked streptavidin beads, and anti-lambda labeled streptavidin beads.

As shown, the streptavidin beads exhibited no clear enrichment for BZ-mCherry when utilizing the anti-lambda beads which was unexpected but believed to be a result of random site biotinylation of the anti-lambda used in this assay. The randomized biotinylated will have resulted in improper display of anti-lambda on the beads thus rendering the selectivity for the oligomannose positive cell population in effective. To explore a different approach, we looked to provide a site specific display of the anti-lambda on the beads by using proteinA magnetic beads, wherein the proteinA will selectively bind the Fc region of the anti-lambda antibody allowing the complementarity determining region to be preferentially displayed on the bead surface. Indeed we see that comparing the anti-lambda beads to a non-specific antibody labeled on the beads we saw significant enrichment of the mock FL cells (BZ-mCherry); however, we also saw enrichment for the proteinA beads alone. When utilizing Tween-20 in the assay we continued to see enrichment for the BZ-mCherry cells for the anti-lambda beads while the proteinA bead enrichment and non-specific antibody bead controls remained low.

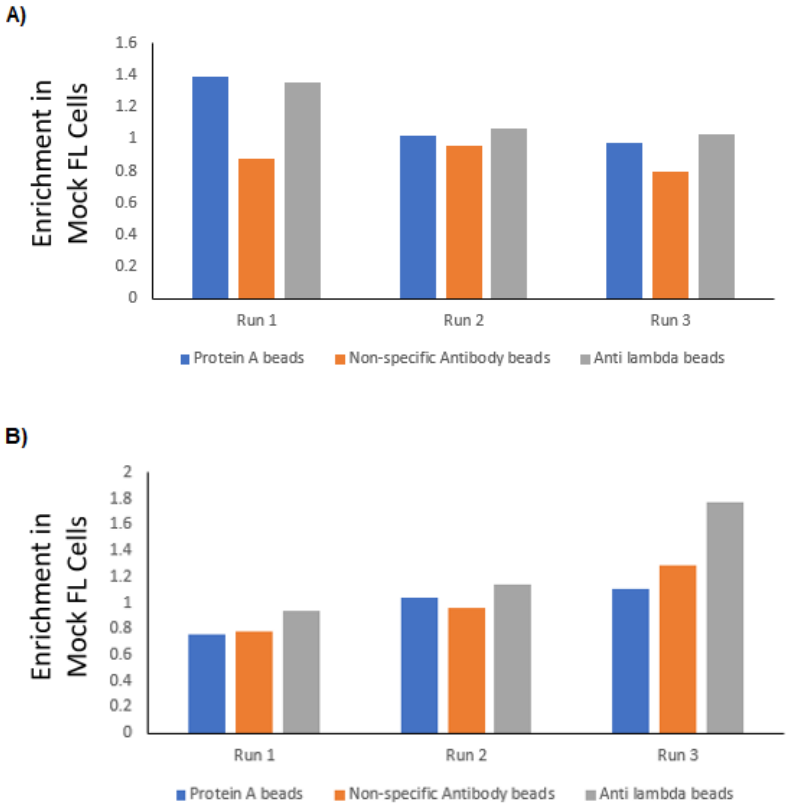

Figure 38: Enrichment level of mock FL cells (BZ-mCherry) relative to HEK cells as determined from FACS after selection using proteinA beads, proteinA beads with non-specific antibody labeling, and proteinA beads with anti-lambda labeling. Comparison is made A) without or B) with Tween-20 in assay.

Here we find that our optimization of the anti-lambda reporter was successful with a clear benefit of using Tween-20 in our assay format; however, there are certain drawbacks. For our PFA-based oligomannose receptor, we cannot utilized the proteinA beads as our lectin possessed a biotin-mimetic tag and thus required the streptavidin bead system. In addition, the use of Tween-20 would not be conducive to the examination of non-fixed living cells. Future works in this realm will be sure to provide a means for overcoming the limitations we have encountered and we suggest further optimization of the system before it may be implemented into a clinically relevant diagnostic platform. Nonetheless, we see a clear path forward by which we may improve our system to meet the diagnostic needs including the need to use our newly established mock FL cell line in order to explore more selective oligomannose recognition moieties.

5.4) Conclusions and Future Directions

In this work, we demonstrated our steps toward an oligomannose-specific flow cytometry probe which was in response to the unmet need for a clinically relevant approach to cell surface glycan detection. Toward this goal, we coupled our two recent developments of a mock follicular lymphoma cell line to serve as a screening tool along with our engineered lectin with high affinity for oligomannose. The coupling of the receptive element (lectin) with the reporter element of a magnetic bead is particularly innovative and if hurdles are overcome may prove to shift clinical paradigms for classification of B cell malignancies into new subsets based on their display of oligomannose. We aim for future developments and optimization to provide a newfound set of diagnostic capabilities by integrating this oligomannose probe to enhance existing flow cytometry panel diagnostics for monitoring the presence and extent of certain diseases for which oligomannosylation is evident. In turn, a future probe could be used in larger studies to examine the prognostic and predictive value of the oligomannose feature in concert with existing pathological parameters. The implementation of a flow cytometry probe for oligomannose may someday lead to innovations in clinical pathology labs in providing additional features for augmenting their diagnostic algorithm development and inherently serve to improve assessment of disease occurrence, reoccurrence, or minimum residual disease. In providing a means for more accurately defining the patient population based on oligomannose presence in the context of being able to identify new immunophenotypic features, the results of this work could someday lead to

improvements in patient stratification to assist in selection of disease management strategies and could benefit the selection of appropriately defined cohorts in the design of new clinical trials.

While the clinical impact discussed above provides a clear route for how this work could lead to new paradigms in considering the inclusion of oligomannosylation of cells within diagnostic algorithms. In looking at the broader scientific significance of this work, overcoming the lack of immunophenotyping probes for oligomannose in the context of clinically relevant flow cytometry may help to move toward other relevant glycan-specific probes that may be integrated into standard diagnostic practice. Because there is a growing but limited knowledge of how many glycan moieties play a role in human health, work in glycan-specific probe development in general will help uncover clinical evidence of presence of certain glycans (such as oligomannosylation) but also provide a tool for basic science research. We expect the ongoing success of this project to enhance the field in terms of access to new information about oligomannose presentation on cell populations discovered through the use of this probe will provide the foundation for future work in improving our scientific understanding of the role of oligomannosylation in the pathogenesis of disease states other than the B cell malignancies mentioned above (for example, oligomannosylation of other membrane proteins has been reported in patients with high grade prostate cancer as well as in some cases of ovarian cancer). Other impact areas of this work are the use of this probe as a component of pre-clinical assessment of disease progression/regression in animal models of B-cell lymphomas possessing this representative oligomannosylation in order to screen the efficacy of new therapeutics.

Literature Cited

1. Strout MP. Sugar-coated signaling in follicular lymphoma. Blood. 2015;126(16):1871-2.

2. Schüler F, Dölken L, Hirt C, Kiefer T, Berg T, Fusch G, et al. Prevalence and frequency of circulating t(14;18)-MBR translocation carrying cells in healthy individuals. International journal of cancer Journal international du cancer. 2009;124(4):958-63. doi: 10.1002/ijc.23958. PubMed PMID: PMC4216731.

3. Argos BV, Chiodin G, Forconi F, Burack R, Rock P, Packham G, et al. Lymphoma-Specific Subversion of B-Cell Receptor Signaling By Macrophage Lectins. Am Soc Hematology; 2018.

4. Limpens J, Stad R, Vos C, De Vlaam C, De Jong D, Van Ommen G, et al. Lymphoma-associated translocation t (14; 18) in blood B cells of normal individuals. Blood. 1995;85(9):2528-36.

5. Calarese DA, Scanlan CN, Zwick MB, Deechongkit S, Mimura Y, Kunert R, et al. Antibody Domain Exchange Is an Immunological Solution to Carbohydrate Cluster Recognition. Science. 2003;300(5628):2065-71. doi: 10.1126/science.1083182.

6. Godon A, Moreau A, Talmant P, Baranger-Papot L, Genevieve F, Milpied N, et al. Is t(14;18)(q32;q21) a constant finding in follicular lymphoma? An interphase FISH study on 63 patients. Leukemia. 2003;17(1):255-9.

7. Lossos IS, Gascoyne RD. Transformation of follicular lymphoma. Best practice & research Clinical haematology. 2011;24(2):147-63.

8. Bahler DW, Levy R. Clonal evolution of a follicular lymphoma: evidence for antigen selection. Proceedings of the National Academy of Sciences. 1992;89(15):6770-4.

9. Sachen KL, Strohman MJ, Singletary J, Alizadeh AA, Kattah NH, Lossos C, et al. Self-antigen recognition by follicular lymphoma B-cell receptors. Blood. 2012;120(20):4182-90.

10. Zhu D, McCarthy H, Ottensmeier CH, Johnson P, Hamblin TJ, Stevenson FK. Acquisition of potential N-glycosylation sites in the immunoglobulin variable region by somatic mutation is a distinctive feature of follicular lymphoma. Blood. 2002;99(7):2562-8.

11. Coelho V, Krysov S, Ghaemmaghami AM, Emara M, Potter KN, Johnson P, et al. Glycosylation of surface Ig creates a functional bridge between human follicular lymphoma and microenvironmental lectins. Proceedings of the National Academy of Sciences. 2010;107(43):18587-92. doi: 10.1073/pnas.1009388107.

12. van de Bovenkamp FS, Hafkenscheid L, Rispens T, Rombouts Y. The emerging importance of IgG Fab glycosylation in immunity. The Journal of Immunology. 2016;196(4):1435-41.

13. McCann KJ, Ottensmeier CH, Callard A, Radcliffe CM, Harvey DJ, Dwek RA, et al. Remarkable selective glycosylation of the immunoglobulin variable region in follicular lymphoma. Molecular immunology. 2008;45(6):1567-72.

14. Zhu D, Ottensmeier CH, Du MQ, McCarthy H, Stevenson FK. Incidence of potential glycosylation sites in immunoglobulin variable regions distinguishes between subsets of Burkitt's lymphoma and mucosa-associated lymphoid tissue lymphoma. British journal of haematology. 2003;120(2):217-22.

15. Stevenson FK, Krysov S, Davies AJ, Steele AJ, Packham G. B-cell receptor signaling in chronic lymphocytic leukemia. Blood. 2011;118(16):4313-20.

16. Krysov S, Potter KN, Mockridge CI, Coelho V, Wheatley I, Packham G, et al. Surface IgM of CLL cells displays unusual glycans indicative of engagement of antigen in vivo. Blood. 2010;115(21):4198-205.

17. Choi WW, Weisenburger DD, Greiner TC, Piris MA, Banham AH, Delabie J, et al. A new immunostain algorithm classifies diffuse large B-cell lymphoma into molecular subtypes with high accuracy. Clinical Cancer Research. 2009;15(17):5494-502.

18. Haidar JH, Shamseddine A, Salem Z, Mrad YA, Nasr MR, Zaatari G, et al. Loss of CD20 expression in relapsed lymphomas after rituximab therapy. European journal of haematology. 2003;70(5):330-2.

19. Lohr JG, Stojanov P, Lawrence MS, Auclair D, Chapuy B, Sougnez C, et al. Discovery and prioritization of somatic mutations in diffuse large B-cell lymphoma (DLBCL) by whole-exome sequencing. Proceedings of the National Academy of Sciences. 2012;109(10):3879-84.

20. Johns TG, Mellman I, Cartwright GA, Ritter G, Old LJ, Burgess AW, et al. The antitumor monoclonal antibody 806 recognizes a high-mannose form of the EGF receptor that reaches the cell surface when cells over-express the receptor. The FASEB journal. 2005;19(7):780-2.

21. Sato Y, Kubo T, Morimoto K, Yanagihara K, Seyama T. High mannose-binding Pseudomonas fluorescens lectin (PFL) downregulates cell surface integrin/EGFR and induces autophagy in gastric cancer cells. BMC cancer. 2016;16(1):63.

22. Ruhaak LR, Taylor SL, Stroble C, Nguyen UT, Parker EA, Song T, et al. Differential N-glycosylation patterns in lung adenocarcinoma tissue. Journal of proteome research. 2015;14(11):4538-49.

23. Holst S, Deuss AJ, van Pelt GW, van Vliet SJ, Garcia-Vallejo JJ, Koeleman CA, et al. N-glycosylation profiling of colorectal cancer cell lines reveals association of fucosylation with differentiation and caudal type homebox 1 (CDX1)/Villin mRNA expression. Molecular & Cellular Proteomics. 2016;15(1):124-40.

24. Wang D, Dafik L, Nolley R, Huang W, Wolfinger RD, Wang LX, et al. Anti-oligomannose antibodies as potential serum biomarkers of aggressive prostate cancer. Drug development research. 2013;74(2):65-80.

25. Newsom-Davis TE, Wang D, Steinman L, Chen PF, Wang L-X, Simon AK, et al. Enhanced immune recognition of cryptic glycan markers in human tumors. Cancer Research. 2009;69(5):2018-25.

26. Fuhrmann U, Bause E, Legler G, Ploegh H. Novel mannosidase inhibitor blocking conversion of high mannose to complex oligosaccharides. Nature. 1984;307(5953):755.

27. Linley A, Krysov S, Ponzoni M, Johnson PW, Packham G, Stevenson FK. Lectin binding to surface Ig variable regions provides a universal persistent activating signal for follicular lymphoma cells. Blood. 2015;126(16):1902-10.

28. Férir G, Huskens D, Noppen S, Koharudin LM, Gronenborn AM, Schols D. Broad anti-HIV activity of the Oscillatoria agardhii agglutinin homologue lectin family. Journal of antimicrobial chemotherapy. 2014;69(10):2746-58.

29. Koharudin LM, Kollipara S, Aiken C, Gronenborn AM. Structural insights into the anti-HIV activity of the Oscillatoria agardhii agglutinin homolog lectin family. Journal of Biological Chemistry. 2012;287(40):33796-811.

30. Sato Y, Okuyama S, Hori K. Primary structure and carbohydrate binding specificity of a potent anti-HIV lectin isolated from the filamentous cyanobacterium Oscillatoria agardhii. Journal of Biological Chemistry. 2007;282(15):11021-9.

31. Council NR, Glycoscience IT. A Roadmap for the Future (ed. Walt, D.) 85–89. The National Academies Press, Washington, DC; 2012.

32. Sterner E, Flanagan N, Gildersleeve JC. Perspectives on anti-glycan antibodies gleaned from development of a community resource database. ACS chemical biology. 2016;11(7):1773-83.

33. Huber M, Le KM, Doores KJ, Fulton Z, Stanfield RL, Wilson IA, et al. Very Few Substitutions in a Germ Line Antibody Are Required To Initiate Significant Domain Exchange. Journal of virology. 2010;84(20):10700-7. doi: 10.1128/jvi.01111-10.

34. Joyce JG, Krauss IJ, Song HC, Opalka DW, Grimm KM, Nahas DD, et al. An oligosaccharide-based HIV-1 2G12 mimotope vaccine induces carbohydrate-specific antibodies that fail to neutralize HIV-1 virions. Proceedings of the National Academy of Sciences. 2008;105(41):15684-9. doi: 10.1073/pnas.0807837105.

35. Doores KJ, Bonomelli C, Harvey DJ, Vasiljevic S, Dwek RA, Burton DR, et al. Envelope glycans of immunodeficiency virions are almost entirely oligomannose antigens. Proceedings of the National Academy of Sciences. 2010;107(31):13800-5. doi: 10.1073/pnas.1006498107.

36. Scanlan CN, Pantophlet R, Wormald MR, Ollmann Saphire E, Stanfield R, Wilson IA, et al. The Broadly Neutralizing Anti-Human Immunodeficiency Virus Type 1 Antibody 2G12 Recognizes a Cluster of α1→2 Mannose Residues on the Outer Face of gp120. Journal of virology. 2002;76(14):7306-21. doi: 10.1128/jvi.76.14.7306-7321.2002.

37. Zhu, D. *et al.* Acquisition of potential N-glycosylation sites in the immunoglobulin variable region by somatic mutation is a distinctive feature of follicular lymphoma. *Blood* **99**, 2562-2568 (2002).

38. Zhu, D., Ottensmeier, C. H., Du, M. Q., McCarthy, H. & Stevenson, F. K. Incidence of potential glycosylation sites in immunoglobulin variable regions distinguishes between subsets of Burkitt's lymphoma and mucosa-associated lymphoid tissue lymphoma. *British journal of haematology* **120**, 217-222 (2003).

39. McCann, K. J. *et al.* Remarkable selective glycosylation of the immunoglobulin variable region in follicular lymphoma. *Molecular immunology* **45**, 1567-1572 (2008).

40. Coelho, V. *et al.* Glycosylation of surface Ig creates a functional bridge between human follicular lymphoma and microenvironmental lectins. *Proceedings of the National Academy of Sciences* **107**, 18587-18592, doi:10.1073/pnas.1009388107 (2010).

41. Krysov, S. *et al.* Surface IgM of CLL cells displays unusual glycans indicative of engagement of antigen in vivo. *Blood* **115**, 4198-4205 (2010).

42. Stevenson, F. K., Krysov, S., Davies, A. J., Steele, A. J. & Packham, G. B-cell receptor signaling in chronic lymphocytic leukemia. *Blood* **118**, 4313-4320 (2011).

43. Linley, A. *et al.* Lectin binding to surface Ig variable regions provides a universal persistent activating signal for follicular lymphoma cells. *Blood* **126**, 1902-1910 (2015).

44. Chiodin, G. *et al.* (American Society of Hematology Washington, DC, 2019).

45. Odabashian, M. *et al.* IGHV sequencing reveals acquired N-glycosylation sites as a clonal and stable event during follicular lymphoma evolution. *blood* **135**, 834-844 (2020).

46. van de Bovenkamp, F. S., Hafkenscheid, L., Rispens, T. & Rombouts, Y. The emerging importance of IgG Fab glycosylation in immunity. *The Journal of Immunology* **196**, 1435-1441 (2016).

47. Argos, B. V. *et al.* (Am Soc Hematology, 2018).

48. Küppers, R. & Stevenson, F. K. Critical influences on the pathogenesis of follicular lymphoma. *Blood* **131**, 2297-2306 (2018).

49. Roulland, S. Sugar-coated BCR kept during FL clonal evolution. *Blood* **135**, 784-785 (2020).

50. Taylor, M. E. & Drickamer, K. *Introduction to glycobiology*. (Oxford university press, 2011).

51. Ohtsubo, K. & Marth, J. D. Glycosylation in cellular mechanisms of health and disease. *Cell* **126**, 855-867 (2006).

52. Fuhrmann, U., Bause, E., Legler, G. & Ploegh, H. Novel mannosidase inhibitor blocking conversion of high mannose to complex oligosaccharides. *Nature* **307**, 755 (1984).

53. MacCallum, R. M., Martin, A. C. & Thornton, J. M. Antibody-antigen interactions: contact analysis and binding site topography. *Journal of molecular biology* **262**, 732-745 (1996).

54. Amé-Thomas, P. & Tarte, K. in *Seminars in cancer biology.* 23-32 (Elsevier).

55. Eray, M. *et al.* Follicular lymphoma cell lines, an in vitro model for antigenic selection and cytokine-mediated growth regulation of germinal centre B cells. *Scandinavian journal of immunology* **57**, 545-555 (2003).

56. Eray, M. *et al.* Cross-linking of surface IgG induces apoptosis in a bcl-2 expressing human follicular lymphoma line of mature B cell phenotype. *International immunology* **6**, 1817-1827 (1994).

57. Goval, J.-J. *et al.* The prevention of spontaneous apoptosis of follicular lymphoma B cells by a follicular dendritic cell line: involvement of caspase-3, caspase-8 and c-FLIP. *haematologica* **93**, 1169-1177 (2008).

58. Kagami, Y. *et al.* Establishment of a follicular lymphoma cell line (FLK-1) dependent on follicular dendritic cell-like cell line HK. *Leukemia* **15**, 148-156 (2001).

59. Knuutila, S. *et al.* Two novel human B-cell lymphoma lines of lymphatic follicle origin: cytogenetic, molecular genetic and histopathological characterisation. *European journal of haematology* **52**, 65-72 (1994).

60. Mättö, M., Nuutinen, U. M., Ropponen, A., Myllykangas, K. & Pelkonen, J. CD45RA and RO isoforms have distinct effects on cytokine-and B-cell-receptor-mediated signalling in human B cells. *Scandinavian journal of immunology* **61**, 520-528 (2005).

61. Fukushima, P. I., Nguyen, P. K. T., O'grady, P. & Stetler-Stevenson, M. Flow cytometric analysis of kappa and lambda light chain expression in evaluation of specimens for B-cell neoplasia. *Cytometry: The Journal of the International Society for Analytical Cytology* **26**, 243-252 (1996).

62. Alamyar, E., Giudicelli, V., Li, S., Duroux, P. & Lefranc, M.-P. IMGT/HighV-QUEST: the IMGT® web portal for immunoglobulin (IG) or antibody and T cell receptor (TR) analysis from NGS high throughput and deep sequencing. *Immunome res* **8**, 26 (2012).

63. Li, S. *et al.* IMGT/HighV QUEST paradigm for T cell receptor IMGT clonotype diversity and next generation repertoire immunoprofiling. *Nature communications* **4**, 1-13 (2013).

64. Brochet, X., Lefranc, M.-P. & Giudicelli, V. IMGT/V-QUEST: the highly customized and integrated system for IG and TR standardized VJ and VDJ sequence analysis. *Nucleic acids research* **36**, W503-W508 (2008).

65. Alamyar, E., Giudicelli, V., Duroux, P. & Lefranc, M. IMGT/HighV-QUEST: A high-throughput system and Web portal for the analysis of rearranged nucleotide sequences of antigen receptors-High-throughput version of IMGT/V-QUEST. *V-QUEST 11èmes Journées Ouvertes en Biologie, Informatique et Mathématiques (JOBIM)*, 7-9 (2010).

66. Rao, R. S. P. & Bernd, W. Do N-glycoproteins have preference for specific sequons? *Bioinformation* **5**, 208 (2010).

67. Marks, J. D. *et al.* By-passing immunization: human antibodies from V-gene libraries displayed on phage. *Journal of molecular biology* **222**, 581-597 (1991).

68. Marks, J. D., Tristem, M., Karpas, A. & Winter, G. Oligonucleotide primers for polymerase chain reaction amplification of human immunoglobulin variable genes and design of family-specific oligonucleotide probes. *European journal of immunology* **21**, 985-991 (1991).

69. Callahan, B. J. *et al.* DADA2: High-resolution sample inference from Illumina amplicon data. *Nature Methods* **13**, 581-583, doi:10.1038/nmeth.3869 (2016).

70. Katoh, K. & Standley, D. M. MAFFT multiple sequence alignment software version 7: improvements in performance and usability. *Molecular biology and evolution* **30**, 772-780 (2013).

71. Crooks, G. E., Hon, G., Chandonia, J.-M. & Brenner, S. E. WebLogo: a sequence logo generator. *Genome research* **14**, 1188-1190 (2004).

72. Council, N.R.; Glycoscience, I.T. *A Roadmap for the Future*; Walt, D., Ed.; The National Academies Press: Washington, DC, USA, 2012; pp. 85–89.

73. Shivatare, S.S.; Chang, S.-H.; Tsai, T.-I.; Tseng, S.Y.; Shivatare, V.S.; Lin, Y.-S.; Cheng, Y.-Y.; Ren, C.-T.; Lee, C.-C.D.; Pawar, S. Modular synthesis of N-glycans and arrays for the hetero-ligand binding analysis of HIV antibodies. *Nat. chem.* 2016, **8**, 338–349.

74. Stick, R.V.; Williams, S. *Carbohydrates: The essential molecules of life*; Elsevier: Amsterdam, Netherlands, 2010.

75. Pabst, M.; Altmann, F. Glycan analysis by modern instrumental methods. *Proteomics* 2011, **11**, 631–643.

76. Bielik, A.M.; Zaia, J. Historical overview of glycoanalysis. In *Functional Glycomics*; Springer: Berlin, Germany, 2010; pp. 9–30.

77. Schwarz, R.T.; Schmidt, M.F.; Anwer, U.; Klenk, H.-D. Carbohydrates of influenza virus. I. Glycopeptides derived from viral glycoproteins after labeling with radioactive sugars. *J. Virol.* 1977, **23**, 217–226.

78. Nakamura, K.; Bhown, A.S.; Compans, R.W. Glycosylation sites of influenza viral glycoproteins Tryptic glycopeptides from the A/WSN (H0N1) hemagglutinin glycoprotein. *Virology* 1980, **107**, 208–221.

79. Matsumoto, A.; Yoshima, H.; Kobata, A. Carbohydrates of influenza virus hemagglutinin: Structures of the whole neutral sugar chains. *Biochemistry* 1983, **22**, 188–196.

80. Spik, G.; Debruyne, V.; Montreuil, J.; van Halbeek, H.; Vliegenthart, J.F. Primary structure of two sialylated triantennary glycans from human serotransferrin. *FEBS lett.* 1985, **183**, 65–69.

81. Schmitz, B.; Klein, R.A.; Duncan, I.A.; Egge, H.; Gunawan, J.; Peter-Katalinic, J.; Dabrowski, U.; Dabrowski, J. MS and NMR analysis of the cross-reacting determinant glycan from Trypanosoma brucei brucei MITat 1.6 variant specific glycoprotein. *Biochem. Biophys. Res. Commun.* 1987, **146**, 1055–1063.

82. Keil, W.; Geyer, R.; Dabrowski, J.; Dabrowski, U.; Niemann, H.v.; Stirm, S.; Klenk, H. Carbohydrates of influenza virus. Structural elucidation of the individual glycans of the FPV hemagglutinin by two-dimensional 1H nmr and methylation analysis. *EMBO J.* 1985, **4**, 2711–2720.

83. Madera, M.; Mechref, Y.; Novotny, M.V. Combining lectin microcolumns with high-resolution separation techniques for enrichment of glycoproteins and glycopeptides. *Anal.Chem.* 2005, **77**, 4081–4090.

84. McDonald, C.A.; Yang, J.Y.; Marathe, V.; Yen, T.-Y.; Macher, B.A. Combining results from lectin affinity chromatography and glycocapture approaches substantially improves the coverage of the glycoproteome. *Mol. Cell. Proteom.* 2009, **8**, 287–301.

85. Xu, Y.; Wu, Z.; Zhang, L.; Lu, H.; Yang, P.; Webley, P.A.; Zhao, D. Highly specific enrichment of glycopeptides using boronic acid-functionalized mesoporous silica. *Anal. Chem.* 2008, **81**, 503–508.

86. Zhang, H.; Li, X.-j.; Martin, D.B.; Aebersold, R. Identification and quantification of N-linked glycoproteins using hydrazide chemistry, stable isotope labeling and mass spectrometry. *Nat. biotechnol.* 2003, **21**, 660–666.

87. Hase, S. Precolumn derivatization for chromatographic and electrophoretic analyses of carbohydrates. *J. Chromatogr. A* 1996, **720**, 173–182.

88. Pabst, M.; Kolarich, D.; Pöltl, G.; Dalik, T.; Lubec, G.; Hofinger, A.; Altmann, F. Comparison of fluorescent labels for oligosaccharides and introduction of a new postlabeling purification method. *Anal. Biochem.* 2009, **384**, 263–273.

89. Rosenfeld, R.; Bangio, H.; Gerwig, G.J.; Rosenberg, R.; Aloni, R.; Cohen, Y.; Amor, Y.; Plaschkes, I.; Kamerling, J.P.; Maya, R.B.-Y. A lectin array-based methodology for the analysis of protein glycosylation. *J. Biochem. Biophys. Methods* 2007, **70**, 415–426, doi:10.1016/j.jbbm.2006.09.008.

90. Chan, K.; Bun Ng, T. Lectin glycoarray technologies for nanoscale biomedical detection. *Protein Pept. Lett.* 2010, **17**, 1417–1425.

91. Loris, R.; De Greve, H.; Dao-Thi, M.-H.; Messens, J.; Imberty, A.; Wyns, L. Structural basis of carbohydrate recognition by lectin II from Ulex europaeus, a protein with a promiscuous carbohydrate-binding site. *J. Mol. Biol.* 2000, **301**, 987–1002.

92. Zhao, Y.-P.; Xu, X.-Y.; Fang, M.; Wang, H.; You, Q.; Yi, C.-H.; Ji, J.; Gu, X.; Zhou, P.-T.; Cheng, C. Decreased core-fucosylation contributes to malignancy in gastric cancer. *PloS ONE* 2014, **9**, e94536.

93. Lee, H.K.; Scanlan, C.N.; Huang, C.Y.; Chang, A.Y.; Calarese, D.A.; Dwek, R.A.; Rudd, P.M.; Burton, D.R.; Wilson, I.A.; Wong, C.H. Reactivity-based one-pot synthesis of oligomannoses: Defining antigens recognized by 2G12, a broadly neutralizing anti-HIV-1 antibody. *Angew. Chem. Int. Ed.* 2004, **43**, 1000–1003.

94. Radcliffe, C.M.; Arnold, J.N.; Suter, D.M.; Wormald, M.R.; Harvey, D.J.; Royle, L.; Mimura, Y.; Kimura, Y.; Sim, R.B.; Inogès, S. Human follicular lymphoma cells contain oligomannose glycans in the antigen-binding site of the B-cell receptor. *J. Biol. Chem.* 2007, **282**, 7405–7415.

95. Stroop, C.J.; Weber, W.; Gerwig, G.J.; Nimtz, M.; Kamerling, J.P.; Vliegenthart, J.F. Characterization of the carbohydrate chains of the secreted form of the human epidermal growth factor receptor. *Glycobiol.* 2000, **10**, 901–917.

96. Aebi, M.; Hennet, T. Congenital disorders of glycosylation: Genetic model systems lead the way. *Trends Cell Biol.* 2001, **11**, 136–141.

97. Pan, S.; Cheng, X.; Sifers, R.N. Golgi-situated endoplasmic reticulum α-1, 2-mannosidase contributes to the retrieval of ERAD substrates through a direct interaction with γ-COP. *Mol. Biol. Cell* 2013, **24**, 1111–1121.

98. Olson, L.J.; Orsi, R.; Peterson, F.C.; Parodi, A.J.; Kim, J.-J.P.; D'Alessio, C.; Dahms, N.M. Crystal structure and functional analyses of the lectin domain of glucosidase II: Insights into oligomannose recognition. *Biochemistry* 2015, **54**, 4097–4111.

99. Wang, S.-K.; Liang, P.-H.; Astronomo, R.D.; Hsu, T.-L.; Hsieh, S.-L.; Burton, D.R.; Wong, C.-H. Targeting the carbohydrates on HIV-1: Interaction of oligomannose dendrons with human monoclonal antibody 2G12 and DC-SIGN. *Proc. Natl. Acad. Sci. USA* 2008, **105**, 3690–3695.

100. Martínez, J.D.; Valverde, P.; Delgado, S.; Romanò, C.; Linclau, B.; Reichardt, N.C.; Oscarson, S.; Ardá, A.; Jiménez-Barbero, J. Unraveling Sugar Binding Modes to DC-SIGN by Employing Fluorinated Carbohydrates. *Molecules* 2019, **24**, 2337.

101. Valverde, P.; Delgado, S.; Martinez, J.D.; Vendeville, J.-B.; Malassis, J.; Linclau, B.; Reichardt, N.-C.; Cañada, F.J.; Jiménez-Barbero, J.; Arda, A. Molecular insights into DC-SIGN binding to self-antigens: The interaction with the blood group A/B antigens. *ACS Chem. Biol.* 2019, **14**, 1660–1670.

102. Fujimoto, Z.; Tateno, H.; Hirabayashi, J. Lectin structures: Classification based on the 3-D structures. In *Lectins*; Springer: Berlin, Germany, 2014; pp. 579–606.

103. Sato, Y.; Okuyama, S.; Hori, K. Primary structure and carbohydrate binding specificity of a potent anti-HIV lectin isolated from the filamentous cyanobacterium Oscillatoria agardhii. *J. Biol. Chem.* 2007, **282**, 11021–11029.

104. Koharudin, L.M.; Kollipara, S.; Aiken, C.; Gronenborn, A.M. Structural insights into the anti-HIV activity of the Oscillatoria agardhii agglutinin homolog lectin family. *J. Biol. Chem.* 2012, **287**, 33796–33811.

105. Pritchard, L.K.; Spencer, D.I.; Royle, L.; Bonomelli, C.; Seabright, G.E.; Behrens, A.-J.; Kulp,D.W.; Menis, S.; Krumm, S.A.; Dunlop, D.C. Glycan clustering stabilizes the mannose patch of HIV-1 and preserves vulnerability to broadly neutralizing antibodies. *Nat. Commun.* 2015, **6**, 7479.

106. Férir, G.; Huskens, D.; Noppen, S.; Koharudin, L.M.; Gronenborn, A.M.; Schols, D. Broad anti-HIV activity of the Oscillatoria agardhii agglutinin homologue lectin family. *J. Antimicrob. Chemother.* 2014, **69**, 2746–2758.

107. Kwak, E.-A.; Kydd, L.; Lim, B.; Jaworski, J. IR-783 Labeling of a Peptide Receptor for 'Turn-On'Fluorescence Based Sensing. *Chemosensors* 2018, **6**, 47.

108. Skerra, A.; Schmidt, T.G.M. Applications of a peptide ligand for streptavidin: The Strep-tag. *Biomol. Eng.* 1999, **16**, 79–86, doi:10.1016/S1050-386s2(99)00033-9.

109. Hundsberger, H.; Önder, K.; Schuller-Götzburg, P.; Virok, D.P.; Herzog, J.; Rid, R. Assembly and use of high-density recombinant peptide chips for large-scale ligand screening is a practical alternative to synthetic peptide libraries. *BMC Genom.* 2017, **18**, 450, doi:10.1186/s12864-017-3814-3.

110. Pöhlmann, S.; Soilleux, E.J.; Baribaud, F.; Leslie, G.J.; Morris, L.S.; Trowsdale, J.; Lee, B.; Coleman, N.; Doms, R.W. DC-SIGNR, a DC-SIGN homologue expressed in endothelial cells, binds to human and simian immunodeficiency viruses and activates infection in trans. *Proc. Natl. Acad. Sci. USA* 2001, **98**, 2670–2675.

111. Hirabayashi, J.; Tateno, H.; Shikanai, T.; Aoki-Kinoshita, K.; Narimatsu, H. The lectin frontier database (LfDB), and data generation based on frontal affinity chromatography. *Molecules* 2015, **20**, 951–973.

112. Yu, H.; Zhao, G.; Dou, W. Simultaneous detection of pathogenic bacteria using agglutination test based on colored silica nanoparticles. *Curr. Pharm. Biotechnol.* 2015, **16**, 716–723.

113. Zhu, M.; Jia, Y.; Peng, L.; Ma, J.; Li, X.; Shi, F. A highly sensitive dual-color lateral flow immunoassay for brucellosis using one-step synthesized latex microspheres. *Anal. Methods* 2019, **11**, 2937–2942.

114. Hoorelbeke B, Van Damme EJ, Rougé P, Schols D, Van Laethem K, Fouquaert E, et al. Differences in the mannose oligomer specificities of the closely related lectins from Galanthus nivalis and Zea maysstrongly determine their eventual anti-HIV activity. Retrovirology. 2011;**8(1)**:10. doi: 10.1186/1742-4690-8-10.

115. Doores KJ, Fulton Z, Huber M, Wilson IA, Burton DR. Antibody 2G12 Recognizes Di-Mannose Equivalently in Domain- and Nondomain-Exchanged Forms but Only Binds the HIV-1 Glycan Shield if Domain Exchanged. Journal of virology. 2010;**84(20)**:10690-9. doi: 10.1128/jvi.01110-10.

116. Kamiya Y, Kamiya D, Yamamoto K, Nyfeler B, Hauri H-P, Kato K. Molecular Basis of Sugar Recognition by the Human L-type Lectins ERGIC-53, VIPL, and VIP36. Journal of Biological Chemistry. 2008;**283(4)**:1857-61. doi: 10.1074/jbc.M709384200.

117. Kwak E-A, Kydd L, Lim B, Jaworski J. IR-783 Labeling of a Peptide Receptor for 'Turn-On' Fluorescence Based Sensing. Chemosensors. 2018;**6(4)**:47. PubMed PMID: doi:10.3390/chemosensors6040047.